



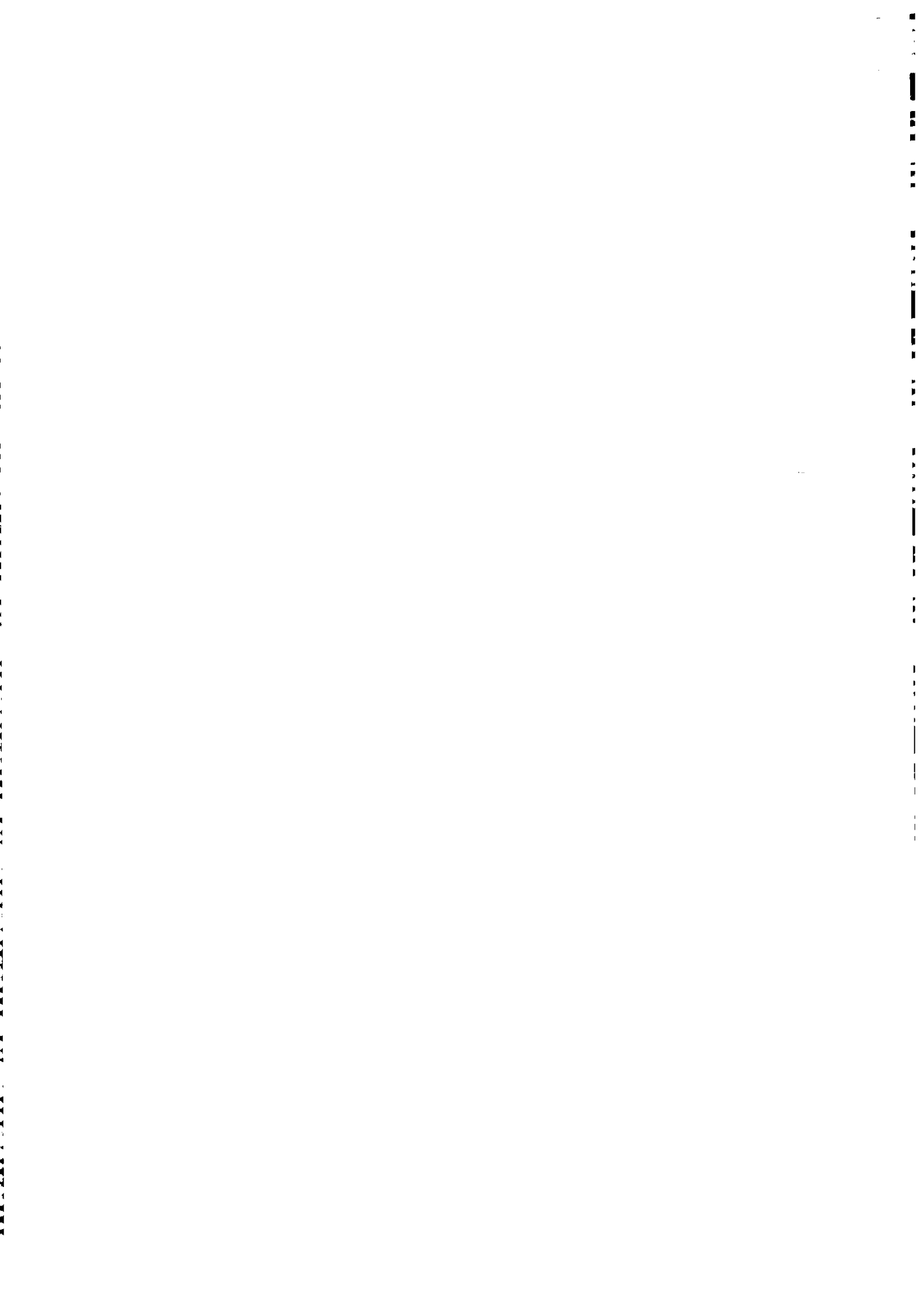
SMR.1065 - 3

**COLLEGE ON SOIL PHYSICS
14 - 30 APRIL 1998**

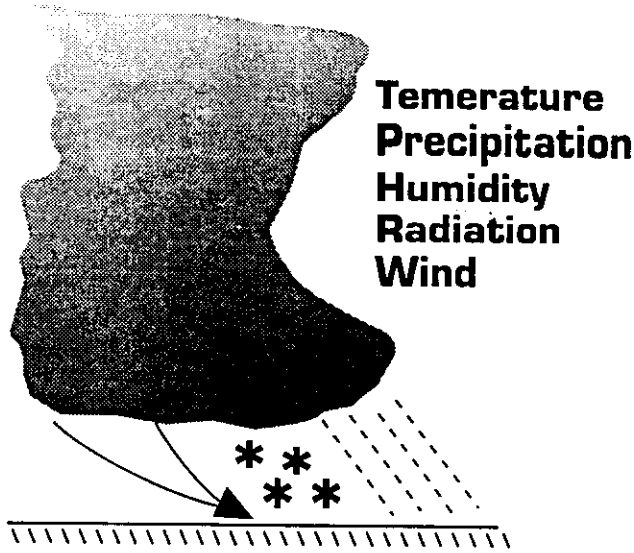
**"Wind Erosion Prediction System"
Part 1**

**Edward L. SKIDMORE
United States Department of Agriculture
Agricultural Research Service - Central Plains Area
Wind Erosion Research Unit
Throckmorton Hall
Kansas State University
Kansas 66506
Manhattan
U.S.A.**

These are preliminary lecture notes, intended only for distribution to participants

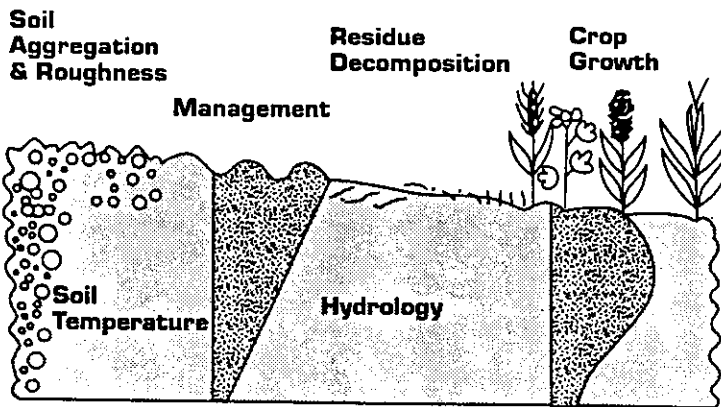


Weather



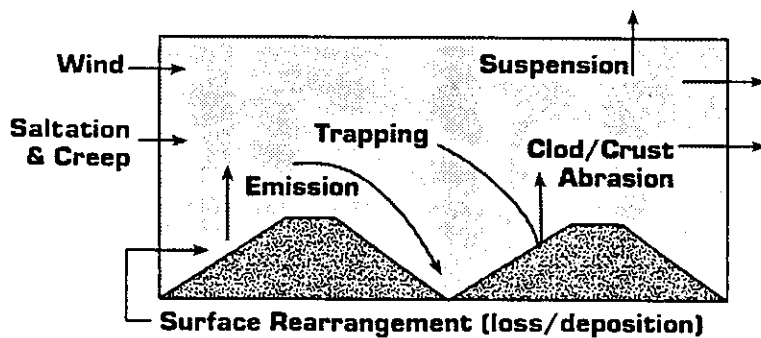
USDA Wind Erosion Prediction System

Temporal Erodiability




Technical Description


Erosion



 Agricultural Research Service

 Natural Resources Conservation Service

 Bureau of Land Management

 Environmental Protection Agency

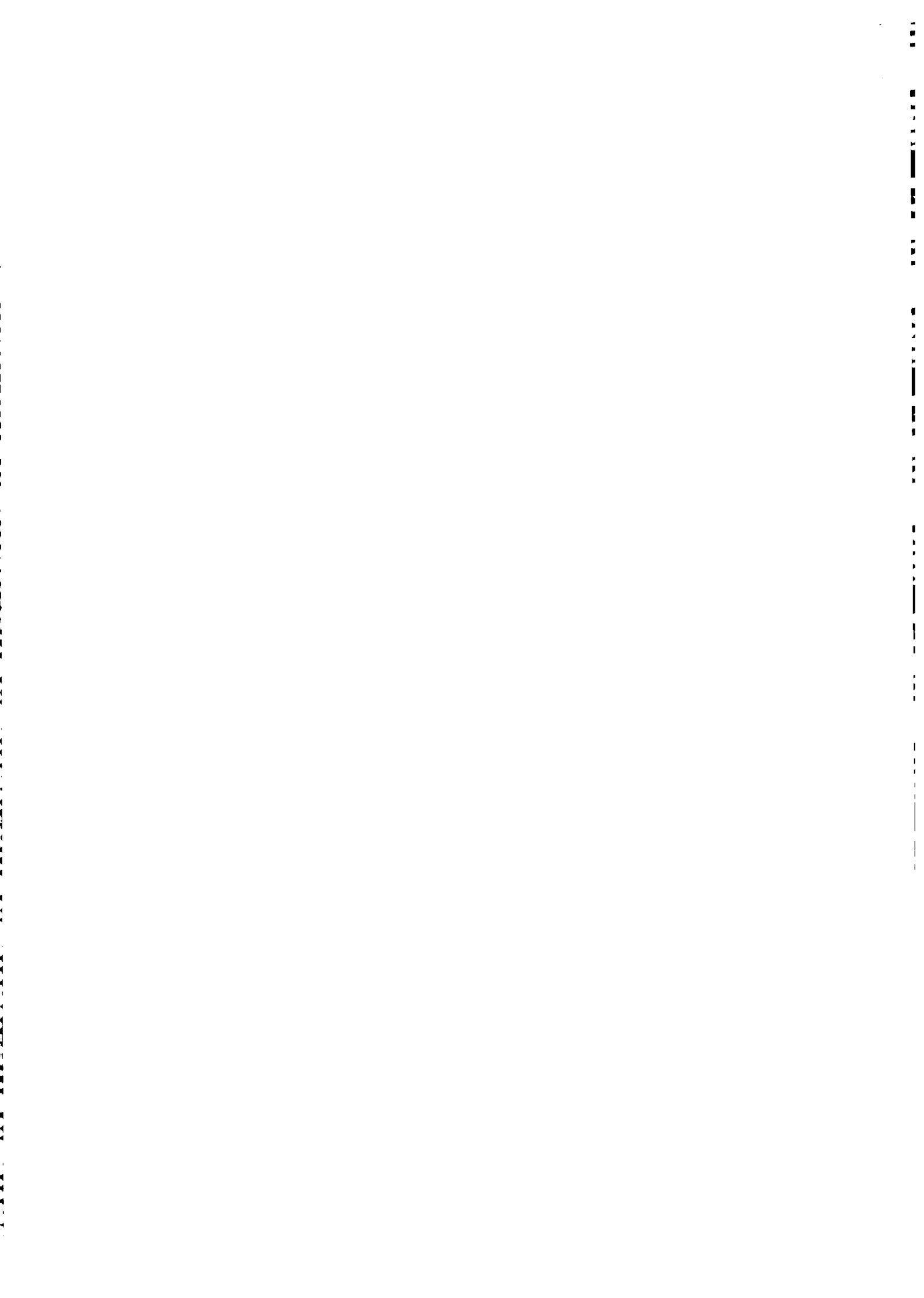


Table of Contents

	Page
PREFACE	x
ACKNOWLEDGMENTS	xi
WIND EROSION PREDICTION SYSTEM (WEPS)	I-1
INTRODUCTION	I-1
OBJECTIVES	I-1
THE SIMULATION REGION	I-1
SIMULATED PROCESSES	I-2
MODEL DESIGN CONCEPTS	I-3
Discrete Time and Discrete Space.	I-3
MODELING TECHNIQUES: WEPS compared to WEQ	I-5
IMPLEMENTATION	I-6
Software	I-6
Hardware	I-6
Operation	I-7
LIMITATIONS	I-7
WEPS UPDATES	I-7
REFERENCES	I-8
MAIN PROGRAM	M-1
INTRODUCTION	M-1
PROGRAM DESCRIPTION	M-1
MAIN VARIABLE, SUBROUTINE, AND FUNCTION LISTS AND	
DEFINITIONS	M-3
Local Variables	M-3
Subroutines Called	M-5
Functions Called	M-6
WEATHER SUBMODEL	W-1
INTRODUCTION	W-1
WINDGEN DEVELOPMENT	W-2
Compact Database	W-2
Determination of Wind Direction	W-7
Determination of Wind Speed	W-7

SUBROUTINE CALCWU	W-8
CLI_WIND PROGRAM	W-11
OUTPUT FILE	W-11
SUMMARY	W-11
LIST OF SYMBOLS	W-13
LITERATURE CITED	W-14
EROSION SUBMODEL	E-1
INTRODUCTION	E-1
OBJECTIVES	E-6
EROSION SUBMODEL CONTROL SECTIONS	E-6
DETERMINE FRICTION VELOCITY	E-6
DETERMINE STATIC THRESHOLD FRICTION VELOCITY	E-15
GENERATION OF THE SIMULATION GRID	E-21
INITIALIZATION OF THE SIMULATION GRID	E-21
HILLS	E-21
WIND BARRIERS	E-21
COMPUTATION OF SOIL LOSS/DEPOSITION	E-24
CONSERVATION OF MASS FOR SALTATION AND CREEP ...	E-24
SOURCE/SINK EQUATIONS FOR SALTATION AND CREEP ..	E-27
CONSERVATION OF MASS FOR SUSPENSION	E-37
SOURCE/SINK EQUATIONS FOR SUSPENSION	E-37
CONSERVATION OF MASS FOR PM-10	E-38
SOURCE/SINK EQUATIONS FOR PM-10	E-38
SURFACE REARRANGEMENT	E-39
EROSION EFFECT ON LOOSE SOIL ON CRUST	E-40
EROSION EFFECT ON CRUST THICKNESS AND COVER	E-40
EROSION EFFECT ON SURFACE ROUGHNESS	E-41
EROSION EFFECT ON AGGREGATE-SIZE DISTRIBUTION ...	E-42
UPDATE OF GLOBAL SUBREGION VARIABLES	E-44
OUTPUT FROM EROSION TO FILES	E-46
REFERENCES	E-47
HYDROLOGY SUBMODEL	H-1
INTRODUCTION	H-1
SUBMODEL DEVELOPMENT AND DESCRIPTION	H-4
Snow Melt	H-4
Surface Runoff	H-4
Soil Water Storage	H-9
Potential Evapotranspiration	H-9
Potential Soil Evaporation and Plant Transpiration	H-15

Actual Plant Water Uptake and Water Stress Factor H-15

Soil Water Redistribution H-17

Estimating Soil Hydraulic Properties H-24

Soil Wetness at the Soil-Atmosphere Interface H-29

Simulation of Soil Temperature H-36

The Structure and Procedures of the HYDROLOGY Submodel H-38

Winter Routines H-46

SUBMODEL TESTING AND EVALUATION H-47

LIST OF SYMBOLS H-52

REFERENCES H-61

MANAGEMENT SUBMODEL T-1

INTRODUCTION T-1

 Purpose T-1

 Objectives T-1

 Assumptions and Limitations T-2

SUBMODEL DESCRIPTION T-3

PHYSICAL PROCESSES MODELED T-6

 Soil Surface Manipulation T-7

 Soil Mass Manipulation T-9

 Biomass Manipulation T-15

 Soil Amendments T-16

SUBMODEL IMPLEMENTATION T-16

 Submodel Logic T-16

 Management File Format Description T-24

 Subroutine Code Descriptions T-28

LIST OF SYMBOLS T-32

REFERENCES T-35

SOIL SUBMODEL S-1

INTRODUCTION S-1

SOIL SUBMODEL COMPUTATION SCHEME S-2

PROCESS EFFECTS ON SOIL TEMPORAL PROPERTIES S-4

 RIDGE AND FURROW DIKE HEIGHT S-4

 RANDOM ROUGHNESS S-5

 CRUST S-6

 CRUST THICKNESS S-6

 CRUST COVER FRACTION S-7

 CRUST STABILITY S-7

 LOOSE ERODIBLE MATERIAL ON CRUST S-7

 DRY AGGREGATE STABILITY S-9

 AGGREGATE SIZE DISTRIBUTION - ASD S-11

Replaced

BULK DENSITY	S-14
CRUST AND AGGREGATE DENSITY	S-15
REFERENCES	S-16
LIST OF SYMBOLS, DEFINITIONS, AND UNITS	S-18
CROP SUBMODEL	C-1
ABSTRACT	C-1
INTRODUCTION	C-1
MODEL DESCRIPTION:	C-2
Crop Parameters:	C-2
Phenological development	C-2
Day length	C-3
Emergence	C-4
Biomass production	C-4
Partitioning of biomass	C-5
Leaf and stem area growth	C-6
Leaf area index decline	C-6
Plant height	C-7
GROWTH CONSTRAINTS	C-7
Water stress	C-8
Temperature stress	C-8
Nutrient stress	C-9
VALIDATION	C-9
Materials and methods	C-9
Results and Discussion	C-9
REFERENCES	C-11
LIST OF SYMBOLS	C-13
RESIDUE DECOMPOSITION SUBMODEL	D-1
MODEL OVERVIEW	D-1
DECOMPOSITION	D-3
CHANGES IN STANDING RESIDUE BIOMASS AND POPULATION ..	D-4
PERCENT SOIL COVER FROM STANDING AND SURFACE RESIDUES	D-5
RESIDUE DISTRIBUTION BY HEIGHT	D-5
MODIFYING VARIABLES DUE TO TILLAGE OPERATIONS	D-6
CROP RESIDUE DECOMPOSITION SUBMODEL SUMMARY	D-6
REFERENCES	D-8

APPENDIX AA:

WEPS-RELATED LITERATURE AA-1
 PAPERS BY THE WEPS CORE TEAM MEMBERS AA-1
 ABSTRACTS BY THE WEPS CORE TEAM MEMBERS AA-11

Appendix BB:

Variable Naming Conventions and Global Variable List BB-1
 WEPS VARIABLE CONVENTIONS BB-1
 VARIABLE USAGE BB-2
 VARIABLE NAMES BB-2
 State Variables BB-2
 Local Variables BB-4
 Parameters BB-4
 Example of Code Using Constants BB-5
 WEPS Common Blocks BB-6
 WEPS Fortran Parameters BB-6
 WEPS Global Variables BB-7

*Appendix CC: Extensions/updater of EROSION
 submodel. It has been accepted for
 publication in Int Sci Soc, Am J. 1998*

List of Tables

	Page
Table W-1. Monthly joint wind speed/direction frequency values.	W-3
Table W-2. Ratio of maximum to minimum hourly wind speed (max/min) and hour of maximum wind speed.	W-5
Table W-3. Wind direction distribution by month in percent.	W-5
Table W-4. Weibull shape parameters by month and direction.	W-6
Table W-5. Weibull scale parameters by month and direction in m/s.	W-6
Table H-1. Runoff curve numbers for hydrologic soil-cover complexes (Class II antecedent moisture conditions).	H-6
Table H-2. Criteria for selecting the correct hydrologic soil group.	H-7
Table H-3. Soil hydraulic parameters classified by soil textural class (water contents on volumetric basis).	H-28
Table H-4. Soil hydraulic parameters classified by soil textural class (water contents on gravimetric basis).	H-29
Table T-1. Management operation classes.	T-4
Table T-2. MANAGEMENT submodel processes.	T-5
Table T-3. Parameters of crushing model for four types of tillage tools.	T-13
Table T-4. Rules of thumb for determining degree of crushing from parameters. . .	T-13
Table T-5. Embedded operations/processes for selected MANAGEMENT tasks. . .	T-24
Table T-6. Operation and process parameters.	T-25
Table T-7. Sample MANAGEMENT input file.	T-26
Table S-1. Soil Submodel State Variable and Process Matrix.	S-21
Table C-1. Parameters of linear regression of measured on simulated plant variables	C-16
Table D-1. Required Inputs From Other Submodels.	D-9
Table D-2. Decomposition Variable List.	D-10
Table D-3. Variables That MANAGEMENT Must Modify.	D-12

List of Figures

	Page
Figure I-1. WEPS simulation geometries.	I-2
Figure I-2. Structure of the WEPS model.	I-4
Figure M-1. Flowchart for MAIN program.	M-2
Figure W-1. Flowchart for subdaily wind subroutine 'calcwu'.	W-9
Figure W-2. Example of a 'real data' subdaily wind speed file, where day mo year are the day , month, and year of the wind data, dir is the wind direction in degrees from North, and wind speeds are the 24 subdaily wind speeds.	W-10
Figure W-3. Example of WINDGEN output where day, mo, and year are the day, month, and year of simulation; dir is the wind direction in degrees from North; umax and umin are maximum and minimum wind speed for the day; and hrmax is the hour at which the wind speed is maximum.	W-12
Figure E-1. Simulation region geometry. End points of barriers and opposite corners of rectangular simulation region, subregions, and accounting regions must be input by user.	E-2
Figure E-2. Illustration of random roughness shelter angles (SA) and oriented roughness spacing (SX-RG) and height (SZ-RG) used in EROSION.	E-3
Figure E-3. Illustration of surface cover fraction descriptions used in EROSION. The rock > 2.0 mm (SF-ROC), aggregated (SF-AG), and crusted (SF-CR) soil constitute the lowest layer, and their fractions sum to 1. The second layer is cover fraction loose soil on the crust (SF-LOS), and it cannot exceed crust fraction. The third layer is the biomass flat fraction of cover (BFF-CV), which is assumed to have random distribution over the entire surface.	E-4
Figure E-4. Diagram illustrating above-canopy friction velocity (WU^*v), which is reduced by drag of the biomass (BRcd) to the below-canopy friction velocity (WU^*). The latter is used to drive EROSION.	E-5
Figure E-5. Partial flowchart of subroutine "Sberos" illustrating testing of subregions to determine if daily maximum friction velocity exceeds threshold friction velocity.	E-7
Figure E-6. Ratio of aerodynamic roughness to ridge height as a function of the ridge height to spacing ratio; predicted is equation E-1. (Hagen and Armbrust, 1992).	E-9
Figure E-7. Aerodynamic roughness of random rough surfaces as a function of the Weibull scale factor of the shelter angle distribution of the random rough surfaces; predicted is equation E-4.	E-10
Figure E-8. Biomass aerodynamic roughness as a function of effective drag coefficient of the biomass; predicted is equation E-6.	E-12

- Figure E-9.** Reduction in friction velocity through biomass canopy as a function of biomass drag coefficient; predicted is equation E-10 (Lyles and Allison, 1976; van de Ven, Fryrear, and Spaan, 1989). E-14
- Figure E-10.** Predicted threshold friction velocities for various levels of aerodynamic roughness and surface cover; predicted is equations E-14 and E-15. E-17
- Figure E-11.** Predicted threshold friction velocities as a function of measured threshold friction velocities on random rough and ridged surfaces (Hagen, 1991b; Hagen and Armbrust, 1992). E-18
- Figure E-12.** Increase in static threshold friction velocity of erodible sand; predicted is equation E-17 (0.29-0.42 mm diameter) caused by flat biomass cover (Hagen, 1995). E-19
- Figure E-13.** Static threshold friction velocity change with water content relative to 1.5 MPa water content; predicted slope is equation E-18 (Saleh and Fryrear, 1995). E-20
- Figure E-14.** Partial flow chart of subroutine "Sberos" illustrating calls to create simulation region grid and initialize it for each day. E-22
- Figure E-15.** Barrier function velocity reduction patterns along the wind direction used to modify friction velocity near barriers; predictions are equations E-20 and E-21. E-23
- Figure E-16.** Partial flow chart of subroutine "Sberos" illustrating testing for subhourly friction velocities above the threshold and then computing soil loss/deposition in subroutine "Sberod." E-25
- Figure E-17.** Diagram of control volume with a ridged bare soil illustrating the sources and sinks used in the EROSION submodel. E-26
- Figure E-18.** Reduction in emission of loose soil as a function of increasing biomass flat cover; predicted is equation E-29 (Hagen, 1995). E-29
- Figure E-19.** Predicted reduction in emission of loose soil as a fraction of both soil fraction with shelter angle greater than 12 degrees and fraction of soil not emitting; predicted is equation E-30. E-30
- Fig. E-20.** Predicted reduction is emission of loose soil compared to values measured in the wind tunnel; predicted is equation E-30 (Hagen, 1991b). E-31
- Figure E-21.** Abrasion coefficients as a function of crushing energy for soil aggregates and crusts; predicted is equation E-49 (Hagen, Skidmore, and Saleh, 1992). E-36
- Figure E-22.** Partial flowchart of subroutine "Sberos" illustrating updating of global subregion variables and output to files from the EROSION submodel. Viewing the results and printing output are controlled by the MAIN control subroutines of WEPS. E-45
- Figure H-1.** Measured hourly soil water contents at the soil-atmosphere interface versus measured evaporation ratios from the 1971 Arizona experiment (data for March 6 & 7 were missing). H-32

Figure H-2. Regression analysis between measured and simulated hourly evaporation ratios from the 1971 Arizona experiment excluding March 6 & 7. H-33

Figure H-3. Measured hourly soil water contents at the soil-atmosphere interface versus measured and simulated evaporation ratios from the 1971 Arizona experiment (March 6 & 7 evaporation ratios were simulated). H-34

Figure H-4. Simplified flowchart of the HYDROLOGY submodel of WEPS. H-41

Figure H-5. Simplified flowchart of the HYDROLOGY submodel of WEPS (continued). H-42

Figure H-6. Simplified flowchart of the HYDROLOGY submodel of WEPS (continued). H-43

Figure H-7. Simplified flowchart of the HYDROLOGY submodel of WEPS (continued). H-44

Figure H-8. Simplified flowchart of the HYDROLOGY submodel of WEPS (continued). H-45

Figure H-9. Regression analysis between measured and simulated daily evaporation rates from Bushland, TX, 1991 validation experiment. H-49

Figure H-10. Measured vs. simulated hourly soil water contents from the eight simulation layers, Bushland, TX 1991, validation experiment. H-50

Figure H-11. Measured soil water contents in the uppermost 2 mm versus simulated hourly soil water contents at the soil-atmosphere interface, Bushland, TX, validation experiment. H-51

Figure T-1. MANAGEMENT file record/location pointers. T-17

Figure T-2. WEPS MAIN routine. T-19

Figure T-3. Top-level MANAGEMENT subroutine. T-20

Figure T-4. MANAGEMENT select operation routine. T-21

Figure T-5. Individual MANAGEMENT operation routine. T-22

Figure T-6. MANAGEMENT select process routine. T-23

Figure S-1. Typical example of temporal variable, (ie., ratio of ridge height to ridge spacing) affected by two processes. S-3

Figure C-1. Comparison of simulated versus measured data for soybeans, corn, grain sorghum, winter wheat, and oats. C-15

Figure D-1. Biomass distribution and transfer between residue pools. D-1

PREFACE

Wind erosion is a serious problem on agricultural lands throughout the United States as well as the world. The ability to accurately predict soil loss by wind is essential for, among other things, conservation planning, natural resource inventories, and reducing air pollution from wind blown sources.

The Wind Erosion Equation (WEQ) is currently the most widely used method for assessing average annual soil loss by wind from agricultural fields. The primary user of WEQ is the United States Department of Agriculture, Natural Resources Conservation Service (USDA-NRCS). When WEQ was developed more than 30 years ago, it was necessary to make it a simple mathematical expression, readily solvable with the computational tools available. Since its inception, there have been a number of efforts to improve the accuracy, ease of application, and range of WEQ. Despite efforts to make such improvements, the structure of WEQ precludes adaptation to many problems.

The USDA appointed a team of scientists to take a leading role in combining the latest in wind erosion science and technology with databases and computers, to develop what should be a significant advancement in wind erosion prediction technology. The Wind Erosion Prediction System (WEPS) incorporates this new technology and is designed to be a replacement for WEQ.

Unlike WEQ (and RWEQ), WEPS is a process-based, continuous, daily time-step model that simulates weather, field conditions, and erosion. It is a user friendly program that has the capability of simulating spatial and temporal variability of field conditions and soil loss/deposition within a field. WEPS can also simulate complex field shapes, barriers not on the field boundaries, and complex topographies. The saltation, creep, suspension, and PM10 components of eroding material also can be reported separately by direction in WEPS. WEPS is designed to be used under a wide range of conditions in the U.S. and easily adapted to other parts of the world.

The objective of this release is to facilitate communication among potential users of WEPS and to allow for Beta testing of the model.

We anticipate future updates and enhancements to WEPS including extension to range and other non-cropped disturbed lands.

ACKNOWLEDGMENTS

The Wind Erosion Prediction System (WEPS) resulted from the work of many individuals representing several agencies and institutions. In particular, appreciation is extended to the WEPS Core Team members: D.V. Armbrust, J.D. Bilbro, G.W. Cole (retired), D.J. Ding, A.A. Durar, D.W. Fryrear, R.B. Grossman, L. Lyles (retired), A. Retta, A. Saleh, H.H. Schomberg, H.R. Sinclair, E.L. Skidmore, J.L. Steiner, J. Tatarko, P.W. Unger, L.E. Wagner, and T.M. Zobeck; the Agency liasons to the Core Team, including: M.S. Argabright, NRCS (retired), H. Bogusch, NRCS, R. Dunkins, EPA, and C. Voigt, BLM; the ARS NPL including: C.R. Amerman, S. Rawlins, and W.D. Kemper; and NRCS leaders including D. Schertz, D. Woodward, and K. Flach (retired).

Gratitude is also expressed to the many cooperators and other individuals who have contributed to the development of WEPS through their valuable research, criticisms, and comments. These individuals include: J.K. Aase, A. Black, W. Blackburn, P. Bullock, D.A. Gillette, J. Gregory, J.R. Kiniry, J. Laflen, J.A. Lamb, F. Larney, J.B. Layton, M.J. Lindstrom, S.D. Merrill, N. Mirzamostafa, D.L. Mokma, A. Moulin, A. Nicks, K.N. Potter, R. Savabi, K. Saxton, J. Stout, G. Tibke, E.D. Vories, and J. Williams.

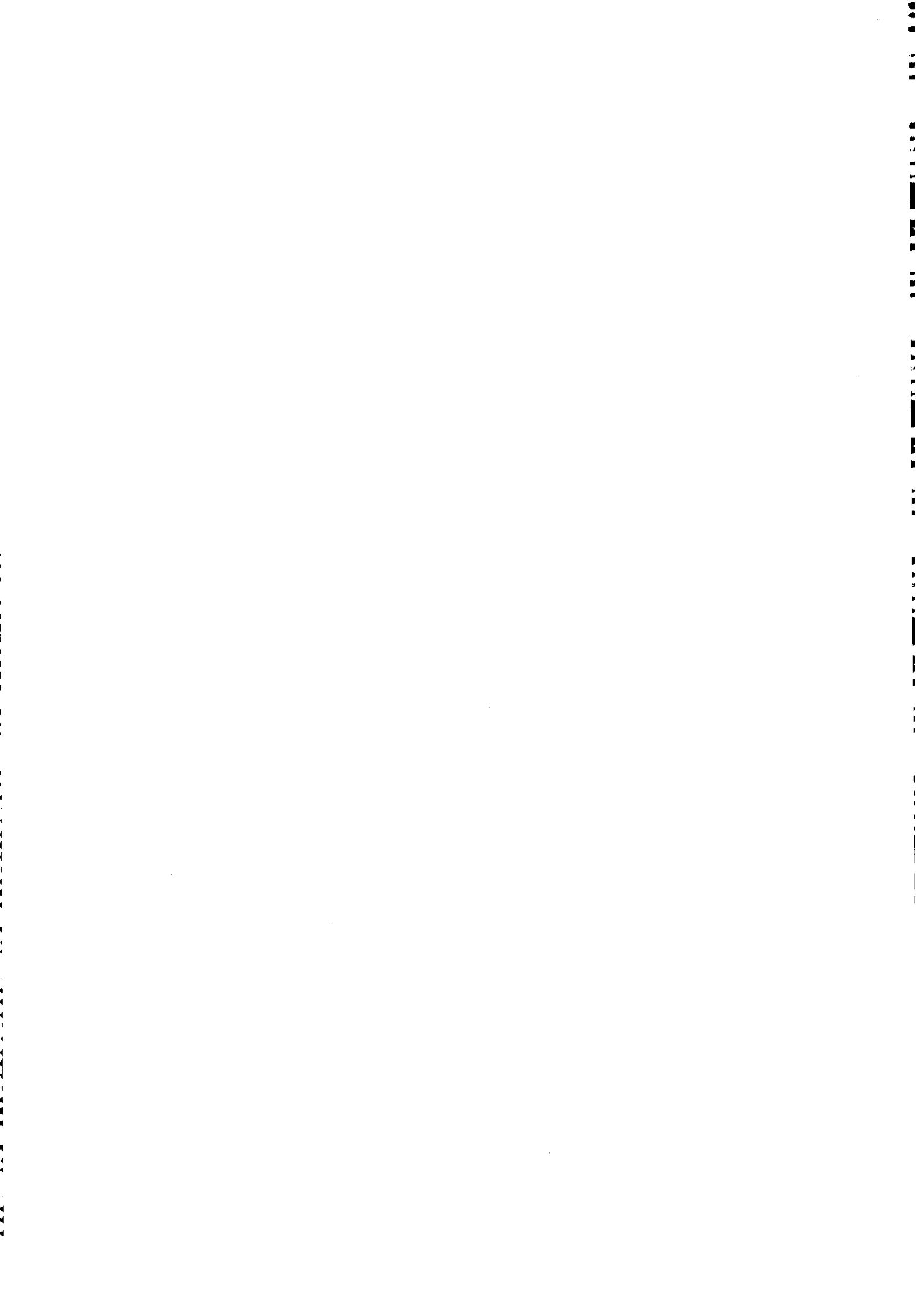
I would also like to recognize the contribution of the NRCS state and field offices and other individuals who participated in the WEPS validation studies.

Finally, acknowledgment is made of the many other individuals who have made this release of WEPS possible by reviewing this document and those who contributed through fundamental research on which many of the underlying concepts of WEPS are based.

Lawrence J. Hagen
WEPS Project Leader

WIND EROSION PREDICTION SYSTEM (WEPS)





WIND EROSION PREDICTION SYSTEM (WEPS)

L.J. Hagen, L.E. Wagner, and J. Tatarko

INTRODUCTION

The Wind Erosion Prediction System (WEPS) is a process-based, continuous, daily time-step model that simulates weather, field conditions, and erosion. It is intended to replace the predominately empirical Wind Erosion Equation (WEQ) (Woodruff and Siddoway, 1965) as a prediction tool for those who plan soil conservation systems or provide environmental planning and assessment. A listing of WEPS-related literature is given in Appendix AA.

OBJECTIVES

The objectives of this report are to summarize the structure of the WEPS model and to describe the design and modeling techniques.

THE SIMULATION REGION

In WEPS, the simulation region is a field or, at most, a few adjacent fields (Fig. I-1). Users must input the geometry of the simulation region and any subregions that have differing soil, management, or crop conditions. Users must also input initial conditions for the surface and four to ten layers. WEPS output is average soil loss/deposition over user-selected time intervals and accounting regions within the simulation region. Multiple and overlapping accounting regions can be selected by the user to obtain output averaged over various spatial scales in the simulation region. WEPS also has an option to provide users with individual soil loss components of creep-saltation and suspension soil-size fractions. The latter is particularly useful as an aid in estimating off-site impacts of wind erosion.

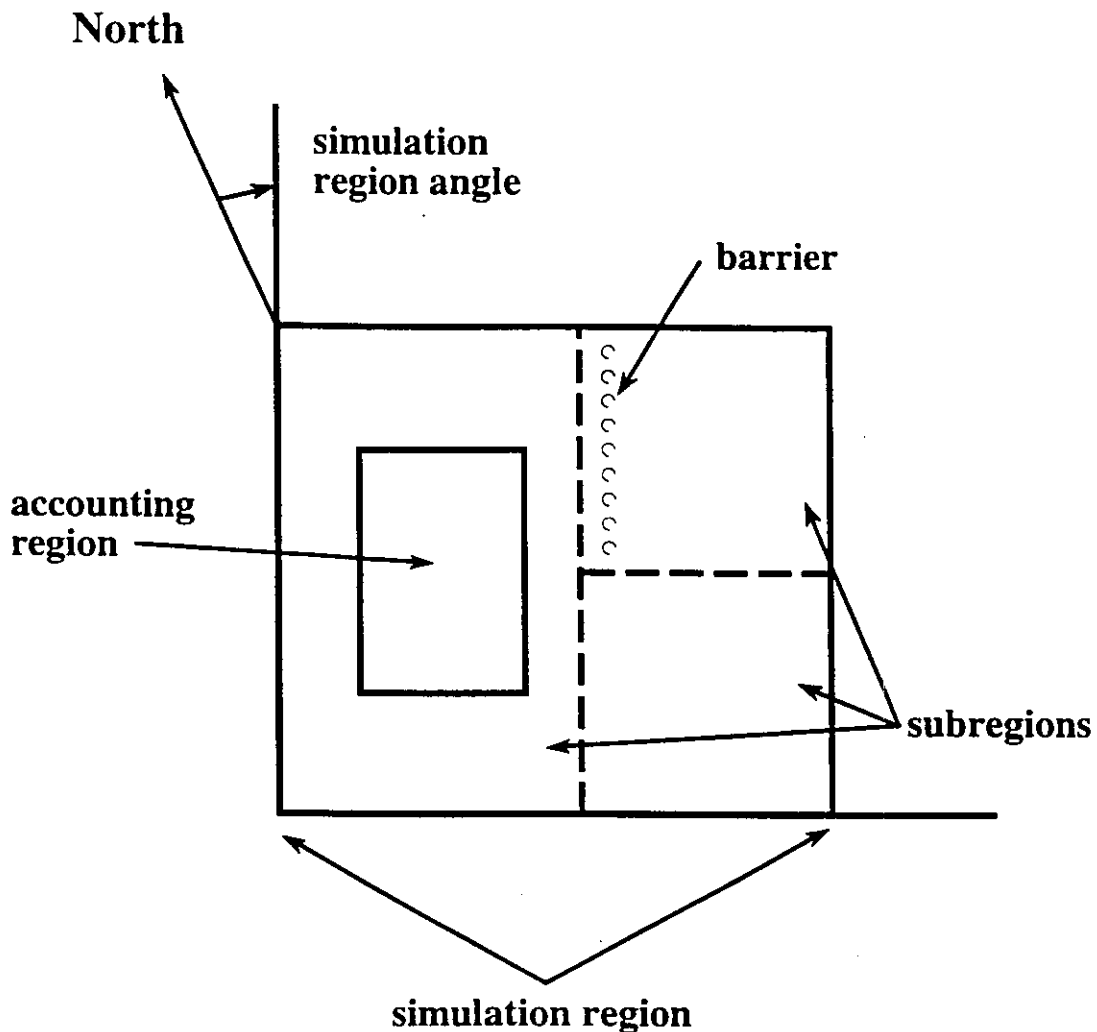


Figure I-1. WEPS simulation geometries.

SIMULATED PROCESSES

Soil erosion by wind is initiated when the wind speed exceeds the saltation threshold velocity for a given soil and biomass condition. After initiation, the duration and severity of an erosion event depends on the wind speed distribution and the evolution of the surface condition. Because WEPS is a continuous, daily, time-step model, it simulates not only the basic wind erosion processes, but also the processes that modify a soil's susceptibility to wind erosion.

The structure of WEPS is modular and consists of a user-interface, a MAIN (supervisory) routine, seven submodels, and four databases (Fig. I-2). The user-interface is used to create "input run" files using information from the data bases and the weather generator. In practical application, new "run" files usually will be created by editing default "run" files within the user-interface.

Most of the submodels within WEPS use daily weather as the natural driving force for the physical processes that change field conditions. The HYDROLOGY submodel accounts for changes in the temperature and water status of the soil. Changes in the soil properties between management events are simulated in the SOIL submodel. The growth of crop plants is simulated in the CROP submodel, and their decomposition is accounted for in the DECOMPOSITION submodel. Finally, the power of the wind on a subhourly basis is used to drive the EROSION submodel.

Step changes in the soil and biomass conditions are generated from typical management practices such as tillage, planting, harvesting, and irrigation. These events and their influence on the "state" of the system are grouped together by function and modeled within the MANAGEMENT submodel of WEPS.

MODEL DESIGN CONCEPTS

WEPS has a modular design, and each subroutine in WEPS is contained in a separate file. This allows individual components of the WEPS submodels to be easily maintained, modified, or replaced if necessary. This modular concept also enhances the possibility of future simulation models borrowing specific components from individual submodels in WEPS with little code modification. It also eases the task of any potential recoding into another programming language, if needed. Other WEPS design concepts are listed below.

Discrete Time and Discrete Space.

The time step is controlled by the main program. To reduce computation time, a daily time step is used in WEPS, except for selected subroutines in the HYDROLOGY and EROSION submodels, which use hourly or subhourly time steps. Submodels are called by MAIN in the order shown in Fig. I-2. Individual submodels control the sequence of calculations within each submodel. However, in MANAGEMENT, actions are simulated sequentially according to the order in which they appear in the management plan. When the last action listed in a management plan is performed, the plan is repeated again. Currently, management plans must cover at least a single year and may cover multiple years. The management plan can be initiated on any given day of the year, however the WEPS model simulation must begin when there is no growing crop. Only management plans covering discrete yearly intervals are allowed.

Wind Erosion Prediction System (WEPS)

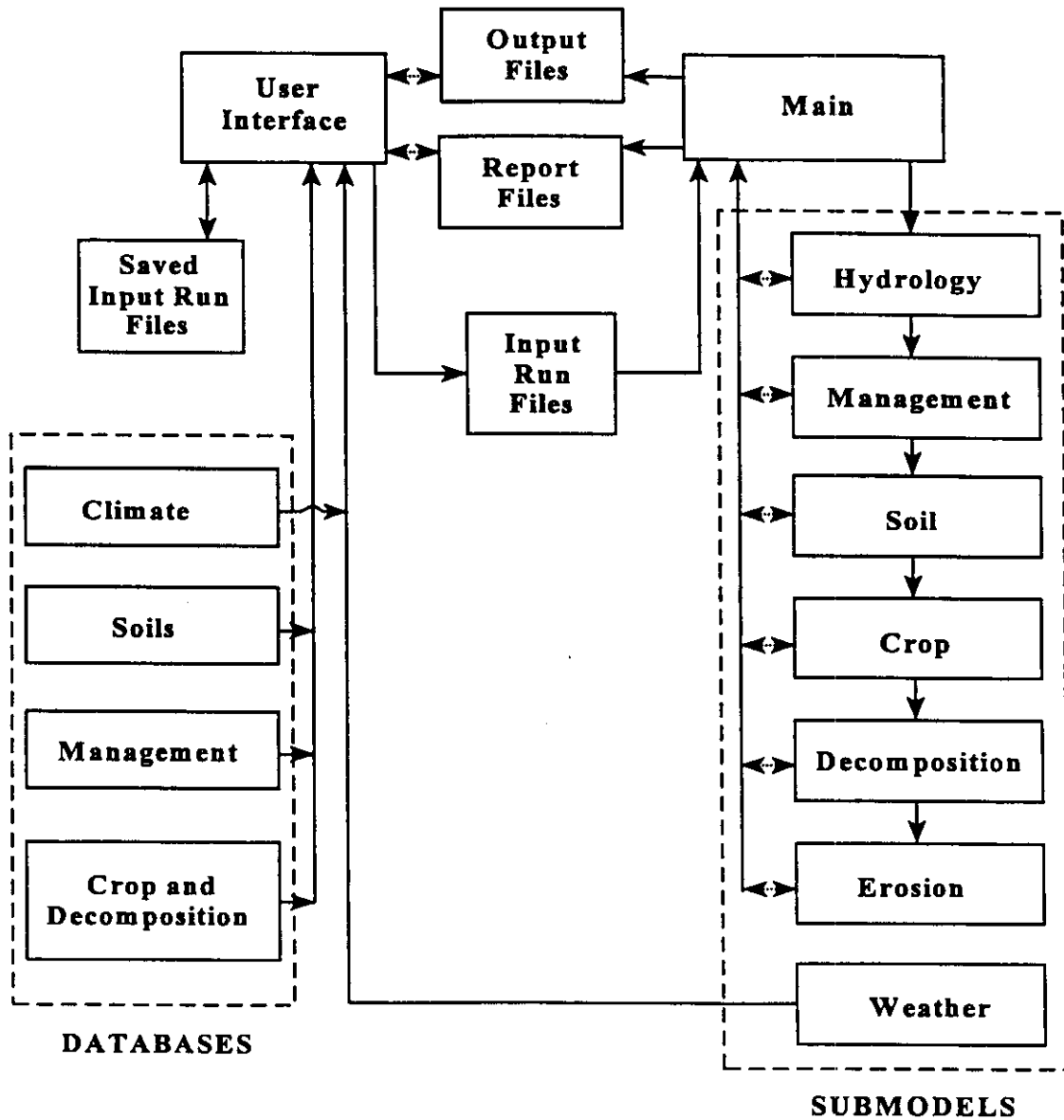


Figure I-2. Structure of the WEPS model.

The WEPS model simulates nonhomogeneous sites by partitioning them into homogeneous subregions and maintaining the individual subregion soil and biomass "states" independently. "Homogeneous" means that the soil type, biomass, and management are similar over a subregion. Therefore, the basic WEPS submodels (except EROSION) were developed so that individual submodels do not require information on how MAIN internally handles nonhomogeneous sites.

MODELING TECHNIQUES: WEPS compared to WEQ

Users of wind erosion prediction technology encounter a wide range of challenging environmental problems that require solutions. WEQ was unable to meet some of these needs. After extensive consultations with users, the WEPS structure was designed with the capabilities to meet the needs that were identified. As such, WEPS represents new technology and is not merely an improvement and recoding of WEQ technology. Also, WEPS is not a "research model" and contains numerous simplifications in order to maintain reasonable computation times. Most users of wind erosion prediction technology are familiar with WEQ. To facilitate understanding of WEPS modeling techniques, a brief comparison of WEPS and WEQ follows.

WEQ predicts soil loss for a single, uniform, isolated field. In contrast, WEPS provides capability to handle nonuniform areas and also "look inside" the simulation region to obtain predictions for specific areas of interest. In WEPS, spatial variation of the surface is input by describing a simulation region as series of subregions including subregions that are merely sinks (i.e. deposition regions for saltation/creep) such as a water body or drainage ditch. This treatment of spatial variability allows one to determine deposition in critical areas. It also allows one to simulate the interaction of areas with varying erosion rates on soil loss/deposition. For example, a region simulated in isolation may be a soil loss area, but simulated as interacting with other region may actually be a deposition area.

WEQ predicts erosion along line-transects across the field, while WEPS treats the field as two-dimensional. The WEPS EROSION submodel simulates soil loss/deposition at grid points over the entire simulation region. This feature allows users to "look inside" by specifying arbitrary accounting regions within the simulation region, and thus, obtain results averaged over grid points within the accounting region.

WEQ predicts only long-term, average soil loss. WEPS calculates on a daily basis and allows users to specify the output intervals. Thus, users can obtain outputs ranging from single storms to multiple years. By simulating for multiple years, the probability of various levels of erosion during any period of the year also can be determined.

The largest contrast between WEQ and WEPS technology occurs, because WEPS simulates a wide range of processes to describe field surface conditions and wind erosion. The WEQ depends on users to input correct estimates of the field surface conditions. Unfortunately, erosion does not vary linearly with residue cover and other temporal field conditions. Hence, simply specifying average field conditions as inputs will not likely yield the best estimates of long-term average erosion.

In WEQ there is no feedback loop which modifies the field in response to weather or erosion. In WEPS, the weather driving forces cause the field surface temporal properties to change. Thus, in a year with high rainfall, the field soil roughness may be reduced below average, while biomass production is above average. However, in a drought year biomass and aggregate size may be below average and erosion may fill ridges to reduce roughness.

The modeling techniques used to simulate processes in WEPS vary. The WEATHER submodel generates stochastic simulated weather variables. Mechanistic and statistical relations are generally used to represent processes in the other submodels. However, there was a structured design methodology. First, the major wind erosion processes such as emission, abrasion, trapping, etc. were identified. Next, the individual temporal soil and biomass properties that affect the wind erosion processes were selected. Then, WEPS submodels were designed to simulate the general processes that control both the surface temporal properties and the erosion processes. Finally, parameters from the databases were used to make the simulation of various processes unique for specific soil, crop, or management actions.

Where suitable simulation technology was already available in the literature, it was selected. Thus, the generalized crop growth simulation from EPIC was selected and modified for use in WEPS. Similarly, the stochastic weather generator used for WEPP is also used in WEPS, except for the simulation of winds.

IMPLEMENTATION

Implementation of the WEPS model has several requirements.

Software

The current WEPS model is coded in FORTRAN conforming to the ANSI FORTRAN 77 standard. All discussion of and reasons for this language choice are omitted here. The coding guidelines used are outlined in the "Water Erosion Prediction Project (WEPP) Fortran-77 Coding Convention" (Carey, et al., 1989). These guidelines contain a few minor modifications and additions for WEPS.

Hardware

The model can be run in both a DOS and Unix environment. Therefore, portability, size, and speed constraints are present in order for the model to work satisfactorily in both environments.

Operation

The operation of WEPS is fully documented in the WEPS Users Guide which is distributed with the WEPS program diskette set.

LIMITATIONS

The current version of WEPS is limited to fields growing a single crop at one time period. This limitation is imposed because the CROP submodel does not provide competition among different plant species. There are also limitations on the number of parameters available in the databases on soils, management operations, and crop species. The database parameters currently available are listed in the WEPS Users Guide.

At present, the climate database contains only statistics for 672 U.S. locations.

WEPS UPDATES

The WEPS model will be improved continually and updated periodically. The USDA-ARS Wind Erosion Research Unit (WERU) has established several means for others to obtain the latest release of the WEPS model, databases, documents, and other related information as they become available.

For users with Internet access, an anonymous FTP site is available for downloading the desired information. The FTP address is: *ftp.weru.ksu.edu*. Login is accomplished by entering "anonymous" at the "Name" prompt, and your E-mail address when asked for a "Password". This site contains readme files at each directory level which should help the user to locate the desired materials. WERU has also established a World Wide Web site. The WERU Home Page URL for this site is: *http://weru.ksu.edu*. This site contains all the information available by FTP as well as information about wind erosion research conducted at WERU. Specific WEPS information also can be obtained through E-Mail at *office@weru.ksu.edu*.

Users without Internet access can obtain WEPS update information by contacting:

USDA-ARS, NPA
Wind Erosion Research Unit
Throckmorton Hall
Kansas State University
Manhattan, KS 66506

Phone: (913) 532-6495
FAX: (913) 532-6528

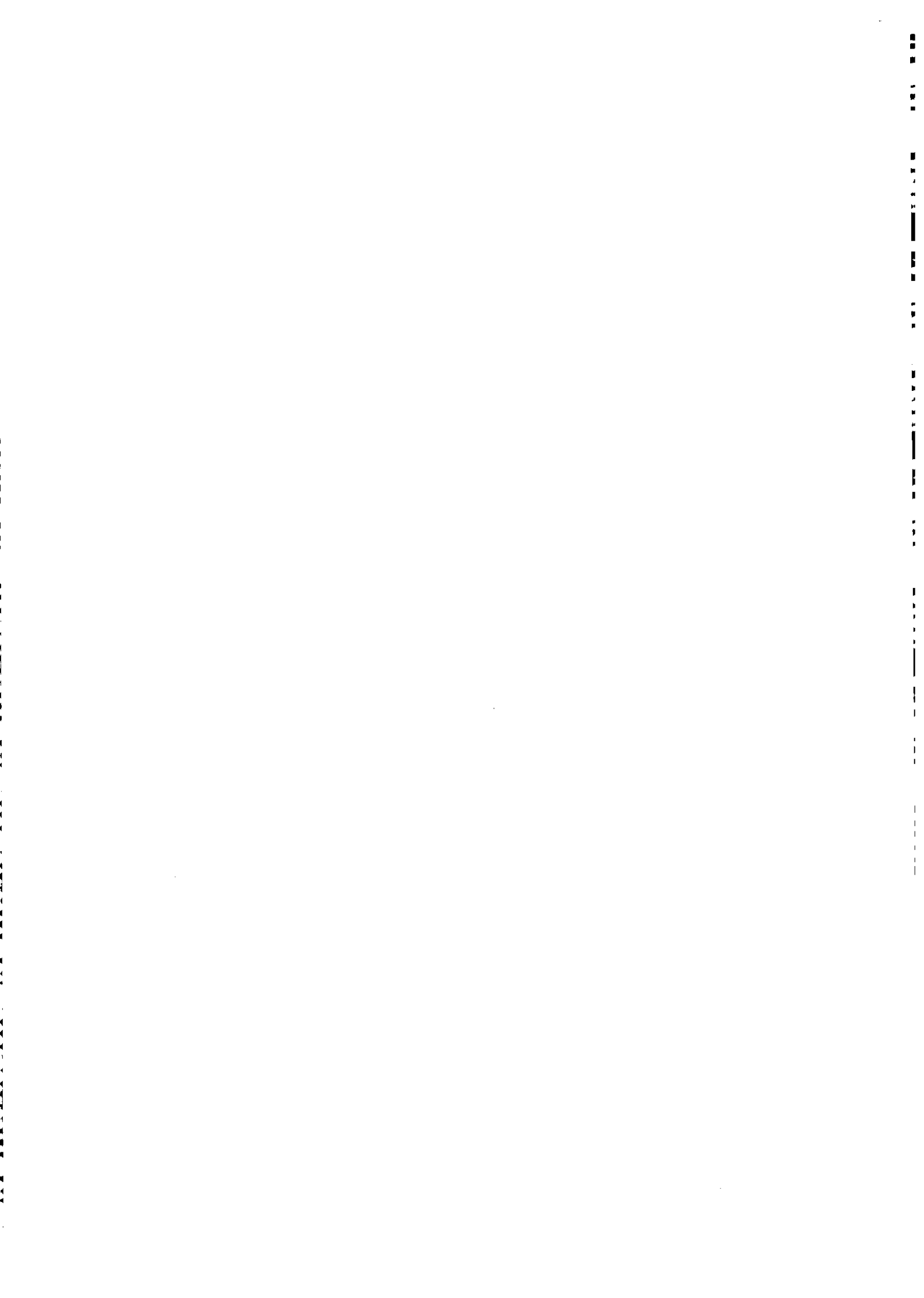
REFERENCES

Carey, W., T. Elledge, D. Flanagan, E. Night, O. Lee, C. Meyer, and P. Swetik. 1989. Water Erosion Prediction Project (WEPP) Fortran-77 coding convention. Draft.

Woodruff, N.P. and F.H. Siddoway. 1965. A wind erosion equation. Soil Sci. Soc. Am. Proc. 29(5):602-608.

MAIN PROGRAM





MAIN PROGRAM

John Tatarko

INTRODUCTION

The purpose of the MAIN program is to control the initialization and execution of the Wind Erosion Prediction System (WEPS). It calls subroutines that read the input data and outputs the general report. In addition, MAIN calls submodels on a daily timestep, which update the field conditions. If the maximum wind speed for the day exceeds a set value (i.e., 8 m/s), MAIN calculates subdaily (e.g., hourly) wind speed and then calls the EROSION submodel to simulate erosion processes. The current version of WEPS reads in the climate data produced by the WEATHER submodel; performs daily simulation of the hydrologic and soil conditions, crop growth, and residue decomposition; and accounts for management effects. Finally, the model determines soil erosion by wind for the desired simulation period.

PROGRAM DESCRIPTION

The current version of MAIN requires the following files for a WEPS simulation run: a) a simulation run file; b) initial field conditions file; d) a tillage/management file; and e) two climate files, one each in the CLIGEN and WINDGEN output formats, that provide climate data on a daily basis. The creation of these files for a WEPS simulation run and their contents are discussed in the WEPS Users Guide. A flowchart of the MAIN program operation is given in Fig. M-1.

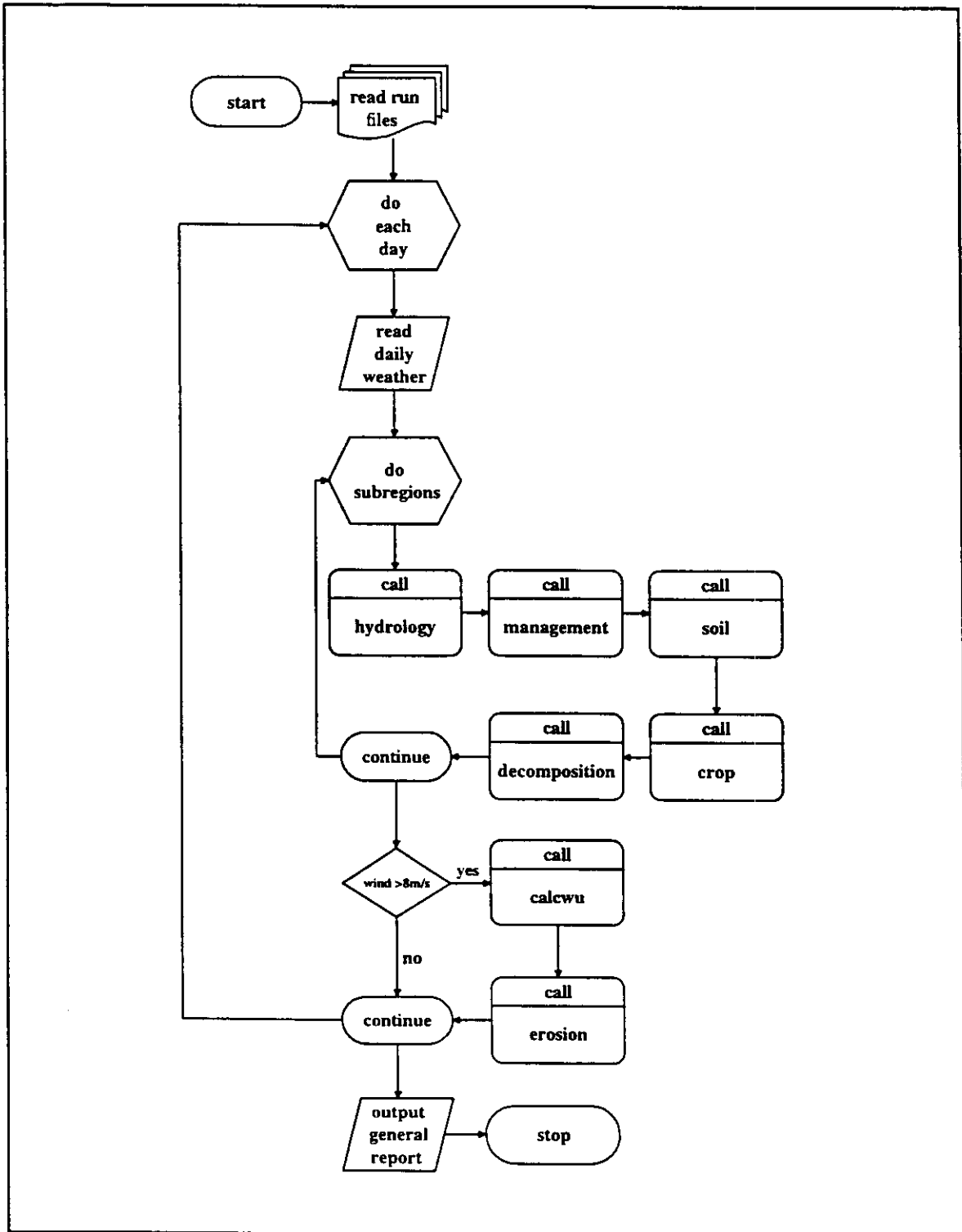


Figure M-1. Flowchart for MAIN program.

The MAIN program begins by initializing local variables and then calls the subroutine INPUT which reads the simulation run file and the initial field conditions file. The simulation then is executed as a daily loop that controls the counters for the current day and an embedded subregion loop. The model can perform any length of simulation on a daily time step and currently allows only one subregion (but up to four are anticipated). For each simulation day, the daily weather is read from the CLIGEN and WINDGEN data files. As some of the submodels are executed, summary information may be compiled for output. All submodels except EROSION are called within the subregion loop. Once field conditions are updated, if maximum wind speed for the day exceeds a set minimum (i.e., 8 m/s), a subdaily wind speed

distribution is read or generated. The EROSION submodel then is called to determine threshold conditions and compute soil erosion. Finally, the MAIN program calls subroutine GENREP, which outputs a series of user-selected output forms with general information about the simulation run.

WEPS was developed using Microsoft¹ FORTRAN, which conforms to the ANSI FORTRAN 77 standard. One known Microsoft extension to the ANSI standard used in WEPS. This extension is the use of \$INCLUDE statements. Communication between submodels is accomplished primarily through COMMON blocks that are contained in include files (i.e., *.inc). Each submodel as well as MAIN contain one or more \$INCLUDE statements, which cause FORTRAN to insert the contents of the specified text file (i.e., common blocks) into the source code at that location during compilation. For those who must use only the ANSI standard with no extensions, the "include files" must be inserted into the appropriate subroutines at the location of the \$INCLUDE statements. A description of WEPS variable naming conventions is given in Appendix BB.

MAIN VARIABLE, SUBROUTINE, AND FUNCTION LISTS AND DEFINITIONS

Local Variables

- am0*fl** These are switches for production of submodel output, where the asterisk represents the first letter of the submodel name.
- am0eif** This variable is an initialization flag for the EROSION submodel.
- am0ifl** This variable is an initialization flag that is set to .false. after the first simulation day.

¹ Trade names are for information only and do not constitute endorsement by the USDA.

ararea	This variable holds the accounting region area (m ²).
ccd	The current day of the CLIGEN file.
ccm	The current month of the CLIGEN file.
ccy	The current year of the CLIGEN file.
cflag	This logical variable controls output of warning messages for mismatch of CLIGEN and simulation dates.
cd	The current day of simulation month.
cm	The current month of simulation year.
cy	The current year of simulation run.
clifil	This variable holds the CLIGEN file name.
cwd	The current day of the WINDGEN file.
cwm	The current month of the WINDGEN file.
cwy	The current year of the WINDGEN file.
daysim	This variable holds the total current days of simulation.
diff	This variable holds the number of simulation days.
div	This variable holds the number of simulation days between screen output during execution.
header	Dummy variable to read in character values that are not used.
i	This variable is a counter for simulation loops.
id,im,iy	The initial day, month, and year of simulation.
ijday	This variable contains the initial Julian day of the simulation run.
isr	This variable holds the subregion index.
l	This variable is an index on soil layers.
lchar	This variable holds the character position in a string so as to ignore leading blanks in that string.
ld,lm,ly	The last day, month, and year of simulation.
line	This character variable is used to read the comment lines in the run files.
ljday	This variable contains the last Julian day of the simulation run.
nslay	The number of soil layers.
nsubr	This variable holds the total number of subregions.
runfil	This variable holds the simulation run input file name.
sarea	This variable holds the simulation region area.
series	This character variable holds the soil series name.
simout	This variable holds the simulation output file name.
sinfil	This character variable holds the initial field conditions file name.
srarea	This variable holds the subregion area.
subfil	This variable holds the subdaily wind information file name for use by subroutine 'calcwu'.
subflg	This logical variable is used to read header information in the subdaily wind file (if .true., read header).

WEPS**MAIN PROGRAM**

M-5

usrld	This character variable is an identification string to aid the user in identifying the simulation run.
usrloc	This character variable holds a location description of the simulation site.
usrnam	This character variable holds the user's name.
winfil	This variable holds the WINDGEN input file name.
wflag	This logical variable controls output of a warning message for mismatch of WINDGEN and simulation dates.
wcflag	This logical variable controls output of a warning message for mismatch of CLIGEN and WINDGEN dates.

Subroutines Called

CALCWU	This subroutine generates a subdaily wind speed distributions for the EROSION submodel. If real subdaily wind speed data exists they are used; if not, they are generated.
CALDAT	This subroutine converts Julian day to day, month, and year.
CDEBUG	This subroutine prints selected global variables immediately before and after the call to CROP.
CROP	This is a modified version of the EPIC crop growth model and calculates potential growth of leaves, stems, yield, and root components.
DDEBUG	This subroutine prints selected global variables immediately before and after the call to DECOMP.
DECOMP	The purpose of this model is to account for the biomass residues in the standing, flat, and buried categories.
EROSION	This is a simulation model to compute soil loss/deposition and make new estimates of the surface erodibility parameters.
GENREP	This subroutine controls the output of the general report file.
HDEBUG	This subroutine prints selected global variables immediately before and after the call to HYDRO.
HYDRO	This is a simulation model of the soil water and energy balance.

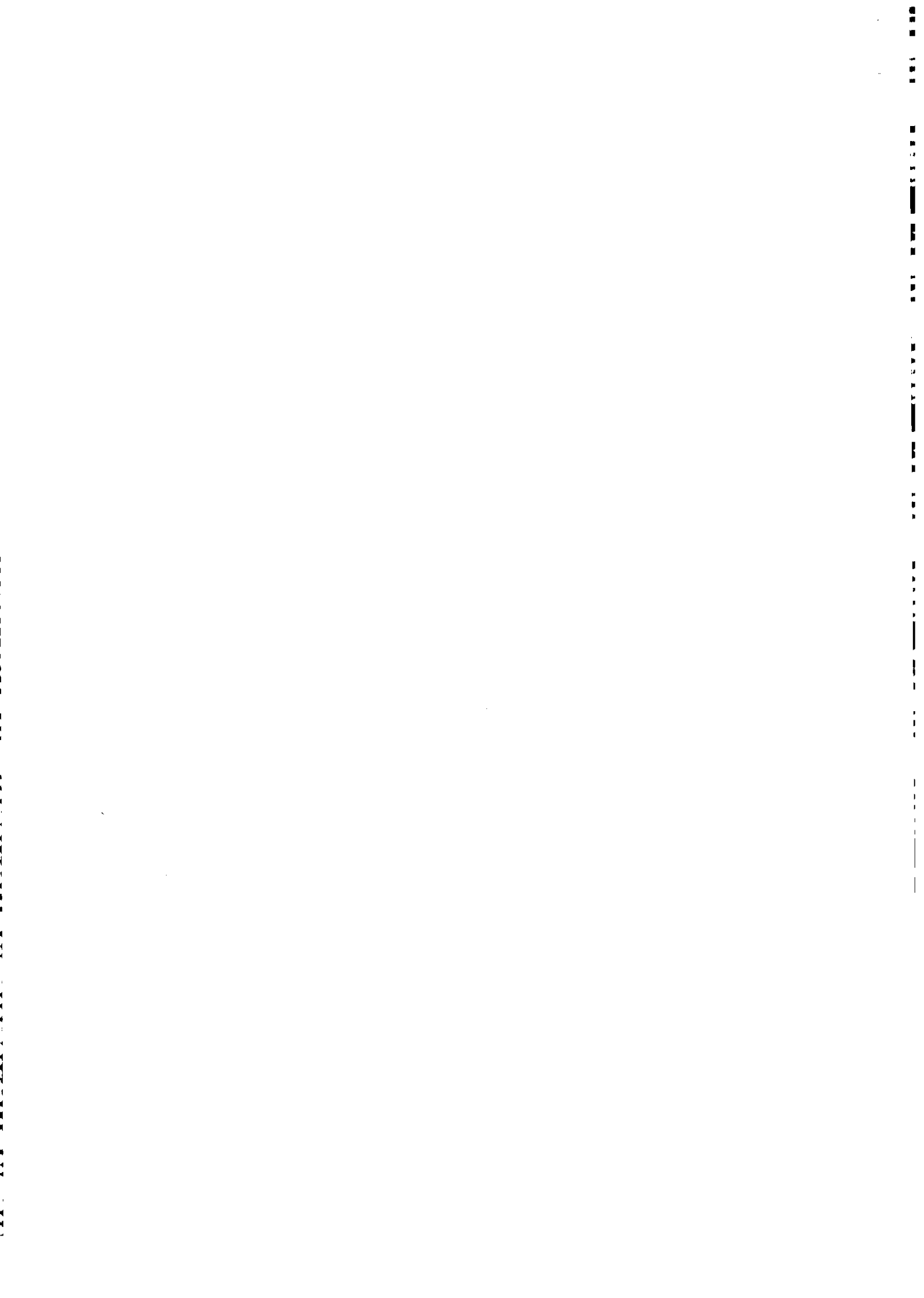
M-6	MAIN PROGRAM	WEPS
INPUT	This subroutine controls the input of the various run files. It performs some interactive error checking on these files.	
MANAGE	This is a model that assesses the effects of tillage on both temporal soil properties and surface configuration. It also simulates biomass manipulation resulting from tillage operations.	
MFINIT	This subroutine initializes MANAGE. It searches the management data file, marking the start sections of each subregion, while storing the number of years in each subregion's management cycle.	
SDEBUG	This subroutine prints selected global variables immediately before and after the call to SOIL.	
SOIL	This is a model that modifies the temporal soil profile properties as well as surface configuration between erosion and tillage events.	

Functions Called

JULDAY	This function determines the Julian date, given a day, month, and year.
LSTDAY	This function determines the last day of a given month for the given year.

WEATHER SUBMODEL





WEATHER SUBMODEL

John Tatarko, E.L. Skidmore, and L.E. Wagner

INTRODUCTION

The Wind Erosion Prediction System (WEPS) requires wind speed and direction in order to simulate the process of soil erosion by wind. These and other weather variables are also needed to drive temporal changes in hydrology, soil erodibility, crop growth, and residue decomposition in WEPS. The weather generator of WEPS consists of the programs WINDGEN and CLIGEN as well as a user interface and it is capable of simulating the needed weather variables on a daily basis and wind speed on a subdaily basis.

WINDGEN is the program that simulates wind speed and direction for WEPS (Skidmore and Tatarko, 1990; Wagner et al., 1992). It was developed specifically for use with WEPS and stochastically simulates wind direction and maximum and minimum wind speed on a daily basis. In addition, WINDGEN provides the hour at which the maximum wind speed occurs for each day based on historical records. Subdaily wind speeds are generated from within WEPS by the subroutine 'calcwu'.

CLIGEN is the weather generator developed for the Water Erosion Prediction Project (WEPP) family of erosion models (Nicks et al., 1987). It is used with WEPS to generate an average annual air temperature as well as daily precipitation, maximum and minimum temperature, solar radiation, and dew point temperature. Average daily air temperature and elevation for the site are used to calculate average daily air density within WEPS. CLIGEN will not be described in this document. However, those interested in CLIGEN and how it simulates these variables should consult the WEPP documentation (Nicks and Lane, 1989). Both CLIGEN and WINDGEN may be executed separately from the command line, or they may be executed together under a menu driven program called 'CLI_WIND'. This is a stand-alone program that allows the generation of weather output from CLIGEN and WINDGEN through a user-friendly menu-driven interface.

WINDGEN DEVELOPMENT

Prediction of wind speed and direction, like most meteorological variables, is extremely difficult. Even with advanced technology such as sophisticated numerical models and super computers, using climatological means is only as accurate as predicting meteorological variables a few days in advance (Tribbia and Anthes, 1987). Therefore, we resort to historical statistical information about most meteorological variables and use stochastic techniques to determine likelihood of various levels of those variables.

Various models have been used to describe wind speed distribution. A glance at a frequency versus wind speed histogram shows that the distribution is not best described by the familiar normal distribution. Distributions that have been used to describe wind speed include the one-parameter Rayleigh (Hennessey, 1977; Corotis et al., 1978), the two parameter gamma (Nicks and Lane, 1989), and the two-parameter Weibull (Takle and Brown, 1978; Corotis et al., 1978). The Weibull is undoubtedly the most widely used model of common wind behavior representing wind speed distributions.

We developed a stochastic wind simulator to furnish wind direction and wind speed as needed by the Wind Erosion Prediction System described by Hagen (1991).

Compact Database

One important requirement of a wind simulator for wind erosion modeling is to develop a compact database. Although described elsewhere (Skidmore and Tatarko, 1990, 1991), we give here some of the details of creating the compact database. Our database was created from historical monthly summaries of wind speed and wind direction contained in the extensive Wind Energy Resource Information System (WERIS) database at the National Climatic Data Center, Asheville, North Carolina (NCC TD 9793). The WERIS database is described further in Appendix C of Elliot et al. (1986). Data were extracted from WERIS tables and, in some cases, analyzed further to create a database suitable for our needs.

We used data from WERIS Table 12 A-L, joint wind speed/direction frequency by month (e.g., Table W-1), to calculate scale and shape parameters of the Weibull distribution function for each of the 16 cardinal wind directions by month.

The cumulative Weibull distribution function $F(u)$ and the probability density function $f(u)$ are defined by:

$$F(u) = 1 - \exp[-(u/c)^k] \quad (1)$$

and

$$f(u) = dF(u)/du = (k/c)(u/c)^{k-1} \exp[-(u/c)^k] \tag{2}$$

where u is wind speed, c is scale parameter (units of velocity), and k is shape parameter (dimensionless) (Apt, 1976). Because anemometer heights varied from location to location, all wind speeds (e.g., Column 1, Table W-1) were adjusted to a 10 m reference height according to the following:

$$u_2 = u_1(z_2/z_1)^{1/7} \tag{3}$$

where u1 and u2 are wind speeds at heights z1 and z2, respectively (Elliot, 1979).

Table W-1. Monthly joint wind speed/direction frequency values.

Wind Speed (m/s)	Wind Direction																	Total	
	N	NNE	NE	ENE	E	ESE	SE	SSE	S	SSW	SW	WSW	W	WNW	NW	NNW	Calm		
Calm	.0	.0	.0	.0	.0	.0	.0	.0	.0	.0	.0	.0	.0	.0	.0	.0	.0	1.7	1.7
1	.0	.0	.0	.0	.0	.0	.0	.0	.0	.0	.0	.0	.0	.0	.0	.0	.0	.0	.0
2	.3	.1	.1	.0	.1	.1	.2	.1	.3	.1	.5	.5	.6	.4	.5	.2	.0	.0	4.1
3	.7	.3	.5	.4	.9	.4	.6	.5	.9	.4	1.1	1.1	1.5	.8	.7	.3	.0	.0	11.1
4	1.0	.6	.8	.4	1.1	.9	1.0	.8	1.9	.6	.8	1.2	1.6	1.2	.7	.5	.0	.0	15.1
5	.9	.6	.8	.5	.9	.9	1.0	1.3	2.1	.9	1.2	1.2	1.6	.5	.4	.5	.0	.0	15.4
6	.7	.7	.6	.4	.6	.5	.9	.6	1.6	1.0	1.1	1.2	.7	.6	.3	.5	.0	.0	12.2
7	1.0	.6	.6	.4	.2	.5	.4	.5	1.6	1.0	1.4	.8	.7	.5	.3	.2	.0	.0	10.0
8	1.0	.6	.8	.2	.5	.3	.6	.3	1.4	1.2	1.0	.6	.7	.4	.4	.2	.0	.0	10.1
9	.8	.4	.6	.2	.3	.1	.2	.4	1.0	.8	.7	.6	.6	.4	.2	.3	.0	.0	7.6
10	.3	.4	.2	.2	.1	.0	.1	.2	.8	.4	.2	.3	.4	.3	.1	.1	.0	.0	4.3
11	.3	.4	.1	.1	.0	.0	.1	.1	.5	.2	.3	.3	.5	.1	.1	.1	.0	.0	3.1
12	.2	.1	.0	.0	.0	.0	.0	.0	.1	.0	.1	.1	.2	.4	.1	.1	.0	.0	1.6
13	.2	.1	.0	.0	.0	.0	.0	.0	.0	.8	.2	.1	.3	.2	.1	.1	.0	.0	1.3
14	.1	.0	.0	.0	.0	.0	.0	.0	.0	.0	.1	.1	.2	.1	.1	.0	.0	.0	.7
15	.1	.0	.0	.0	.0	.0	.0	.0	.0	.0	.1	.1	.0	.0	.0	.0	.0	.0	.5
16	.0	.0	.0	.0	.0	.0	.0	.0	.0	.0	.0	.1	.1	.0	.0	.0	.0	.0	.2
17	.0	.0	.0	.0	.0	.0	.0	.0	.0	.0	.0	.0	.1	.0	.0	.0	.0	.0	.1
18	.0	.0	.0	.0	.0	.0	.0	.0	.0	.0	.0	.0	.0	.0	.0	.0	.0	.0	.1
19	.0	.0	.0	.0	.0	.0	.0	.0	.0	.0	.0	.0	.0	.0	.0	.0	.0	.0	.1
20	.0	.0	.0	.0	.0	.0	.0	.0	.0	.0	.0	.0	.0	.0	.0	.0	.0	.0	.0
21-25	.0	.0	.0	.0	.0	.0	.0	.0	.0	.0	.0	.0	.0	.0	.0	.0	.0	.0	.0
26-30	.0	.0	.0	.0	.0	.0	.0	.0	.0	.0	.0	.0	.0	.0	.0	.0	.0	.0	.0
31-35	.0	.0	.0	.0	.0	.0	.0	.0	.0	.0	.0	.0	.0	.0	.0	.0	.0	.0	.0
36-40	.0	.0	.0	.0	.0	.0	.0	.0	.0	.0	.0	.0	.0	.0	.0	.0	.0	.0	.0
41-up	.0	.0	.0	.0	.0	.0	.0	.0	.0	.0	.0	.0	.0	.0	.0	.0	.0	.0	.0
Total	7.8	4.8	5.1	2.9	4.9	3.8	5.1	4.9	12.2	6.8	8.9	8.5	9.9	5.7	4.0	3.0	1.7	100.0	
Avg	6.9	7.0	6.1	6.0	5.1	5.2	5.5	5.9	6.2	6.7	6.4	6.2	6.4	6.2	5.6	6.3	.0	6.1	

Table 12c of WERIS for March, Lubbock, TX

The calm periods were eliminated, and the frequency of wind in each speed group was normalized to give a total of 1.0 for each of the 16 cardinal directions. Thus,

W-4

WEATHER SUBMODEL

WEPS

$$F_1(u) = [(F(u) - F_0)/(1 - F_0)] = 1 - \exp[-(u/c)^k] \quad (4)$$

where $F_1(u)$ is the cumulative distribution with the calm periods eliminated, and F_0 is the frequency of the calm periods. The scale and shape parameters were calculated by the method of least squares applied to the cumulative distribution function (Eqn. [W-4]). Equation [W-4] was rewritten as:

$$1 - F_1(u) = \exp[-(u/c)^k] \quad (5)$$

Then by taking the logarithm twice, this becomes:

$$\ln[-\ln(1 - F_1(u))] = -k \ln c + k \ln u \quad (6)$$

If we let $y = \ln[-\ln(1 - F_1(u))]$, $a = -k \ln c$, $b = k$, and $x = \ln u$, Equation [W-6] may be rewritten as:

$$y = a + bx \quad (7)$$

$F_1(u)$ was calculated from information in tables like Table W-1 for each wind speed group to determine y and x in Equation [W-7]. This gave the information needed to use a standard method of least squares to determine the Weibull scale and shape parameters. To recover the real distribution, we can rewrite Equation [W-4] as:

$$F_1(u) = F_0 + (1 - F_0)(1 - \exp[-(u/c)^k]) \quad (8)$$

Wind direction distribution for each location was summarized by month from the "TOTAL" row near the bottom of Table W-1 for each location.

Other pertinent data, obtained from the Wind Energy Resource Atlas of the United States (Elliot et al., 1986), included latitude, longitude, city, state, location name, Weather Bureau Army Navy (WBAN) number, agency responsible for the weather station, period of record, anemometer height and location, and number of observations per 24-hour period.

We eliminated WERIS sites from our database if they represented less than 5 years of data, the anemometer height was not known, or fewer than 8 observations were taken per day. Where more than one satisfactory observation period/site remained in a metropolis, we picked the site with the best combination of the following: (1) maximum number of hours per day observations were taken, (2) longest period of record, (3) 1 hourly versus 3 hourly observations, and (4) best location of anemometer (ground mast > beacon tower > roof top > unknown location). The WINDGEN database currently consists of statistical parameters for 672 locations in the United States.

WEPS

WEATHER SUBMODEL

W-5

From WERIS Table 5, we obtained a ratio of maximum/minimum mean hourly wind speed and hour of maximum wind speed by month (e.g., Table W-2). Tables W-2, W-3, W-4, and W-5 give examples of wind information we compiled into a compact database.

Table W-2. Ratio of maximum to minimum hourly wind speed (max/min) and hour of maximum wind speed.

	Month											
	1	2	3	4	5	6	7	8	9	10	11	12
max/min	1.5	1.5	1.6	1.6	1.6	1.6	1.6	1.7	1.5	1.6	1.6	1.5
hour max	15	12	15	15	18	18	18	15	15	15	12	15

Values from WERIS Table 5 for Lubbock, TX (Skidmore and Tatarko, 1991) where Month 1 = January.

Table W-3. Wind direction distribution by month in percent.

Wind Direction	Month											
	1	2	3	4	5	6	7	8	9	10	11	12
1	8.2	9.7	7.8	5.5	5.3	3.1	2.3	2.9	5.9	6.3	8.8	9.0
2	5.0	4.9	4.8	3.6	3.7	2.2	1.5	2.6	4.8	5.0	4.4	4.8
3	5.0	5.9	5.1	4.1	4.1	3.2	3.9	4.2	6.3	5.3	4.8	4.7
4	3.8	4.2	2.9	4.5	4.8	4.1	3.8	4.7	4.9	4.1	3.1	3.1
5	4.0	4.3	4.9	5.3	5.9	5.0	5.9	6.7	6.3	4.3	4.4	2.2
6	3.1	3.8	3.8	4.7	6.6	6.1	5.7	6.3	5.7	3.0	3.2	1.9
7	3.3	3.8	5.1	6.5	10.5	10.4	10.0	9.7	7.5	4.2	3.4	2.1
8	2.9	3.3	4.9	4.9	8.3	9.5	11.6	14.9	13.6	9.0	5.4	3.7
9	9.8	8.7	12.2	16.4	16.4	26.8	27.4	24.1	18.6	19.7	11.7	9.4
10	6.0	5.7	6.8	6.5	6.9	9.2	8.8	7.2	7.9	9.6	7.5	7.4
11	9.6	8.5	8.9	7.7	7.3	5.9	5.9	5.1	6.2	8.2	9.9	10.1
12	9.6	9.3	8.5	7.9	4.7	3.4	2.4	2.8	3.5	6.0	9.0	9.8
13	12.3	10.8	9.9	6.7	5.1	3.3	2.0	1.7	3.5	6.1	9.0	11.8
14	6.3	6.2	5.7	4.6	3.0	1.5	1.0	1.1	1.7	3.2	5.1	7.7
15	4.7	4.9	4.0	3.4	2.6	1.6	0.8	1.1	2.0	3.0	4.3	5.3
16	3.8	3.4	3.0	3.0	1.8	1.1	0.6	1.1	2.1	2.9	3.0	4.0
17	2.7	2.7	1.7	1.4	1.8	1.5	3.1	5.0	4.0	3.6	4.8	4.3

Directions are clockwise with 1 = north and Month 1 = January. Direction 17 represents calm periods. Values for Lubbock, TX (Skidmore and Tatarko, 1991).

Table W-4. Weibull shape parameters by month and direction.

Wind Direction	Month											
	1	2	3	4	5	6	7	8	9	10	11	12
1	2.5	2.5	2.7	2.6	2.8	2.3	2.2	2.6	2.3	2.5	2.7	2.7
2	2.8	2.4	3.2	2.9	2.8	2.7	3.2	2.3	3.1	2.8	2.7	2.6
3	2.8	3.1	3.3	2.8	2.7	2.9	2.8	3.3	3.2	3.3	3.0	3.2
4	3.9	3.4	3.0	3.5	3.0	2.6	2.8	2.9	3.2	3.1	2.7	3.2
5	3.1	3.2	3.3	2.9	3.0	3.4	3.1	3.2	3.3	3.0	3.6	2.8
6	3.4	3.6	3.9	3.3	3.6	4.4	3.7	3.9	3.3	3.5	3.6	5.1
7	3.7	3.3	3.3	3.3	3.4	3.6	3.5	3.5	3.9	4.1	3.6	5.4
8	3.2	4.1	3.3	3.5	3.3	3.5	3.8	3.7	3.5	2.9	3.0	4.5
9	2.9	3.2	3.6	3.3	3.3	3.7	3.7	3.7	3.4	3.3	3.3	3.2
10	3.1	3.5	3.7	3.7	3.2	3.5	3.9	3.6	4.0	3.2	3.5	3.2
11	3.4	3.2	2.7	3.2	3.2	3.0	3.5	3.0	3.4	3.0	3.2	3.2
12	2.5	2.6	2.5	2.4	2.5	2.9	3.4	3.6	3.0	2.7	2.6	2.6
13	2.1	2.4	2.2	2.5	2.6	2.2	3.3	3.1	3.0	2.4	2.2	2.2
14	2.1	2.2	2.3	2.5	2.4	3.6	4.1	3.5	2.6	2.4	1.8	2.0
15	2.4	2.6	2.2	2.5	2.5	3.1	3.3	2.9	2.9	2.0	2.2	2.3
16	2.2	2.6	2.7	2.3	2.8	3.3	2.6	3.5	2.5	2.1	2.4	2.4
17	2.6	2.6	2.7	2.9	3.0	3.1	3.3	3.2	3.0	2.7	2.6	2.6

The directions are clockwise starting with 1=north. Direction 17 is for total wind. Values are for Lubbock, TX (Skidmore and Tatar, 1991).

Table W-5. Weibull scale parameters by month and direction in m/s.

Wind Direction	Month											
	1	2	3	4	5	6	7	8	9	10	11	12
1	8.0	8.2	8.8	8.3	8.0	7.6	5.8	5.0	6.4	7.5	7.5	7.9
2	8.2	9.2	9.0	8.6	8.3	7.6	6.0	5.7	7.3	7.5	6.7	8.1
3	6.6	7.8	8.0	8.3	7.9	7.2	5.8	5.8	5.9	7.0	6.5	6.8
4	6.5	6.5	7.8	6.9	7.3	6.3	5.9	5.2	5.3	6.2	5.7	6.3
5	6.0	6.3	6.7	6.4	6.6	6.3	5.2	4.8	4.6	5.2	5.0	5.0
6	5.3	6.4	6.8	7.1	7.1	6.2	5.3	5.0	5.2	5.1	5.1	4.2
7	5.5	6.4	7.2	7.2	7.4	6.8	6.0	5.5	5.5	5.3	4.8	5.2
8	5.9	6.1	7.5	8.5	8.0	7.5	6.3	5.8	5.9	6.2	5.8	5.2
9	6.2	7.0	7.9	8.5	8.1	8.0	6.8	6.5	6.5	6.6	6.2	6.5
10	7.2	7.2	8.7	8.5	8.1	7.7	6.9	6.5	6.9	6.9	6.9	7.4
11	7.3	7.6	8.2	8.4	7.6	6.9	6.1	5.9	6.1	6.2	6.5	6.9
12	6.5	7.0	8.0	8.6	7.8	7.0	5.4	5.0	5.2	5.9	6.4	6.0
13	6.7	6.8	8.3	8.8	7.2	6.4	4.9	4.4	5.3	5.1	6.3	6.4
14	7.1	7.2	7.8	8.1	7.0	5.6	4.3	4.2	4.6	5.1	6.0	6.9
15	6.1	6.1	7.2	7.2	7.1	5.3	4.6	4.5	4.4	4.9	6.4	6.5
16	7.1	7.7	7.7	8.3	6.6	5.7	4.8	3.9	4.9	6.4	7.1	7.2
17	6.8	7.3	8.1	8.2	7.7	7.3	6.3	5.8	5.9	6.3	6.4	6.7

Directions are clockwise starting with 1=north. Direction 17 is for total wind. Values for Lubbock, TX. Wind speed adjusted to height of 10 meters (Skidmore and Tatarko, 1991).

The following few paragraphs outline procedures to access the compact database and how it is used to simulate wind direction and wind speed. The actual implementation of these

procedures is accomplished through either a user-friendly interface or command line implemented computer programs (see WEPS Users Guide).

Determination of Wind Direction

Read the wind direction distribution array for the specified month (Table W-3). Calculate the cumulative wind direction distribution so that it ranges from 0.0 to 1.0. Draw a random number, RN, where $0.0 < RN < 1.0$, and compare it with the cumulative wind direction distribution. If the random number is equal to or less than the probability of the wind being from the north (i.e., direction = 1, Table W-3), then the simulated wind direction is north. If the random number is greater than the cumulative probability of the wind being from the north and equal to or less than the probability of the wind being from the north northeast, then the simulated wind direction is north northeast and so on. If the random number is greater than the cumulative probability of the wind being from all of the 16 cardinal directions, then the simulated wind is calm.

Determination of Wind Speed

Once wind direction is simulated, access the database to determine the Weibull scale, c (Table W-4), and shape, k (Table W-5), parameters for that direction and the month under consideration in preparation for the next step.

Rearrange Equation [W-8] to make wind speed, u , the dependent variable:

$$u = c \{-\ln[1 - (F(u) - F_0)/(1 - F_0)]\}^{1/k} \quad (9)$$

Draw a random number, $0.0 < RN < 1.0$, assign its value to $F(u)$, and subtract from it the frequency of calm periods, F_0 . If $F(u) < F_0$, then u is calm. In the rare case that $F(u) = 1.0$, the argument of \ln in Equation [W-9] is zero and does not compute. Therefore, if $F(u) > 0.999$, let $F(u) = 0.999$. Otherwise, calculate u from Equation [W-9] for $F_0 < F(u) < 0.999$ to determine a period simulated wind speed. If the period is 1 day, then u represents simulated daily mean wind speed.

Subdaily wind speeds in WEPS will be calculated whenever the maximum wind speed for the day exceeds a set erosion threshold (i.e., default is 8 m/s). To compute subdaily wind speeds, consider a diurnal variation. We present an example of hourly wind speeds, but shorter or longer periods are permitted in WEPS.

Read from the wind database the ratio of maximum to minimum mean hourly wind speed and the hour of maximum wind speed for the location and month under consideration. Calculate the maximum and minimum wind speed for the day based on the representative wind speed as calculated above and given the ratio of maximum to minimum wind speed:

W-8

WEATHER SUBMODEL

WEPS

$$urep = (umax + umin) / 2 \quad (10)$$

$$uratio = umax / umin \quad (11)$$

where *urep* is the daily mean representative wind speed as calculated from Equation [W-9], *uratio* is the ratio of daily maximum, *umax*, to daily minimum, *umin*, wind speed. Solving Equations [W-10] and [W-11] for *umax* and *umin* gives:

$$umax = 2 uratio urep / (1 + uratio) \quad (12)$$

$$umin = umax / uratio \quad (13)$$

therefore, wind speed for any hour of the day *u(I)* can be simulated from:

$$u(I) = urep + 0.5(umax - umin) \cos[2 \pi(24 - hrmax + I) / 24] \quad (14)$$

where *hrmax* is the hour of the day when wind speed is maximum; *I* is index for hour of day, and the other variables are as previously defined.

SUBROUTINE CALCWU

When daily maximum wind speed is above the erosion threshold, WEPS must be capable of simulating wind speeds on a subdaily basis. This threshold depends on surface conditions of the simulated field. The MAIN program tests for a maximum daily wind speed in excess of a set speed (i.e., 8 m/s). If winds are less than or equal to this value, subdaily wind speeds are not generated. If the maximum wind speed is greater than 8 m/s, subroutine 'calcwu' is called to provide the subdaily wind speed distribution using Equation W-14. If real subdaily wind speeds are available, they may be read from a file by subroutine 'calcwu' as described in the WEPS Users Guide. Once sub-daily wind speeds are generated or read, the EROSION submodel then will determine if threshold conditions are suitable for erosion to occur. A flow chart for subroutine 'calcwu' is shown in Fig. W-1.

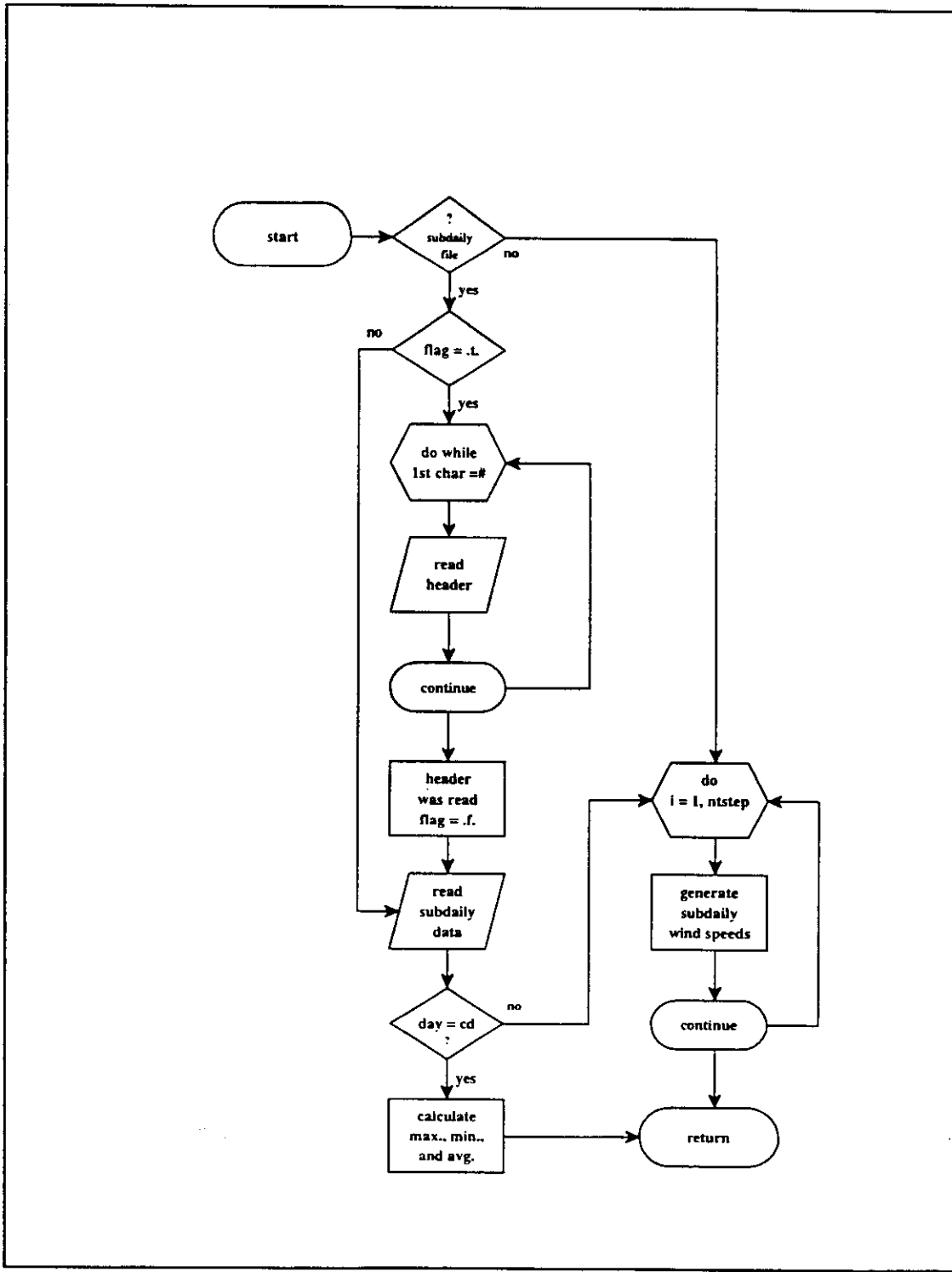


Figure W-1. Flowchart for subdaily wind subroutine 'calcwu'.

The number of time steps used for subdaily wind speeds is user specified (default is 24 one hour steps) within the simulation run file as described in the WEPS Users Guide.

CLI_WIND PROGRAM

CLI_WIND is a stand-alone, menu-driven computer program to generate weather output. The program's main menu allows the user to select for CLIGEN or WINDGEN or both, enter the site selection menu, generate the desired data, modify CLI_WIND configurations, or exit the program. Within the site-selection menu, the user is allowed to change default settings for the database and output file names as well as a random seed number. The user must then select the site for the simulated weather. This site must be within a user-specified distance range from the WEPS simulation site. If no sites within the given distance range are present in the database, the user is prompted for an expanded search range. The user also has the option of selecting output header information, the starting year, as well as the number of years of simulation.

OUTPUT FILE

We illustrate the output of a simulation from WINDGEN in Fig. W-3. These simulations were generated by accessing data from the WEPS database (i.e., Tables W-2, W-3, W-4, and W-5) and performing the operations described previously.

SUMMARY

The weather generator for WEPS consists of statistical databases derived from historical weather records and computer programs to simulate wind direction and speed as well as other climatic variables on a daily basis. It also has the capability of simulating subdaily wind speeds. This weather generator was developed by the US Department of Agriculture-Agricultural Research Service and is suitable for simulating daily data as required by WEPS.

WINDGEN \$Revision: 1.1 \$						
day	mo	year	dir	umax	umin	hrmax
1	1	1985	225.0	5.8	4.1	12.0
2	1	1985	315.0	11.3	8.1	12.0
3	1	1985	112.5	7.5	5.3	12.0
4	1	1985	337.5	2.0	1.4	12.0
5	1	1985	180.0	3.4	2.4	12.0
.
.
30	1	1985	292.5	9.8	7.0	12.0
31	1	1985	247.5	5.2	3.7	12.0
1	2	1985	157.5	7.4	5.3	12.0
2	2	1985	270.0	7.2	5.2	12.0
3	2	1985	247.5	5.3	3.8	12.0
.
.
.

Figure W-3. Example of WINDGEN output where day, mo, and year are the day, month, and year of simulation; dir is the wind direction in degrees from North; umax and umin are maximum and minimum wind speed for the day; and hrmax is the hour at which the wind speed is maximum.

WEPS

WEATHER SUBMODEL

W-13

LIST OF SYMBOLS

<u>Symbol</u>	<u>Description</u>	<u>Unit</u>
a	represents $(-k \ln c)$ in regression equation (Eqn. [W-7])	$m s^{-1}$
b	represents (k) in regression equation (Eqn. [W-7])	-
c	Weibull distribution scale parameter	$m s^{-1}$
$f(u)$	probability density function	-
$F(u)$	cumulative Weibull distribution function	-
$F_1(u)$	cumulative distribution of winds with calm eliminated	-
F_0	frequency of the calm periods	-
hrmax	hour of the day when wind speed is at maximum	-
k	Weibull distribution shape parameter	-
u	wind speed	$m s^{-1}$
u_1	wind speed at height z_1 used in Eqn. [W-3]	$m s^{-1}$
u_2	wind speed at height z_2 used in Eqn. [W-3]	$m s^{-1}$
$u(I)$	wind speed at time I	$m s^{-1}$
umax	daily maximum wind speed	$m s^{-1}$
umin	daily minimum wind speed	$m s^{-1}$
uratio	ratio of daily maximum to daily minimum wind speed	-
urep	daily mean representative wind speed	$m s^{-1}$
x	represents $(\ln u)$ in regression equation (Eqn. [W-7])	$m s^{-1}$
y	represents $(\ln [-\ln(1-F_1(u))])$ in regression equation (Eqn. [W-7])	$m s^{-1}$
z_1	height associated with u_1 in Eqn. [W-3]	m
z_2	height associated with u_2 in Eqn. [W-3]	m

LITERATURE CITED

- Apt, K.E. 1976. Applicability of the Weibull distribution to atmospheric radioactivity data. *Atmospheric Envir.* 10:777-782.
- Corotis, R.B., A.B. Sigl, and J. Klein. 1978. Probability models of wind velocity magnitude and persistence. *Sol. Energy* 20:483-493.
- Elliot, D.L. 1979. Adjustment and analysis of data for regional wind energy assessments. Paper presented at the Workshop on Wind Climate, Ashville, North Carolina, 12-13 November 1979.
- Elliot, D.L., C.G. Holladay, W.R. Barchet, H.P. Foote, and W.F. Sandusky. 1986. Wind energy resource atlas of the United States. DOE/CH 10093-4. Available from National Technical Information Service, Springfield, Virginia.
- Hagen, L.J. 1991. Wind erosion prediction system to meet user needs. *J. Soil and Water Conserv.* 46:105-111.
- Hennessey, J.P. 1977. Some aspects of wind power statistics. *J. Appl. Meteor.* 16:119-128.
- Nicks, A.D. and L.J. Lane. 1989. Weather generator, pp 2.1-2.19. In L.J. Lane and M.A. Nearing (editors), USDA - Water erosion prediction project: Hillslope profile model documentation. NSERL Report No. 2, USDA-ARS, National Soil Erosion Research Laboratory, West Lafayette, Indiana 47907.
- Nicks, A.D., J.R. Williams, C.W. Richardson, and L.J. Lane. 1987. Generating climatic data for a water erosion prediction model. Paper No. 87-2541, International Winter Meeting ASAE, December 15-18, Chicago, IL.
- Skidmore, E. L. and J. Tatarko. 1990. Stochastic wind simulation for erosion modeling. *Trans. ASAE.* 33:1893-1899.
- Skidmore, E.L. and J. Tatarko. 1991. Wind in the Great Plains: speed and direction distributions by month. Pages 245-263 in: J.D. Hanson, M.J. Shaffer, and C.V. Cole (eds.) *Sustainable Agriculture for the Great Plains*, USDA-ARS, ARS-89.
- Takle, E.S. and J.M. Brown. 1978. Note on the use of Weibull statistics to characterize wind speed data. *J. Appl. Meteor.* 17:556-559.

WEPS**WEATHER SUBMODEL****W-15**

Tribbia, J.J. and R.A. Anthes. 1987. Scientific basis of modern weather prediction. *Science* 237:493-499.

Wagner, L.E., J. Tatarko, and E.L. Skidmore. 1992. WIND_GEN - Wind data statistical database and generator. Paper No. 92-2111, International Summer Meeting ASAE. June 21-24, Charlotte, NC.

W-16

WEATHER SUBMODEL

WEPS

EROSION SUBMODEL



EROSION SUBMODEL

L.J. Hagen

INTRODUCTION

The Wind Erosion Prediction System (WEPS) is a process-based, computer model that predicts wind erosion for a rectangular simulation region on a daily time-step basis (Hagen, 1991a). The WEPS is composed of a user-interface, databases, a supervisory program and seven submodels.

The EROSION submodel uses parameters supplied by other submodels that describe the soil surface, flat biomass cover, standing biomass leaf and stem areas, and weather to decide if wind erosion can occur in a simulation region. If erosion can occur, then the submodel simulates the process of soil movement. Finally, the submodel periodically updates any changes in the soil surface caused by soil movement. At the completion of user-selected simulation intervals, the submodel outputs estimates of soil loss/deposition from the simulation region.

The EROSION submodel consists of several subroutines written in FORTRAN 77. Submodel input data are stored in arrays of variable size that usually represent either global subregion variables or local variables for points on a grid of the simulation region. The number of grid points, grid size, output frequency, output type, etc. are selected external to the submodel and passed to the submodel by program control. Thus, it is necessary to specify elsewhere the number of dimensions in arrays that will contain the inputs and outputs from the submodel before running this submodel.

The EROSION submodel considers the simulation region to be rectangular and composed of one or more rectangular subregions (fields) with differing surface conditions (Fig. E-1). The surface conditions considered are combinations of the following:

1. Surface roughness - random and/or oriented measured below the standing biomass canopy (Fig. E-2);

E-2

EROSION SUBMODEL

WEPS

2. Covers - flat, random, biomass cover; crust with loose, erodible soil on crust; aggregated soil with a size distribution; and rock cover (> 2.0 mm dia.) (Fig. E-3);
3. Surface soil moisture; and
4. Standing biomass (Fig. E-4).

**WEPS
Simulation Geometries**

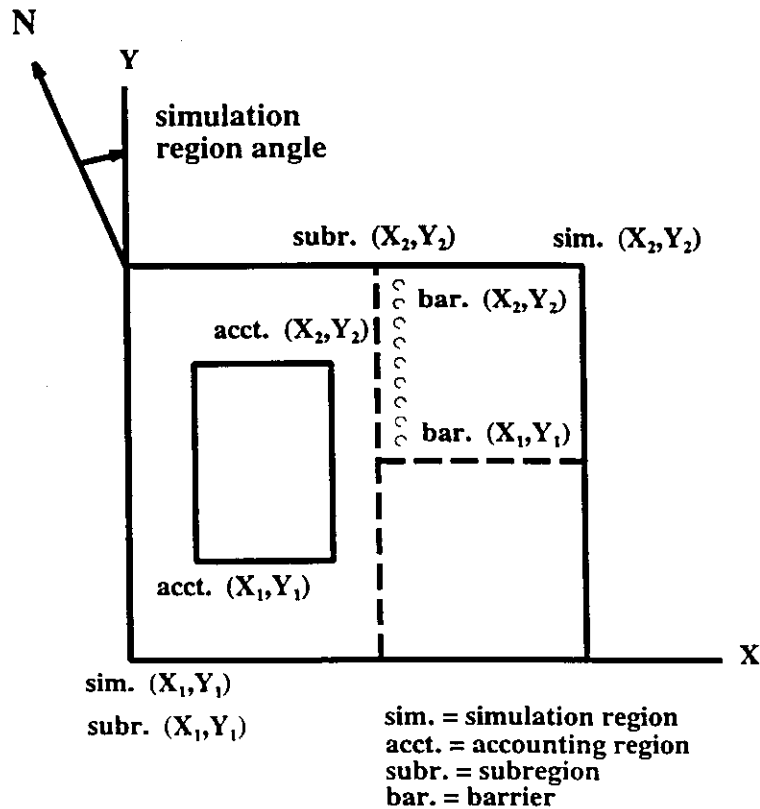


Figure E-1. Simulation region geometry. End points of barriers and opposite corners of rectangular simulation region, subregions, and accounting regions must be input by user.

WEPS

EROSION SUBMODEL

E-3

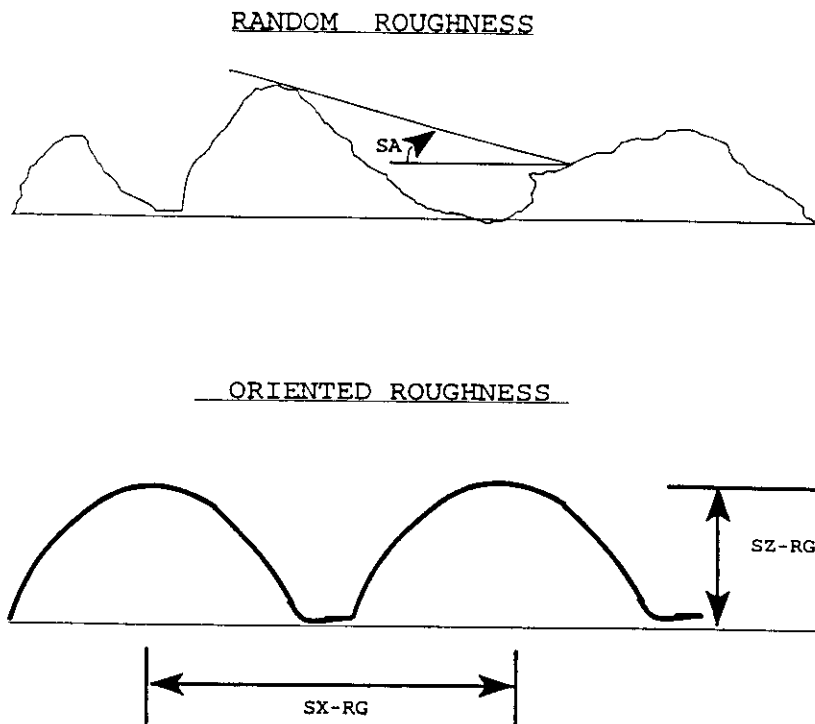


Figure E-2. Illustration of random roughness shelter angles (SA) and oriented roughness spacing (SX-RG) and height (SZ-RG) used in EROSION.

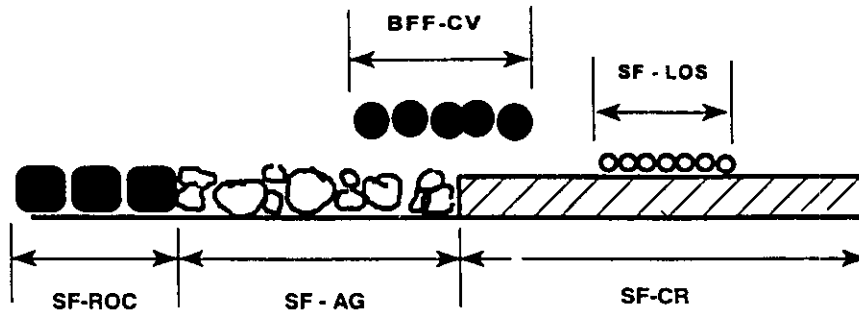


Figure E-3. Illustration of surface cover fraction descriptions used in EROSION. The rock > 2.0 mm (SF-ROC), aggregated (SF-AG), and crusted (SF-CR) soil constitute the lowest layer, and their fractions sum to 1. The second layer is cover fraction loose soil on the crust (SF-LOS), and it cannot exceed crust fraction. The third layer is the biomass flat fraction of cover (BFF-CV), which is assumed to have random distribution over the entire surface.

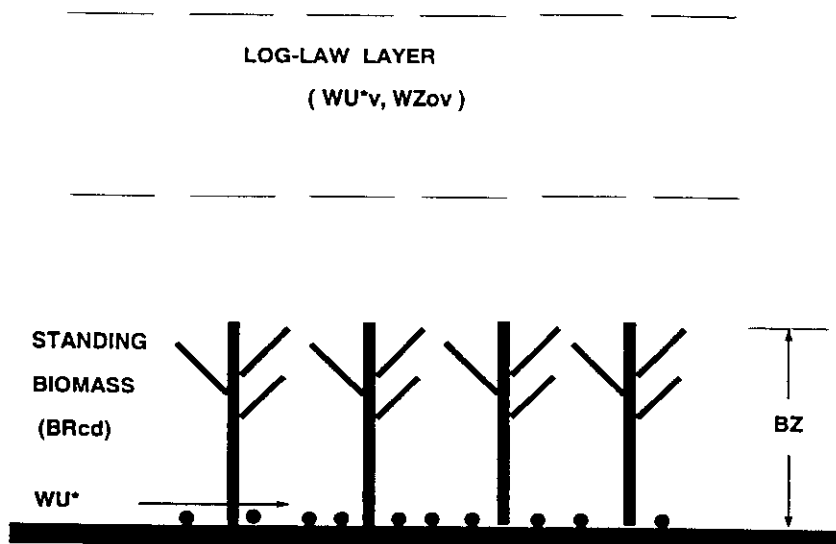


Figure E-4. Diagram illustrating above-canopy friction velocity (WU^*v), which is reduced by drag of the biomass ($BRcd$) to the below-canopy friction velocity (WU^*). The latter is used to drive EROSION.

The EROSION submodel is not called unless maximum daily wind speed at 10 m height reaches 8 m/s. Then, the maximum daily wind speed is used to determine if erosion can occur in any subregion. If snow depth exceeds 20 mm, no erosion occurs in a subregion. If erosion can occur, then generated weather data of subhourly wind speeds and a single wind direction (Skidmore and Tatarko, 1990) for each daily time-step are used to drive the EROSION submodel.

OBJECTIVES

The EROSION submodel is divided into several major functional sections to accomplish the following simulation objectives:

1. Calculate friction velocities in each subregion;
2. Calculate threshold friction velocities in each subregion;
3. Generate the simulation region grid points;
4. Initialize values on simulation region grid points;
5. Compute soil loss/deposition;
6. Update surface variables changed by erosion;
7. Update changed global subregion variables; and
8. Output selected information to files.

EROSION SUBMODEL CONTROL SECTIONS

The subroutine "sberos" serves as the control subroutine for the EROSION submodel (Figs. E-5, E-14, E-16, and E-22) and calls other subroutines which execute the calculations necessary to simulate wind erosion.

DETERMINE FRICTION VELOCITY

In order to determine friction velocity, the aerodynamic roughness term of the log-law wind speed profile must be determined first. For each subregion in the simulation region, the surface aerodynamic roughness as affected by microrelief of the soil and flat biomass cover

WEPS

EROSION SUBMODEL

E-7

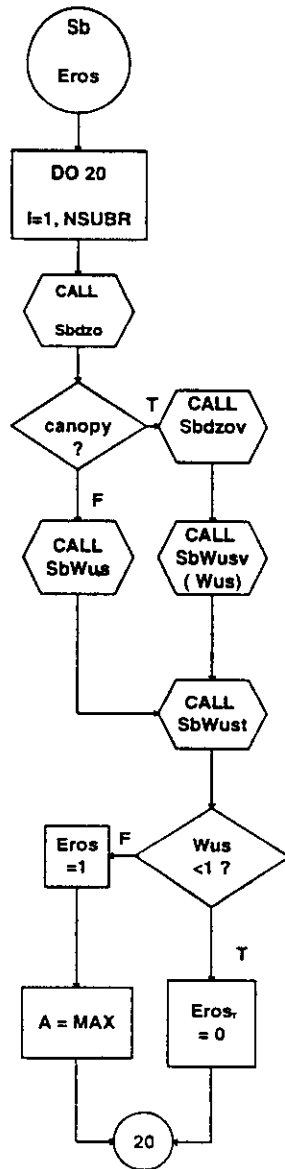


Figure E-5. Partial flowchart of subroutine "Sberos" illustrating testing of subregions to determine if daily maximum friction velocity exceeds threshold friction velocity.

E-8

EROSION SUBMODEL

WEPS

is calculated. In EROSION, tillage ridges are characterized by their height, spacing, orientation, and top bed width. For ridge heights greater than zero, the aerodynamic roughness is (Fig. E-6) (Hagen and Armbrust, 1992):

$$\frac{WZO_{rg}}{SZ_{rg}} = \frac{1}{-64.1 + 135.5 \frac{SZ_{rg}}{SXP_{rg}} + \frac{20.84}{\sqrt{\frac{SZ_{rg}}{SXP_{rg}}}}}, \quad SZ_{rg} > 0 \quad (1)$$

where

- WZO_{rg} = aerodynamic roughness of the ridges (mm),
 SZ_{rg} = ridge height (mm), and
 SXP_{rg} = ridge spacing parallel the wind direction (mm).

The ridge spacing parallel to the wind direction is:

$$SXP_{rg} = \frac{SX_{rg}}{\text{abs}[\sin(\frac{3.1416}{180}(AWA_{dir} - SA_{rg}))]}; \text{denominator} > 0.2 \quad (2)$$

where

- SX_{rg} = ridge spacing (mm),
 AWA_{dir} = daily wind direction (degrees), and
 SA_{rg} = ridge orientation, clockwise from north and parallel to the ridge (degrees).

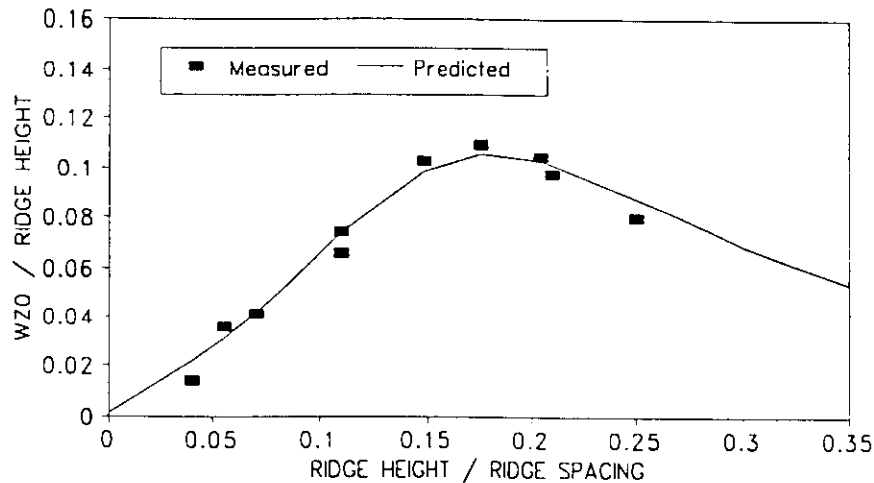


Figure E-6. Ratio of aerodynamic roughness to ridge height as a function of the ridge height to spacing ratio; predicted is equation E-1. (Hagen and Armbrust, 1992).

To describe the fraction of surface sheltered from saltation impacts, the random roughness in EROSION is characterized by shelter angles (Fig. E-2). A shelter angle at a point is defined as the largest angle above horizontal to the top of any upwind point. The shelter angle distribution is described by a two parameter Weibull distribution; the two parameters are a scale factor and a shape factor (Potter, Zobeck, and Hagen, 1990). The average shape factor measured over a range of random roughness was about 0.77 (Potter and Zobeck, 1990). The scale factor was related to the random roughness measurement described by Allmaras et al. (1966) as

$$SAC = 2.3 \sqrt{SZ_{rr}} \quad (3)$$

where

SAC = Weibull scale factor for shelter angle (degrees), and
 SZ_{rr} = random roughness (mm)

Aerodynamic roughness increases with the scale factor and for random roughness (Fig. E-7)(Hagen, 1991b).

E-10

EROSION SUBMODEL

WEPS

$$WZO_{rr} = \exp\left(2.1546 - \frac{14.44}{SAC_{rr}}\right); \quad SAC_{rr} > 2 \quad (4)$$

where

WZO_{rr} = aerodynamic roughness of random roughness including any flat biomass cover (mm), and
 SAC_{rr} = Weibull scale parameter of the shelter angle distribution (degrees).

The aerodynamic roughness for the surface, WZO, then is calculated as the maximum of the ridge or random aerodynamic roughness.

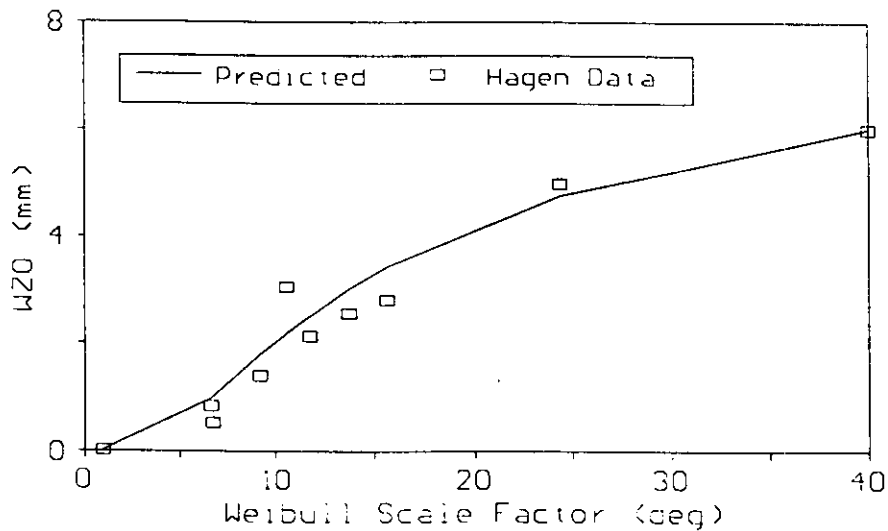


Figure E-7. Aerodynamic roughness of random rough surfaces as a function of the Weibull scale factor of the shelter angle distribution of the random rough surfaces; predicted is equation E-4.

If standing plant biomass is present, the aerodynamic roughness length of the canopy is calculated using the following procedure. First, an effective biomass drag coefficient is calculated as for all crops as (Armbrust and Bilbro, 1995):

$$BR_{cd} = BR_{lai} (0.2 - (0.15)EXP(-8 * BR_{lai})) + BR_{sai} \quad (5)$$

where

- BR_{cd} = effective biomass drag coefficient,
 BR_{lai} = biomass leaf area index (m^2/m^2), and
 BR_{sai} = stem area index, i.e., stem silhouette area per unit horizontal soil surface area (m^2/m^2).

Next, the standing biomass aerodynamic roughness is calculated using an average stem diameter of 20 mm as (Fig. E-8) (Hagen and Armbrust, 1994):

$$WZ0_v = \frac{BZ}{17.27 - \frac{1.254 \ln(BR_{cd})}{BR_{cd}} - \frac{3.714}{BR_{cd}}} \quad (6)$$

Minimum aerodynamic roughness is that of the below-canopy surface. While aerodynamic roughness may decrease slightly with stem diameter of residue, a constant value was assumed in this study.

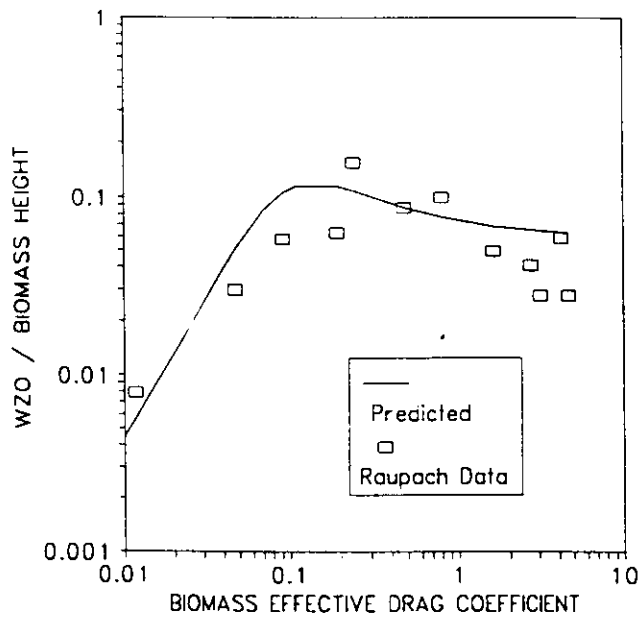


Figure E-8. Biomass aerodynamic roughness as a function of effective drag coefficient of the biomass; predicted is equation E-6.

Friction velocity at the subregion is calculated in two steps. First, the friction velocity at the weather station, where wind speeds are measured, is calculated for strong winds with neutral stability using the log-law profile (Panofsky and Dutton, 1984):

$$WUF = \frac{(0.4)WU}{\ln\left(\frac{WZ}{WZZ0}\right)} \quad (7)$$

where

- WUF = friction velocity at the weather station (m/s),
- WU = wind speed at weather station (m/s),
- WZ = anemometer height at the weather station (mm); (wind speeds were adjusted to 10 m height in WEPS data base), and
- WZZ0 = aerodynamic roughness at weather station, assumed to be 25 mm in WEPS.

Second, the maximum subregion friction velocity is calculated using the daily maximum wind speed. The calculation is based on the ratio of aerodynamic roughness at the subregion to that at the wind speed measurement station. This equation is an approximation of a

WEPS

EROSION SUBMODEL

E-13

procedure suggested by Lettau (Panofsky and Dutton, 1984). If there is no standing biomass, then

$$WU_{.} = WUF \left(\frac{WZO}{WZZO} \right)^{0.067} \quad (8)$$

where

WU^* = friction velocity used to drive the erosion simulation (m/s).

However, if there is standing biomass, then

$$WU_{.,v} = WUF \left(\frac{WZO_v}{WZZO} \right)^{0.067} \quad (9)$$

where

$WU_{.,v}$ = friction velocity above the standing biomass (m/s), and
 WZO_v = as defined by equation E-6.

Next, the subregion friction velocity below the standing biomass is calculated (Fig. E-9) (Hagen and Armbrust, 1994).

$$WU_{.} = WU_{.,v} \left[0.86 \exp\left(\frac{-BR_{cd}}{0.0298}\right) + 0.025 \exp\left(-\frac{BR_{cd}}{0.356}\right) \right] \quad (10)$$

where

$WU_{.}$ = friction velocity below the standing biomass at the surface that is used to drive the erosion simulation (m/s).

At this point in the calculations, the influence of barriers or hills on friction velocity are still neglected

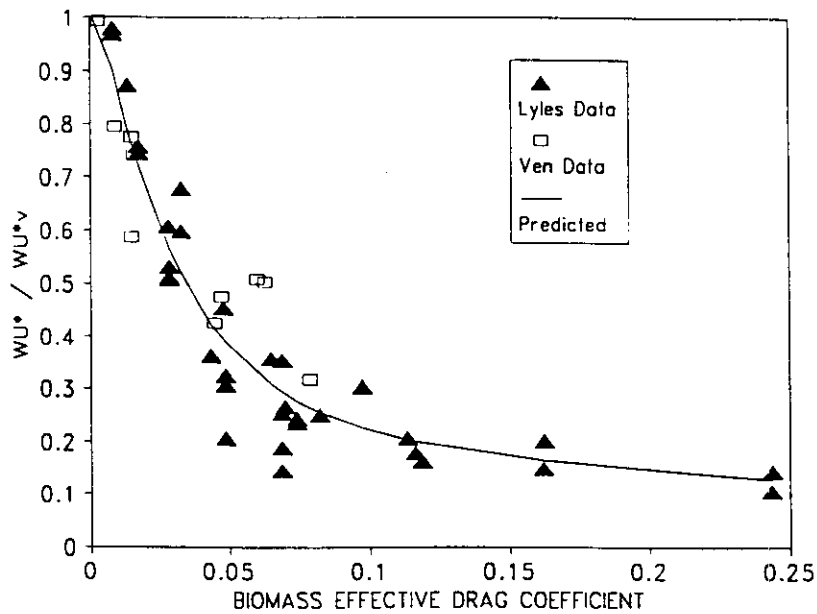


Figure E-9. Reduction in friction velocity through biomass canopy as a function of biomass drag coefficient; predicted is equation E-10 (Lyles and Allison, 1976; van de Ven, Fryrear, and Spaan, 1989).

DETERMINE STATIC THRESHOLD FRICTION VELOCITY

The velocity at which numerous aggregates begin to saltate is defined as the static threshold friction velocity. Static threshold friction velocity is calculated in each subregion as influenced by aggregate size and density, clod/crust cover, surface roughness, flat biomass cover, and surface soil wetness at noon.

Soil scientists generally report the sum of the soil mass fractions less than 2 mm diameter as 1.0 and then report volume of rocks as a separate value in their databases. In WEPS, we have followed this precedent and let the surface fractions of crusted and aggregated soil sum to 1.0. However, to calculate the true fraction of bare surface that does not emit, one must correct for the rock fraction, if it is present. Hence, the fraction of bare surface that does not emit loose soil is :

$$SF_{cv} = [(1 - SF_{cr})(1 - SF_{84}) + SF_{cr} - SF_{los}] [1 - SV_{roc}] + SV_{roc} \quad (11)$$

where

- SF_{cv} = soil fraction covered by clod/crust and rock so it does not emit,
- SF_{cr} = soil fraction covered by crust, but excluding the fraction of rock-covered area,
- SF_{los} = soil fraction covered with loose, erodible soil on the crusted area,
- SV_{roc} = soil volume rock > 2.0 mm. (m^3/m^3), and
- SF_{84} = soil fraction covered with aggregates < 0.84 mm in diameter on the noncrusted area, but excluding the fraction of rock-covered area.

The latter term is calculated from the modified lognormal aggregate size distribution as (Wagner and Ding, 1994):

$$SLT = \frac{(0.84 - SL_{agn})(SL_{agx} - SL_{agn})}{(SL_{agx} - 0.84)SL_{agm}} \quad (12)$$

$$SF_{84} = 0.5 \left[1 + \operatorname{erf} \left[\frac{\ln(SLT)}{\sqrt{2} \ln(SO_{ags})} \right] \right] \quad (13)$$

E-16

EROSION SUBMODEL

WEPS

where

- SL_{agn} = lower limit of size distribution (mm),
 SL_{agx} = upper limit of size distribution (mm),
 SL_{agm} = geometric mean of size distribution (mm), and
 SO_{ags} = geometric standard deviation of size distribution.

To determine threshold friction velocities for bare soil surface, estimating equations were fitted to wind tunnel data (Hagen, 1991b; Chepil and Woodruff, 1963) to give (Figs. E-10 and E-11):

$$WUB_{ts} = 1.7 - (1.35)\exp[-(b2)SF_{cv}] \quad (14)$$

$$b2 = \frac{1}{-0.076 + \frac{1.111}{\sqrt{WZO}}} \quad (15)$$

where

WUB_{ts} = static threshold friction velocity of bare surface (m/s).

The minimum static threshold friction velocity for field surfaces was selected to be 0.35 m/s.

If random flat biomass cover is present, the increase in soil surface area protected from emission is (Fig. E-3):

$$SFC_{cv} = (1 - SF_{cv})BFF_{cv} \quad (16)$$

where

- SFC_{cv} = fraction change in soil surface area protected from emission, and
 BFF_{cv} = biomass fraction of flat cover.

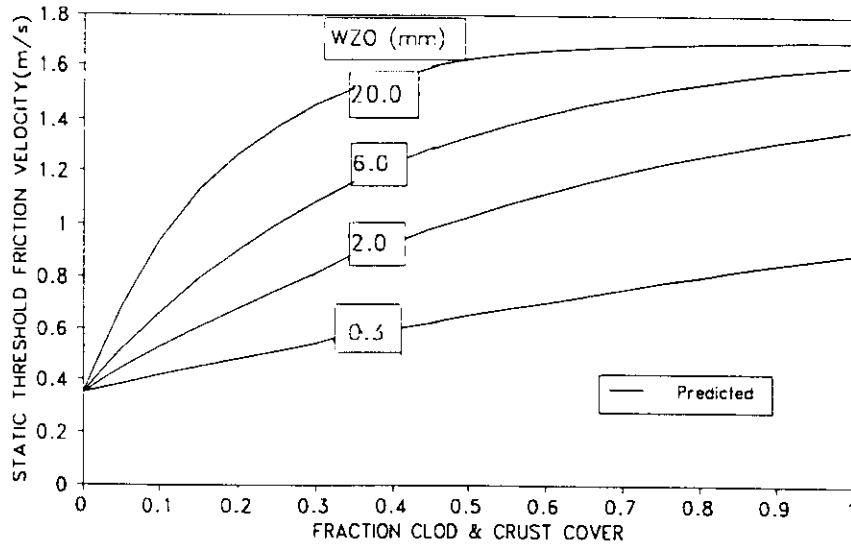


Figure E-10. Predicted threshold friction velocities for various levels of aerodynamic roughness and surface cover; predicted is equations E-14 and E-15.

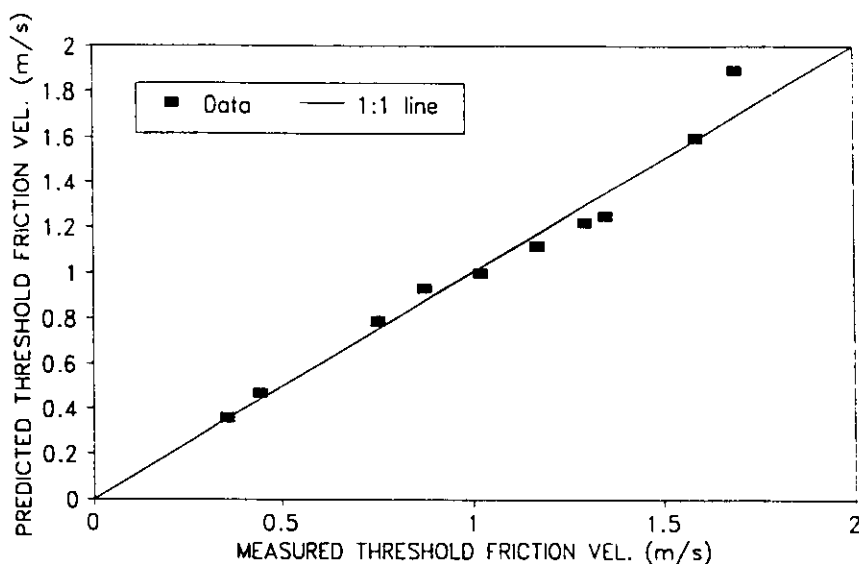


Figure E-11. Predicted threshold friction velocities as a function of measured threshold friction velocities on random rough and ridged surfaces (Hagen, 1991b; Hagen and Armbrust, 1992).

The increase in static threshold friction velocity caused by flat biomass cover is (Fig. E-12) (Hagen, 1995):

$$WUC_{.ts} = 0.02 + SFC_{cv}; \quad SF_{cv} > 0.0 \quad (17)$$

where

$WUC_{.ts}$ = change in static threshold friction velocity caused by flat biomass cover (m/s).

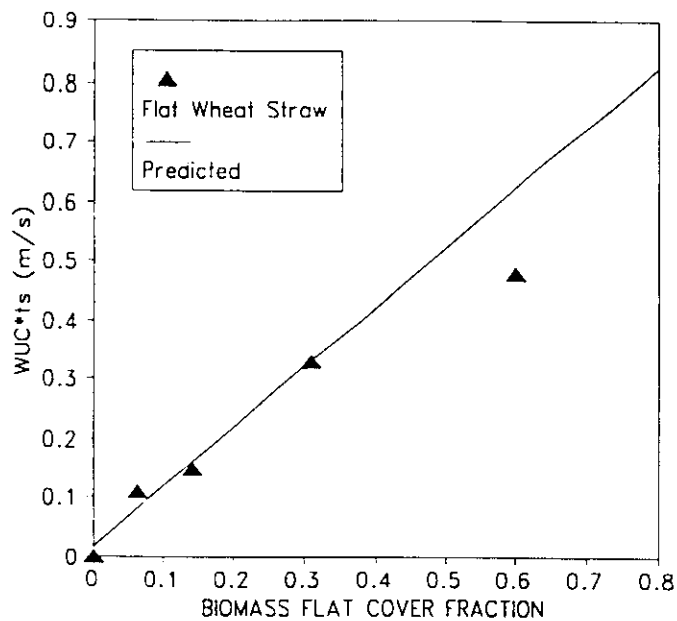


Figure E-12. Increase in static threshold friction velocity of erodible sand; predicted is equation E-17 (0.29-0.42 mm diameter) caused by flat biomass cover (Hagen, 1995).

If the surface is wet, threshold velocity increases as the slope of Fig. E-13 (Saleh and Fryrear, 1995).

$$WUCW_{.ts} = 0.48 \frac{HR0_{wc}}{HR15_{wc}}, \quad \frac{HR0_{wc}}{HR15_{wc}} > 0.2 \quad (18)$$

where

$WUCW_{.ts}$ = increase in static threshold friction velocity from surface wetness (m/s),

$HR0_{wc}$ = surface soil water content (kg/kg), and

$HR15_{wc}$ = surface soil water content at 1.5 MPa (kg/kg).

Finally, static threshold velocity with wetness and flat cover is:

$$WU_{.ts} = WUB_{.ts} + WUC_{.ts} + WUCW_{.ts} \quad (19)$$

where

WU_{ts} = surface static threshold velocity accounting for both flat biomass cover and wetness effects (m/s).

If friction velocity does not exceed threshold in any of the subregions, control is returned to MAIN. If friction velocity exceeds the threshold, further calculations must be done.

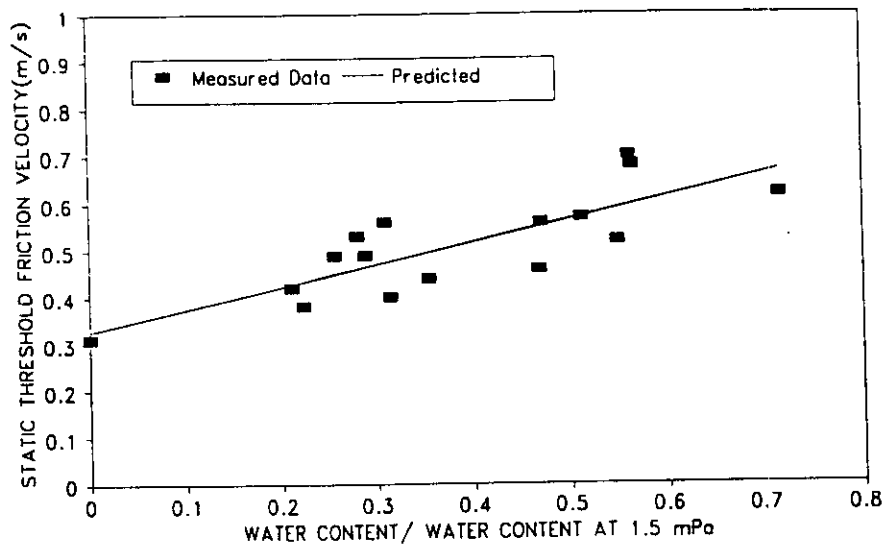


Figure E-13. Static threshold friction velocity change with water content relative to 1.5 MPa water content; predicted slope is equation E-18 (Saleh and Fryrear, 1995).

GENERATION OF THE SIMULATION GRID

Simulation of soil loss/deposition uses finite difference methods to solve partial differential equations that describe the erosion processes. The finite difference procedure requires generation of a grid of computation points on the simulation region. Generation of the grid is started by a flag passed from the supervisory program, MAIN, and is done only once for a simulation run (Fig. E-14). The subroutine "sbgrid" assigns the number and location of the grid points in the simulation region. (Later, inclusion of multigrid techniques or seasonally varying barrier porosity may cause multiple calls to this subroutine.)

INITIALIZATION OF THE SIMULATION GRID

To begin simulation, values of variables must be assigned to each grid point. Thus, at the start of each day with probable erosion, initial values for local and global variables are input at each grid point using the subroutine "sbinit".

HILLS

The subroutine "sbhill" reads an input file that assigns to each grid point a dimensionless wind speed reduction or speed-up factor as influenced by topography. Individual factors are assigned for each of 16 wind directions. Because WEATHER simulates a single wind direction for each day, only one set of factors is used for each day with erosion.

WIND BARRIERS

The subroutine "sbbar" carries out a similar function, but calculates the wind speed reduction factor for each grid point that is influenced by either medium/low or high porosity barriers. Again, a separate reduction factor is assigned for each direction, and only one set of factors is needed each day with erosion. The wind speed reduction factors for high and medium/low porosity barriers are, respectively, (Fig. E-15) (Hagen et al., 1981; van Eimern et al., 1964):

$$FUH_{br} = 1 - \exp[-0.006 xp^2] + 0.913 \exp[-0.033(xp + 4)^{1.52}] \quad (20)$$

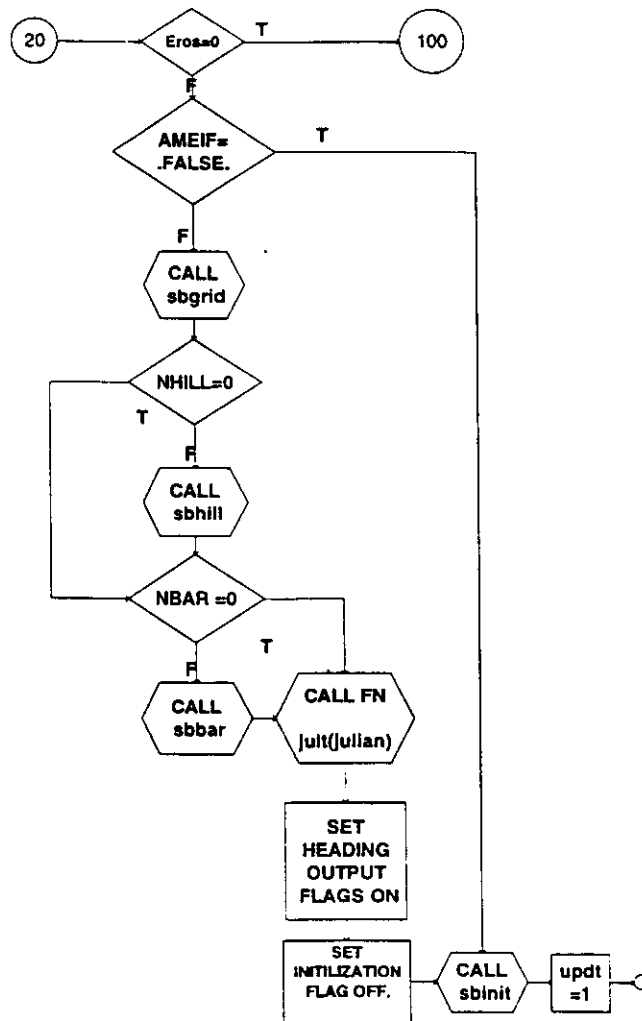


Figure E-14. Partial flow chart of subroutine "Sberos" illustrating calls to create simulation region grid and initialize it for each day.

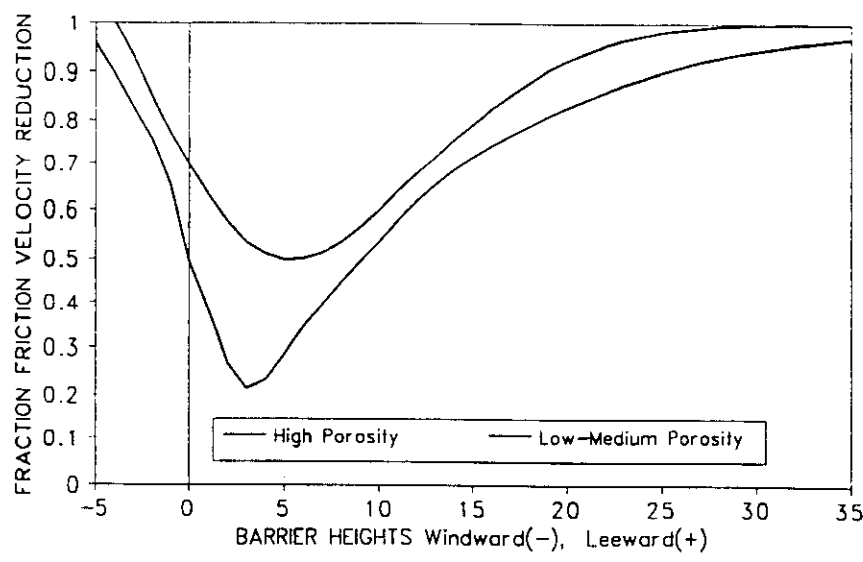


Figure E-15. Barrier function velocity reduction patterns along the wind direction used to modify friction velocity near barriers; predictions are equations E-20 and E-21.

$$FUM_{br} = 1 - \exp[-0.0486|xp|^{1.2}] + 0.671 \exp[-0.000165(xp + 5)^{4.66}] \quad (21)$$

where

- XP = distance from barrier parallel to the wind direction in barrier heights,
 FUH_{br} = fraction friction velocity reduction by high porosity barrier, and
 FUM_{br} = fraction friction velocity reduction by low or medium porosity barriers.

COMPUTATION OF SOIL LOSS/DEPOSITION

This section of the control subroutine, "sberos", steps through the subhourly wind speed values provided by WEATHER and tests whether the friction velocity exceeds the erosion threshold at any point on the simulation grid (Fig. E-16). If the subroutines "sbhill" and "sbbar" are used, this test will account for the effects of both topography and barriers on the friction velocity.

When friction velocity exceeds the erosion threshold, soil loss/deposition is calculated within the subroutine "sberod".

The erosion process is modeled as the time-dependent conservation of mass using linked partial differential equations for three size classes of eroding soil. These are saltation and creep size (0.1 to 2.0 mm), suspension size (<0.1 mm), and PM-10 size (<0.01 mm).

CONSERVATION OF MASS FOR SALTATION AND CREEP

Conservation of saltation and creep size aggregates is simulated with two sources of erodible material (emission and abrasion) and two sinks (surface trapping and suspension). A computational control volume using this scheme for saltation and creep on a bare soil is illustrated in Fig. E-17. The equations for mass conservation of saltation and creep aggregates on a two-dimensional rectangular simulation region can be written as:

$$\frac{\partial(\overline{CH})}{\partial t} = - \frac{\partial q_x}{\partial x} - \frac{\partial q_y}{\partial y} + G_{en} + G_{an} - G_{tp} - G_{ss} \quad (22)$$

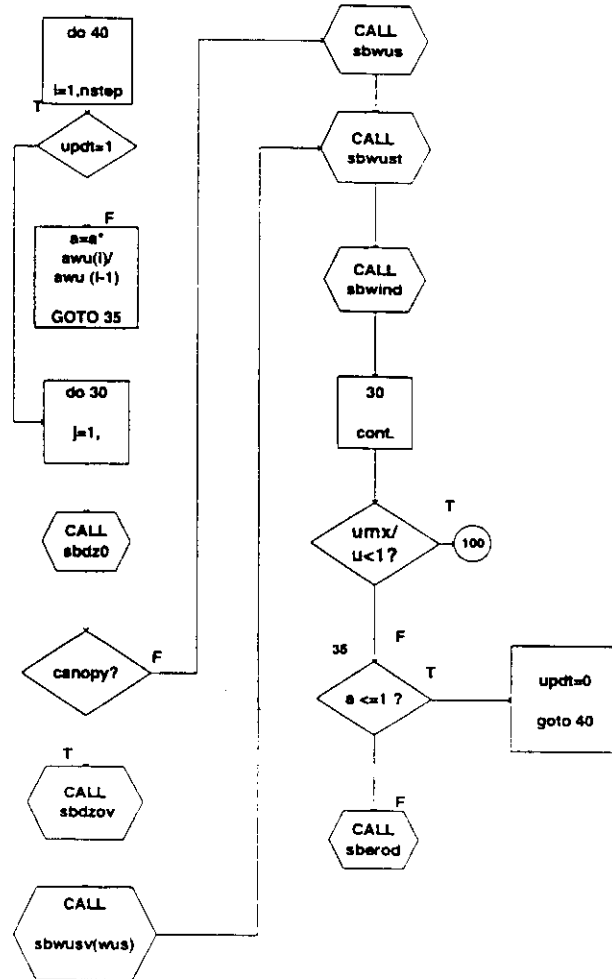


Figure E-16. Partial flow chart of subroutine "Sberos" illustrating testing for subhourly friction velocities above the threshold and then computing soil loss/deposition in subroutine "Sberod."

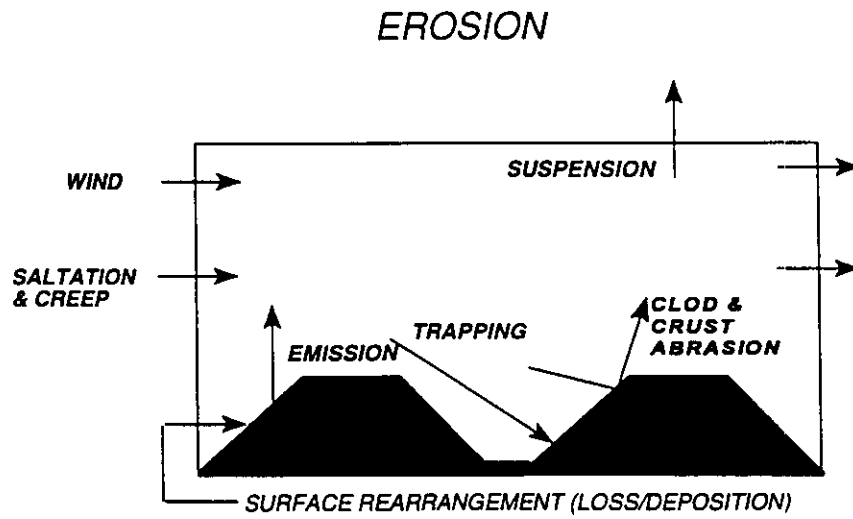


Figure E-17. Diagram of control volume with a ridged bare soil illustrating the sources and sinks used in the EROSION submodel.

E-50

EROSION SUBMODEL

WEPS

van Eimern, J., R. Karschon, L.A. Razumova, and G.W. Roberston. 1964. Windbreaks and shelterbelts. World Meteorol. Organ. Tech. Notes 59, 188pp.

Wagner, L.E. and L.J. Hagen. 1992. Relationship between shelter angle, surface roughness and cumulative sheltered storage depth. Proc. Int. Wind Erosion Workshop of CIGR, Budapest, Hungary.

Wagner, L.E. and D. Ding. 1994. Representing aggregate size distribution as modified lognormal distributions. Trans. Am. Soc. Agric. Engin. 37(3):815-821.

Zobeck, T.M. and D.W. Fryrear. 1986. Chemical and physical characteristics of windblown sediment, I. Quantities and physical characteristics. Trans. Am. Soc. Agric. Engin. 29(4):1032-1036.

Zobeck, T.M. and T.W. Popham. 1991. Influence of abrader flux and soil properties. Soil Sci. Am. J. 55(4):1091-1097.

- Hagen, L.J., N. Mirzamostafa, and A. Hawkins. 1995. The PM-10 component of soil loss for the Wind Erosion Prediction System. (in preparation).
- Hagen, L.J., E.L. Skidmore, and A. Saleh. 1992. Prediction of aggregate abrasion coefficients. *Trans. Am. Soc. Agric. Engin.* 35(6):1847-1850.
- Hagen, L.J., E.L. Skidmore, P.L. Miller, and J.E. Kipp. 1981. Simulation of the effect of wind barriers on airflow. *Trans. Amer. Soc. Agric. Engin.* 24(4):1002-1008.
- Lyles, L. and B.E. Allison. 1976. Wind erosion: the protective role of simulated standing stubble. *Trans. Am. Soc. Agric. Engin.* 19(1):61-64.
- Mirzamostafa, N. and L.J. Hagen. 1995. Suspension component of soil loss for the Wind Erosion Prediction System. (in preparation).
- Panofsky, H.A. and J.A. Dutton. 1984. *Atmospheric turbulence*. New York: John Wiley & Sons, 397 pp.
- Potter, K.N. and T.M. Zobeck. 1990. Estimation of soil microrelief. *Trans. Am. Soc. Agric. Engin.* 33(1):156-161.
- Potter, K.N., T.M. Zobeck and L.J. Hagen. 1990. A microrelief index to estimate soil erodibility by wind. *Trans. Am. Soc. Agric. Engin.* 33(1):151-155.
- Raupach, M.R. 1992. Drag and drag partition on rough surfaces. *Boundary Layer Meteorol.* 60:375-395.
- Saleh, A. and D. W. Fryrear. 1995. Threshold velocities of wet soils as affected by wind blown sand. *Soil Sci.* (in review)
- Skidmore, E.L. and J. Tatarko. 1990. Stochastic wind simulation for erosion modeling. *Trans. Am. Soc. Agric. Engin.* 33(6):1893-1899.
- Stout, J. 1990. Wind erosion within a simple field. *Trans. Am. Soc. Agric. Engin.* 33(5):1597-1600.
- van de Ven, T.A.M., D.W. Fryrear, and W.P. Spaan. 1989. Vegetation characteristics and soil loss by wind. *J. Soil and Water Conserv.* 44:347-349.

REFERENCES

- Allmaras, R.R., R.E. Burwell, W.E. Larson and R.F. Holt. 1966. Total porosity and random roughness of the interrow zone as influenced by tillage. USDA Cons. Res. Rep. 7.
- Armbrust, D.V. and J.D. Bilbro. 1995. Relationship of plant canopy cover and soil transport capacity. (in process)
- Borah, D.K. and P.K. Bordoloi. 1989. Nonuniform sediment transport model. Trans. Am. Soc. Agric. Engin. 32(5):1631-1636.
- Chepil, W.S. and N.P. Woodruff. 1958. Sedimentary characteristics of dust storms: III. Composition of suspended dust. Am. J. Sci. 255:206-213.
- Chepil, W.S. and N.P. Woodruff. 1963. The physics of wind erosion and its control. Adv. in Agron. 15:211-302.
- Greeley, R. and J.D. Iverson. 1985. Wind as a geological process. Cambridge England: Cambridge Univ. Press, 333 pp.
- Hagen, L.J. 1991a. A wind erosion prediction system to meet user needs. J. Soil and Water Conserv. 46:106-111.
- Hagen, L.J. 1991b. Wind erosion: emission rates and transport capacities on rough surfaces. ASAE paper no. 912082, St. Joseph, MI.
- Hagen, L.J. 1991c. Wind erosion mechanics: abrasion of aggregated soil. Trans. Am. Soc. Agric. Engin. 34(4):831-837.
- Hagen, L.J. 1995. Crop residue effects on aerodynamic processes and wind erosion. Theoretical and Applied Climatology (accepted)
- Hagen, L.J. and D.V. Armbrust. 1992. Aerodynamic roughness and saltation trapping efficiency of tillage ridges. Trans. Am. Soc. Agric. Engin. 35(4):1179-1184.
- Hagen, L.J. and D.V. Armbrust. 1994. Plant canopy effects on wind erosion saltation. Trans. Am. Soc. Agric. Engin. 37(2):461-465.

Of course, after the last erosion period of the day, the updated variables are passed to other submodels. For global soil layer variables, only the first layer is updated.

One other problem may occur, if a daily erosion event causes large gradients of global variables to develop across a single subregion. This gradient may affect the erosion on subsequent days, but this is not reflected by using average inputs for each subregion to begin the daily erosion simulation. To reduce this problem, the daily gradients will be retained by the EROSION submodel until the surface is significantly changed by other submodels.

OUTPUT FROM EROSION TO FILES

Two subroutines output files of information from the EROSION submodel (Fig. E-22). The first subroutine, "sbout", is a specialized subroutine that is located within the daily erosion cycle. It is to be modified by those developing, verifying, and validating the EROSION submodel.

The second subroutine, "sbrpt", has several outputs:

1. The Julian day,
2. the total soil loss/deposition at each grid point since last output,
3. the total suspension at each grid point since last output, and
4. the total PM-10 production at each grid point since last output.

The outputs to a file from calls to subroutine "sbrpt" are controlled by a flag from the MAIN subroutine.

The grid points that may be included in each user-selected accounting region must form a rectangle, but there are no other restrictions. However, all the information for standard reports for all potential accounting regions is located in the report file generated by subroutine "sbrpt". When MAIN calls the subroutine "sbrpt" for a printed report, the data in the report file are analyzed for each of the specified accounting regions and printed.

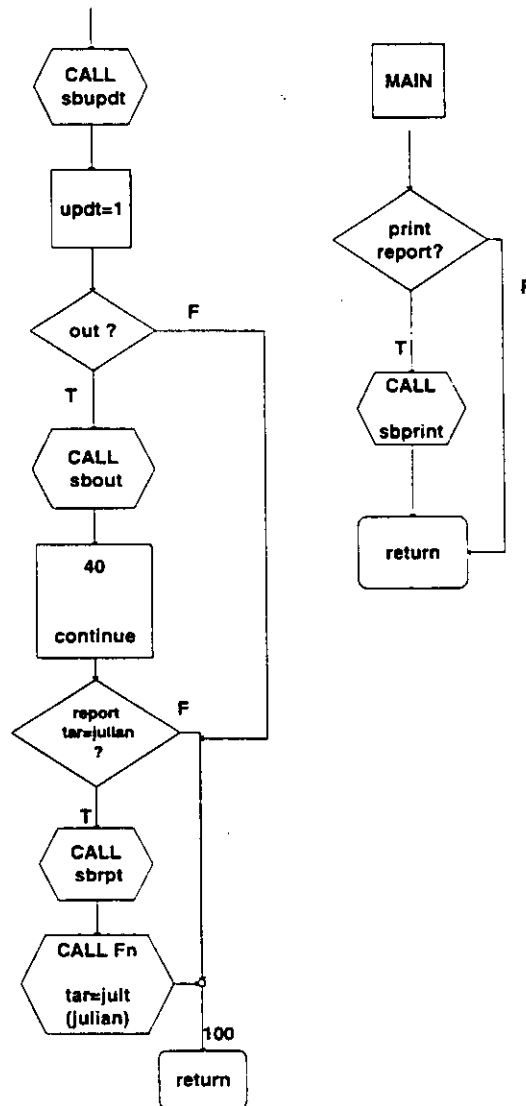


Figure E-22. Partial flowchart of subroutine "Sberos" illustrating updating of global subregion variables and output to files from the EROSION submodel. Viewing the results and printing output are controlled by the MAIN control subroutines of WEPS.

E-44

EROSION SUBMODEL

WEPS

Similarly, for fractions larger than 0.84 mm, say 2.0 mm,

$$\frac{d(SF200)}{dt} = \frac{(1 - SF200)}{(1 - SF84)} \frac{d(SF84)}{dt} \quad (80)$$

UPDATE OF GLOBAL SUBREGION VARIABLES

During an erosion event, the global subregion variables are updated periodically by subroutine "sbupdt" (Fig. E-22). The reason for this update within an erosion day is to allow changes in the soil surface to impact the calculation of the surface friction velocity and other erosion parameters.

specific size ranges in the calculation procedures. Hence, during days when EROSION is simulated, the size ranges will be updated periodically during the day in the active surface layer (zero layer) at each grid area. At the end of each day, new aggregate size distribution parameters are calculated for the first (10 mm) layer of each subregion by averaging the changes over the grid points in the subregion.

To update the grid areas, an active layer mass (zero layer) is defined, similar to the procedure of Borah and Bardoloi (1989) as

$$SM_0 = \frac{0.84}{1 - F84} SD_{ag}, \quad \frac{SM_0}{SD_{blk}} < 10 \text{ mm} \quad (77)$$

where

- SM_0 = soil mass that must be removed by emission in order to armor the surface (kg/m^2),
- SD_{ag} = soil aggregate density (Mg/m^3),
- SD_{blk} = soil bulk density (Mg/m^3), and
- $SF84$ = soil mass fraction less than 0.84 mm diameter.

In the case of a low number of clods, the active layer is restricted to 10 mm depth.

The abrasion and trapping processes increase the fraction less than 0.84 mm, whereas emission decreases it. Thus,

$$\frac{d(F84)}{dt} = \frac{(F_{anag} C_{anag})(G_{an} + GSS_{an}) + SF_{ag} G_{tp}}{SM_0} - \frac{(1 - SF_{cv} - SF_{los})(G_{en} + GSS_{en})}{SM_0} \quad (78)$$

The maximum and minimum size aggregates in the distribution are assumed to remain constant. Hence, size fractions finer than 0.84 mm are modified proportionally as

$$\frac{d(SF10)}{dt} = \frac{SF10}{SF84} \frac{d(SF84)}{dt} \quad (79)$$

where

- $SF10$ = soil fraction less than 0.1 mm diameter.

E-42

EROSION SUBMODEL

WEPS

$$SZ_2 = \frac{2(G_{en} + GSS_{en} + G_{an} + GSS_{an} + G_{\eta})}{SD_{blk}}, SF_{cv} < 0.1 \quad (72)$$

where

SZ_2 = change in height per unit time (mm/s).

The rate of change in ridge height is then

$$\frac{d(SZ_{rg})}{dt} = -SZ_{1,2} \quad (73)$$

Similarly, the effect of erosion on random roughness is approximated as

$$\frac{d(SZ_{sd})}{dt} = -SZ_{1,2} \quad (74)$$

where

SZ_{sd} = soil storage depth in the random roughness (mm).

Analysis of a number of pin meter measurements on random rough surfaces showed the soil storage depth for shelter angles greater than 3 degrees is related to the Weibull scale factor as (Wagner and Hagen, 1992)

$$SAC = 1.563 + 4.534\sqrt{SZ_{sc}} \quad (75)$$

Manipulating the two preceding equations gives

$$\frac{d(SAC)}{dt} = -\frac{10.28 SZ_{1,2}}{(SAC - 1.563)}, \quad SAC > 2.0 \quad (76)$$

where

SAC = the Weibull scale factor of shelter angle distribution (degrees).

EROSION EFFECT ON AGGREGATE-SIZE DISTRIBUTION

The aggregate-size distribution is modeled as an abnormal, log-normal distribution with 4 parameters (Wagner and Ding, 1994). However, the EROSION submodel uses a series of

$$\frac{d(SZ_{cr})}{dt} = - \frac{F_{ancr} C_{ancr} (G_{an} + GSS_{an})}{SD_{blk}} \quad (68)$$

where

SZ_{cr} = crust thickness (mm).

Next, crust cover is reduced in linear proportion to crust thickness and aggregate cover is increased

$$\frac{d(SF_{cr})}{d(SZ_{cr})} = \frac{SF_{cr}}{SZ_{cr}} \quad (69)$$

$$\frac{d(SF_{ag})}{dt} = - \frac{d(SF_{cr})}{dt} \quad (70)$$

where

SF_{cr} = fraction crust cover, and
 SF_{ag} = fraction aggregate cover.

EROSION EFFECT ON SURFACE ROUGHNESS

Typical field surfaces have a clod or crust armor at the highest elevations. During erosion, these elevated points have abrasion losses from the top and trapping or emission in the low areas. The net rate of change in height caused by these processes is approximated as

$$SZ_1 = \frac{2(G_{an} + GSS_{an} - G_{en} - GSS_{en} + G_{\eta})}{SD_{blk}}, \quad SF_{cr} > 0.1 \quad (71)$$

where

SZ_1 = change in height per unit time (mm/s).

The factor two is used because it is assumed that the different process act on only about half the area.

In the case of highly erodible surfaces, there is both emission and abrasion from the top and trapping in the low areas. The net rate of change in height is approximated as

E-40

EROSION SUBMODEL

WEPS

measurements are available to validate the simulated response of field surfaces to erosion. To simulate the surface rearrangement, simple equations based on mass balance of the surface layer were developed for the area represented by each grid point.

EROSION EFFECT ON LOOSE SOIL ON CRUST

The net vertical deposition is

$$SG = G_{ip} - G_{en} - GSS_{en} \quad (65)$$

where

SG = net vertical deposition of loose soil ($\text{kg}/\text{m}^2\text{s}$).

The net vertical deposition then is portioned between the emitting area on the crust and the total emitting area as

$$\frac{d(SM_{los})}{dt} = SG \left[\frac{SF_{los}}{1 - SF_{cv}} \right] \quad (66)$$

where

SM_{los} = soil mass that is loose and erodible on the crust (kg/m^2),
 SF_{los} = soil fraction cover of loose aggregates on crust,
 SF_{cv} = soil fraction covered and not emitting, and
 t = time (s).

The fraction of crusted area covered by loose material is updated as

$$e \frac{d(SF_{los})}{d(SM_{los})} = \frac{SF_{los}}{SM_{los}} \quad (67)$$

EROSION EFFECT ON CRUST THICKNESS AND COVER

Abrasion from the crust is

WEPS

EROSION SUBMODEL

E-39

$$SF10_{en} = \frac{SF_1}{SF_{10}} \quad (60)$$

where

SF_1 = soil surface fraction less than 0.01 mm diameter, and
 SF_{10} = soil surface fraction less than 0.10 mm diameter.

The flux from abrasion is

$$G10_{an} = SF10_{an} SF_{ss_{an}} \sum_{i=1}^m (F_{ani} C_{ani}) q \quad (61)$$

where

$SF10_{an}$ = soil fraction of PM-10 in suspended soil that was abraded from the surface (Hagen, Mirzamostafa, and Hawkins, 1995).

$$SF10_{an} = 0.67 SF_{cla}, \quad SF10_{an} < 0.35 \quad (62)$$

The flux from breakdown of saltation and creep is

$$G10_{ss} = SF10_{bk} C_{bk} q \quad (63)$$

where

$SF10_{bk}$ = soil fraction of PM-10 in suspended soil that was created from breakdown of saltation and creep (Hagen, Mirzamostafa, and Hawkins, 1995).

$$SF10_{bk} = 0.0015 + 0.023 SF_{si}^2 \quad (64)$$

where

SF_{si} = soil fraction silt in surface layer.

SURFACE REARRANGEMENT

Finally, auxiliary equations to describe the changes in the soil surface in response to loss or deposition are needed to complete the system of equations. In general, few field

E-38

EROSION SUBMODEL

WEPS

largest particles, 0.05 to 0.1 mm diameter, are roughly half the mass of the suspension discharge (Chepil and Woodruff, 1958; Zobeck and Fryrear, 1986) and tend to move toward the surface. The process is simulated as

$$G_{ss_{ip}} = C_{dp}(q_{ss} - 0.5 q_{ss_o}), \quad G_{ss_{ip}} > 0.0 \quad (57)$$

where

- q_{ss_o} = maximum q_{ss} calculated (kg/ms), and
 C_{dp} = coefficient of deposition, value about 0.02 (1/m).

CONSERVATION OF MASS FOR PM-10

Conservation of mass for the PM-10 is simulated as a partitioning of the suspension components without any trapping.

$$\frac{\partial(\overline{C10H10})}{\partial t} = -\frac{\partial(q10)_x}{\partial x} - \frac{\partial(q10)_y}{\partial y} + G10_{en} + G10_{an} + G10_{ss} \quad (58)$$

where

- $q10$ = PM-10 discharge (kg/ms),
 $C10$ = mean concentration of PM-10 particles (Mg/m³),
 $H10$ = height of PM-10 region over simulation region (m),
 $G10_{en}$ = net vertical flux of PM-10 from emission of loose soil (kg/m²s),
 $G10_{an}$ = net vertical flux of PM-10 from abrasion of clods and crust (kg/m²s), and
 $G10_{ss}$ = net vertical flux of PM-10 from breakdown of saltation and creep (kg/m²s).

SOURCE/SINK EQUATIONS FOR PM-10

The flux from emission is

$$G10_{en} = SF10_{en} SF_{ss_{en}} C_{en} (q_{en} - q) \quad (59)$$

where

- $SF10_{en}$ = soil fraction of PM-10 in the suspended soil that was emitted from the surface.

Similar to saltation and creep, a set of equations can be written for mass conservation of the suspension component.

$$\frac{\partial(\overline{C_{ss}H_{ss}})}{\partial t} = -\frac{\partial(q_{ss})_x}{\partial x} - \frac{\partial(q_{ss})_y}{\partial y} + G_{ss_{en}} + G_{ss_{an}} + G_{ss} - G_{tp} \quad (54)$$

where

- t = time (s),
- C_{ss} = mean concentration of suspension particles (Mg/m^3),
- q_{ss} = suspension discharge (kg/ms),
- H_{ss} = height of suspension region over simulation region field (m),
- x, y = horizontal distances in perpendicular directions that are parallel to the simulation boundaries,
- $G_{ss_{en}}$ = net vertical flux of suspension from emission of loose soil (kg/m^2s),
- $G_{ss_{an}}$ = net vertical flux of suspension from abrasion of clods and crust (kg/m^2s),
- G_{ss} = net vertical flux to suspension from breakdown of saltation and creep (kg/m^2s), and
- $G_{ss_{tp}}$ = net vertical flux of suspension from trapping of suspension (kg/m^2s).

SOURCE/SINK EQUATIONS FOR SUSPENSION

The emission flux is calculated as:

$$G_{ss_{en}} = SF_{ss_{en}} C_{en} (q_{en} - q) \quad (55)$$

where all the terms have all been defined previously.

The abrasion flux is calculated as

$$G_{ss_{an}} = SF_{ss_{an}} \sum_{i=1}^m (F_{ani} C_{ani}) q \quad (56)$$

The suspension flux from breakdown of saltation and creep, G_{ss} , was defined previously.

Suspension flux by trapping is simulated only when the suspension discharge passes over a subregion without active saltation to maintain the suspension flux near the surface. The

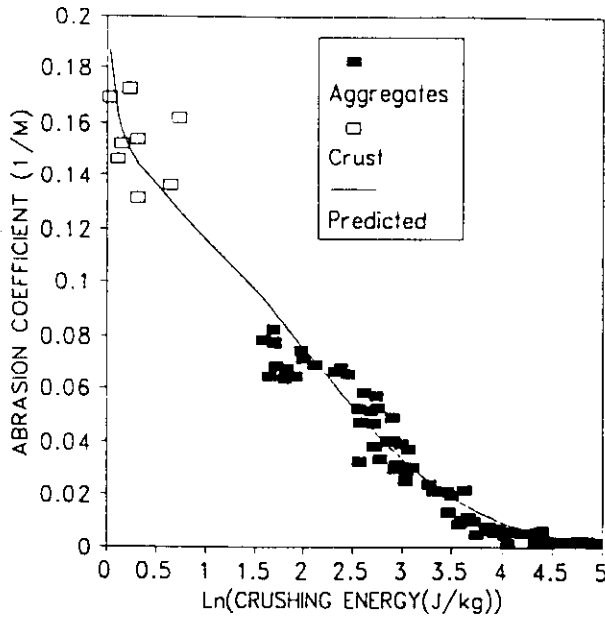


Figure E-21. Abrasion coefficients as a function of crushing energy for soil aggregates and crusts; predicted is equation E-49 (Hagen, Skidmore, and Saleh, 1992).

Suspension Flux:

The suspension component from breakdown of saltation and creep is simulated as

$$G_{ss} = C_{bk} q \tag{52}$$

where

- G_{ss} = suspension flux from breakdown of saltation and creep (kg/m^2s), and
- C_{bk} = coefficient of breakage ($1/m$).

The coefficient of breakage is estimated as

$$C_{bk} = 0.08 C_{canag} \tag{53}$$

CONSERVATION OF MASS FOR SUSPENSION

The preceding calculation assumes that residue and rocks are generally somewhat above the surrounding surface, and thus, intercept more saltation than indicated by their level of cover.

$$F_{anag} = (1 - SF_{84})(1 - SF_{cr}) F_{an} \quad (47)$$

$$F_{ancr} = (SF_{cr} - SF_{los}) F_{an} \quad (48)$$

The abrasion coefficient is a function of aggregate dry stability and was determined experimentally as (Fig. E-21) (Hagen, Skidmore, and Saleh, 1992)

$$C_{anag} = \exp[-2.07 - 0.077 SE_{ags}^{2.5} - 0.119 \ln(SE_{ags})] \quad (49)$$

and an estimate for crust abrasion coefficient is (Zobeck, 1991)

$$C_{ancr} = 1.0 C_{anag} \quad (50)$$

The soil fraction abraded from clod and crust that is of suspension size was determined experimentally as (Mirzamostafa and Hagen, 1995)

$$0.92 SF_{ss_{an}} = 0.92 SF_{cla}, \quad SF_{ss_{an}} < 0.4 \quad (51)$$

where

SF_{cla} = soil fraction clay in surface layer.

Abrasion Flux

The abrasion of soil clods and crust by saltation creates additional erodible aggregates. The abrasion flux from the soil surface area being abraded ($SA < 12$ degrees) can be computed for the surface portion that is not covered with residue, rocks, or aggregates less than creep size (Hagen, 1991c).

$$G_{an} = (1 - SF_{ss_{an}}) \left(\sum_{i=1}^m F_{ani} C_{ani} \right) q \quad (43)$$

where

- G_{an} = abrasion flux ($\text{kg}/\text{m}^2\text{s}$),
- $SF_{ss_{an}}$ = soil fraction of suspension size particles from abrasion
- F_{ani} = fraction of saltation abrading surface with i th abrasion coefficient,
- C_{ani} = abrasion coefficient of i th surface ($1/\text{m}$), and
- q = saltation and creep discharge entering control volume (kg/ms).

Auxiliary equations were developed to calculate the variables in the abrasion flux equation.

$$a2 = \frac{SF_{84} - SF_{10}}{SF_{200} - SF_{10}} \quad (44)$$

$$SF_{sn} = 1 - (1 - a2) \exp\left(-\frac{SFA_{12}}{20}\right) \quad (45)$$

where

- SF_{sn} = fraction of the saltation and creep that is saltation as a function of surface roughness and aggregate size distribution.

The fraction of moving soil abrading clods and crust, F_{an} , is

$$F_{an} = [1 - 4 BFF_{cv} - 2 SV_{roc}(1 - BFF_{cv})] SF_{sn}, \quad F_{an} > 0.0 \quad (46)$$

where

- BFF_{cv} = biomass fraction of flat cover, and
- SV_{roc} = soil volume with rock (m^3/m^3).

WEPS

EROSION SUBMODEL

E-33

$$G_{tp} = C_{tp}(q - q_{cp})q + C_i q \quad (36)$$

where

- C_i = coefficient of interception of standing biomass (1/m),
 C_{tp} = coefficient of trapping (kg s/m^3), and
 q_{cp} = transport capacity for saltation and creep (kg/ms).

Again, auxiliary equations were developed to calculate the variables in the trapping flux equation. For coefficient of interception,

$$C_i = \frac{BR_{sai}}{BZ} \quad (37)$$

For coefficient of trapping of ridged surface,

$$C_{tprg} = 0.75 \frac{SZ_{rg}}{SXP_{rg}} \quad (38)$$

For coefficient of trapping of random rough surface,

$$C_{tprr} = 0.0144 SAC, \quad (39)$$

Finally, choosing the maximum gives

$$C_{tp} = \max(C_{tprg}, C_{tprr}) \quad (40)$$

The transport capacity is calculated as

$$q_{cp} = C_s WU_{.p}^2 (WU_{.p} - WU_{.p}) \quad (41)$$

The threshold velocity for transport capacity depends mainly on the surface roughness and is calculated for a surface with 0.4 fraction of armor as

$$WU_{.p} = 0.8[1.7 - 1.35 \exp(-0.4 b_2)] \quad (42)$$

E-32

EROSION SUBMODEL

WEPS

The value of SFA_{12} can be calculated as follows:

$$SAC_{rg} = 65.4 \left(\frac{SZ_{rg}}{SXP_{rg}} \right)^{0.65} \quad (31)$$

$$SFA_{12} = \left[1 - \exp\left(-\frac{12}{SAC_{rg}}\right)^{0.77} \right] \left[\exp\left(-\frac{12}{sac}\right)^{0.77} \right] \quad (32)$$

The soil fraction of suspensions size in the emitted soil is estimated from the aggregate size distribution

$$SFSS_{en} = \frac{SF_{10}}{SF_{84}} \quad (33)$$

where

- SF_{10} = soil fraction less than 0.10 mm diameter, and
 SF_{84} = soil fraction less than 0.84 mm diameter.

Finally, the emission transport capacity is calculated with a widely used transport equation (Greeley and Iverson, 1985)

$$q_{en} = C_s WU_{.t}^2 (WU_{.t} - WU_{.c}) \quad (34)$$

where

- C_s = saltation transport parameter, value about 0.4 ($\text{kg s}^2/\text{m}^4$).

$$WU_{.t} = 0.8 WU_{.15} \quad (35)$$

The dynamic threshold friction velocity is calculated as

Trapping Flux

The saltation and creep are decreased whenever the discharge exceeds the transport capacity of the wind for a given surface condition. In addition, standing biomass intercepts saltation and creep. The trapping flux is calculated as (Hagen and Armbrust, 1992; Hagen, 1995)

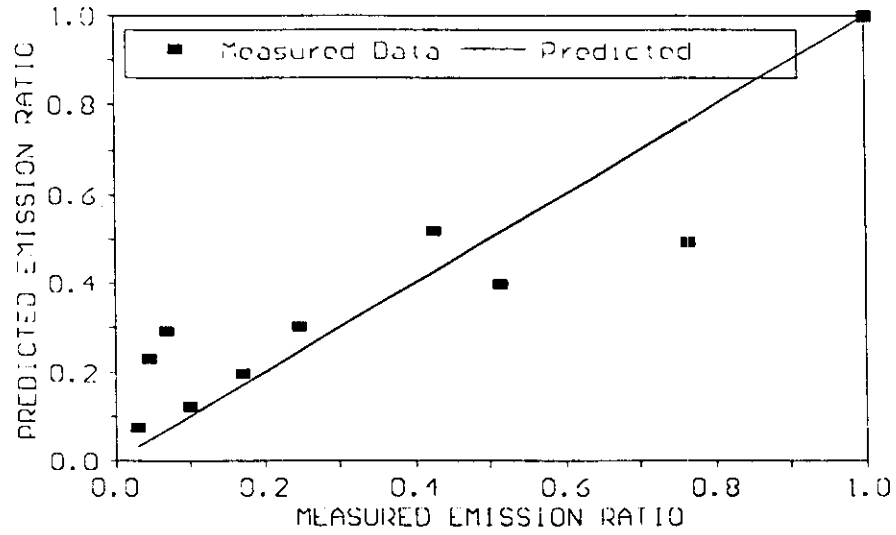


Fig. E-20. Predicted reduction is emission of loose soil compared to values measured in the wind tunnel; predicted is equation E-30 (Hagen, 1991b).

E-30

EROSION SUBMODEL

WEPS

The fractional reduction in emission coefficient to account for roughness and fraction not emitting of a bare soil is (Fig. E-19. and E-20),

$$R_{enb} = (1 - SF_{cv}) \exp(-2.5 SFA_{12}) \quad (30)$$

where

SFA_{12} = soil surface fraction with shelter angles greater than 12 degrees.

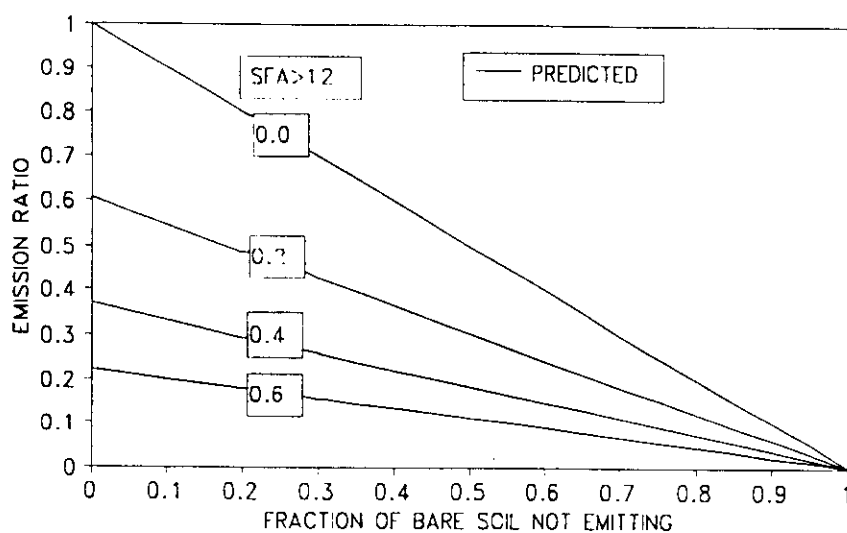


Figure E-19. Predicted reduction in emission of loose soil as a fraction of both soil fraction with shelter angle greater than 12 degrees and fraction of soil not emitting; predicted is equation E-30.

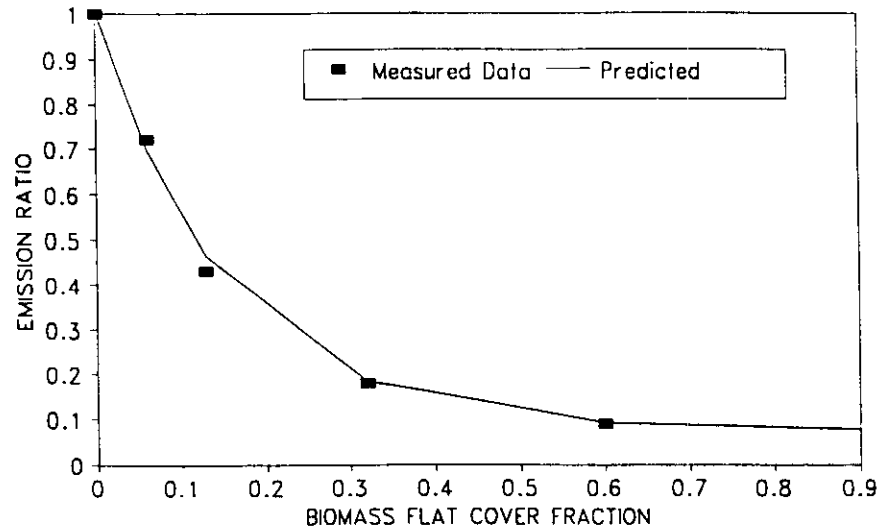


Figure E-18. Reduction in emission of loose soil as a function of increasing biomass flat cover; predicted is equation E-29 (Hagen, 1995).

E-28

EROSION SUBMODEL

WEPS

where

- C_{en} = coefficient of emission (1/m),
 $SF_{ss_{en}}$ = soil fraction of suspension size in loose soil emitted, and
 q_{en} = transport capacity for emission calculated using
 dynamic threshold friction velocity (kg/m² s).

A simplified form of the emission flux equation was tested on a highly erodible, sandy field and provided a good fit to the measured data (Stout, 1990).

For the complex surfaces simulated in EROSION, auxiliary equations were developed to estimate the variables in the emission flux equation. The emission coefficient is calculated as a function of surface complexity as

$$C_{en} = C_{eno} R_{enb} R_{env} \quad (28)$$

where

- C_{eno} = coefficient of emission for a bare, smooth, loose, erodible soil.
 Typical value is about 0.06 (1/m).

The fractional reduction in emission coefficient to account for flat biomass cover is (Hagen, 1995) (Fig. E-18),

$$R_{env} = 0.075 + 0.934 \exp\left(-\frac{BFF_{cv}}{0.149}\right) \quad (29)$$

WEPS

EROSION SUBMODEL

E-27

$$q = (\bar{C}H) \bar{V}_p \quad (23)$$

$$\bar{V}_p = K_p WU. \quad (24)$$

$$q_x = (EU./WU.)q \quad (25)$$

$$q_y = (EV./WU.)q \quad (26)$$

where

- x, y = horizontal distances in perpendicular directions parallel to the simulation region boundaries (m),
 t = time (s),
 C = average concentration of saltating particles in the control volume of height H (kg/m^3),
 q_x, q_y = components of the saltation discharge, q , in the x and y directions, respectively (kg/ms),
 V_p = average horizontal saltation particle velocity (m/s),
 K_p = proportionality coefficient,
 $WU.$ = surface friction velocity (m/s),
 $EU., EV.$ = components of the horizontal friction velocity, $WU.$, in the x and y directions, respectively, (m/s),
 $G_{en}, G_{an}, G_{ip}, G_{ss}$ = Net vertical soil fluxes from emission of loose soil, surface abrasion of aggregates/crusts, trapping of saltation, and suspension of fine particles from breakdown of saltation/creep, respectively ($\text{kg}/\text{m}^2\text{s}$).

SOURCE/SINK EQUATIONS FOR SALTATION AND CREEP

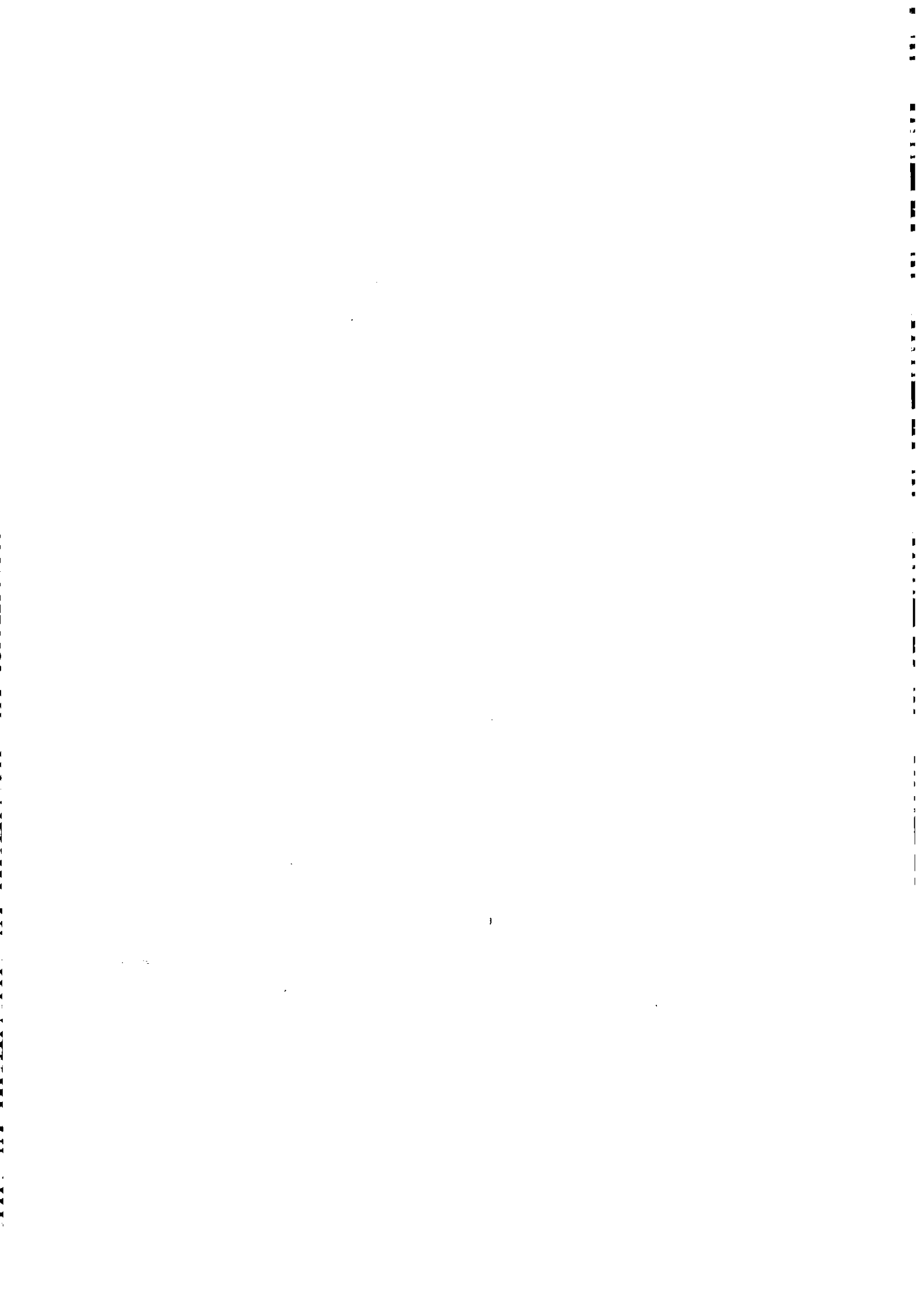
Emission Flux

For the loose, erodible portion of the soil, the emission flux can be simulated as

$$G_{en} = C_{en}(1 - SF_{ss_{en}})(q_{en} - q) \quad (27)$$

HYDROLOGY SUBMODEL





HYDROLOGY SUBMODEL

A. A. Durar and E. L. Skidmore

INTRODUCTION

The HYDROLOGY submodel of the Wind Erosion Prediction System (WEPS) uses inputs generated by other WEPS submodels such as WEATHER, CROP, SOIL, MANAGEMENT, and DECOMPOSITION to predict the water content in the various layers of the soil profile and at the soil-atmosphere interface throughout the simulation period. Accurate simulation by the other WEPS submodels requires prediction of the daily changes in soil water profiles. However, estimating soil wetness at the soil-atmosphere interface is emphasized, because it significantly influences the susceptibility of the soil to wind erosion.

The HYDROLOGY submodel of WEPS maintains a continuous, daily, soil water balance using the equation:

$$SWC = SWCI + (PRCP + DIRG) + SNOW - RUNOFF - ETA - DPRC \quad (1)$$

where SWC is the amount of water on the soil profile in any given day (mm), SWCI is the initial amount of water in the soil profile (mm), PRCP is the amount of daily precipitation (mm), DIRG is the amount of daily irrigation (mm), SNOW is the daily snow melt minus daily snow accumulation (mm), RUNOFF is the amount of daily surface runoff (mm), ETA is the amount of daily actual evapotranspiration (mm), and DPRC is the amount of daily deep percolation (mm).

The amount of daily precipitation (PRCP) is partitioned between rainfall and snowfall on the basis of the average daily air temperature. If the average daily temperature is 0°C or below, the precipitation takes the form of snowfall; otherwise, it takes the form of rainfall.

The snow term (SNOW) can be either positive, equaling the daily snow melt, or negative, equaling the daily snow accumulation. The melted snow is treated as rainfall and added to the precipitation term in Eq. H1 when accounting for daily runoff and infiltration. On the other hand, the accumulated snow is subtracted from the daily precipitation during the estimation of the daily soil water balance with Eq. H-1.

Simulation of soil-water dynamics on a daily basis by the HYDROLOGY submodel involves three major sequences. First, the submodel partitions the total amount of water available from precipitation, irrigation, and/or snow melt into surface runoff and infiltration. The submodel stores the daily amount of water available for infiltration into the soil profile. Second, the submodel determines the influence of ambient climatic conditions by calculating the potential evapotranspiration. Third, the submodel redistributes soil water in the soil profile on an hourly basis, which provides hourly estimations of water content in the soil profile. The submodel estimates the actual rate of evapotranspiration by adjusting the potential rate on the basis of soil water availability. Deep percolation from the soil profile is estimated to be equal to the conductivity of the lowermost simulation layer, assuming a unit hydraulic gradient.

The HYDROLOGY submodel estimates surface runoff and infiltration for each simulation day that has precipitation and/or irrigation. If measured daily runoff associated with the precipitation and/or irrigation event is available, it is entered as an input to the computer simulation of soil-water dynamics, and daily infiltration is computed simply as precipitation and/or irrigation minus runoff. However, if measured runoff data are not readily available, as is often the case, then a daily estimate of runoff is made using a modified version of the Soil Conservation Service (SCS) soil-cover complex method, which usually is referred to as the curve number (SCS-CN) method. The SCS-CN technique relates runoff to soil properties, antecedent soil moisture conditions, hydrologic conditions of the ground cover, and land use and management practices (Soil Conservation Service, 1972). However, the runoff component of the HYDROLOGY submodel contains four major modifications to the standard SCS-CN method. First, the submodel adjusts the tabulated curve numbers to account for the effects of slope on runoff. Second, the HYDROLOGY submodel uses the daily estimates of crop canopy from the CROP submodel to evaluate the daily conditions of the ground cover. Third, the submodel uses the status of soil wetness in the uppermost simulation layer to directly evaluate the antecedent soil moisture conditions instead of using the antecedent rainfall index. Fourth, the submodel includes a provision for estimating the increase in runoff under frozen soil conditions.

The submodel estimates the daily amount of water available for infiltration into the soil by subtracting the amount of daily surface runoff from the amount of daily precipitation, snow melt, and/or irrigation. The infiltration water is stored in the uppermost simulation layer, until its water content reaches field capacity. Any excess water then is added to the succeeding lower layer, where it is stored with the same maximum storage restriction. This is repeated until complete water storage is obtained. Any excess water that flows out from the lowermost simulation layer becomes a part of a deep percolation.

Potential evapotranspiration is calculated using a revised version of Penman's combination method (Van Bavel, 1966). The total daily rate of potential evapotranspiration then is partitioned on the basis of the plant leaf area index into potential soil evaporation and

WEPS**HYDROLOGY SUBMODEL****H-3**

potential plant transpiration. The potential rate of soil evaporation is adjusted to account for the effect of plant residues in the simulation region. Furthermore, the daily potential rates of soil evaporation and plant transpiration are adjusted to actual rates on the basis of water availability in the soil profile.

The HYDROLOGY submodel uses a simplified forward finite-difference technique to redistribute soil water with the one-dimensional Darcy equation for water flow. The time step of the soil water redistribution section is 1 hour, which allows for an hourly estimation of soil wetness as needed for WEPS. Knowledge of the relationship between unsaturated hydraulic conductivity and soil water content is required for solving the governing transport equations of water movement through the soil. The submodel uses Campbell's (1974) method to calculate the unsaturated hydraulic conductivity of the soil from the more readily available soil water characteristic curve and saturated hydraulic conductivity data. Because water release curve data of the soil are not always available, the submodel provides alternative options to estimate the hydraulic parameters of the water release curve that are needed as inputs to run the soil water redistribution segment of the submodel.

The HYDROLOGY submodel predicts on an hourly basis soil wetness at the soil-atmosphere interface by using a combination of two techniques. The submodel extrapolates water content to the soil surface from the three uppermost simulation layers. A numerical solution known as Cramer's rule (Miller, 1982) is used to obtain an estimate of the extrapolated water content at the soil surface by solving the three simultaneous equations that describe the relationship between water content and soil depth for the three uppermost simulation layers. The submodel also interpolates the functional relationship between surface-soil wetness and the hourly evaporation ratio.

SUBMODEL DEVELOPMENT AND DESCRIPTION

Some of the algorithms used in the HYDROLOGY submodel are similar to those used in well-established models such as SPAW (Saxton and Bluhm, 1982; Saxton et al., 1974; 1984; Sudar et al., 1981), CREAMS (Smith and Williams, 1980), and EPIC (Williams et al., 1984; 1990). Significant modifications were made, however, and new algorithms were added to meet the unique requirements of WEPS for fast simulation of the diurnal changes in soil water content, particularly at the soil-atmosphere interface.

Snow Melt

The snow melt component of the HYDROLOGY submodel of WEPS is similar to that of the CREAMS model (Smith and Williams, 1980) and the EPIC model (Williams, 1989; Williams et al., 1984; 1990). If snow is present at any simulation day, it is melted when the maximum daily air temperature exceeds 0°C using the equation:

$$\begin{aligned} SNMLT &= 4.57 TMAX & SNMLT < SNWC \\ SNMLT &= SNWC & SNMLT \geq SNWC \end{aligned} \quad (2)$$

where SNMLT is the rate of snow melt (mm/day), SNWC is the water content of snow before melt occurs (mm), and TMAX is the maximum daily air temperature (°C).

Surface Runoff

The HYDROLOGY submodel estimates daily infiltration for each simulation day that has precipitation and/or irrigation. If measured daily runoff associated with the precipitation and/or irrigation event is available, it is entered as an input to the computer simulation of soil-water dynamics, and daily infiltration is computed simply as precipitation and/or irrigation minus runoff. However, if measured runoff data are not readily available, as is often the case, then a daily estimate of runoff is made by a modified version of the Soil Conservation Service (SCS) soil-cover complex method, which usually is referred to as the curve number (SCS-CN) method. The SCS-CN technique was selected because (1) it is a reliable procedure that has been used for many years by such credible simulation models as SPAW (Saxton and Bluhm, 1982; Saxton et al., 1974; 1984; Sudar et al., 1981), CREAMS (Smith and Williams, 1980), and EPIC (Williams, 1989; Williams et al., 1984; 1990); (2) it is computationally efficient; (3) it uses readily available data such as daily rainfall as an input; and (4) it relates runoff to soil properties, antecedent soil moisture conditions, hydrologic conditions of the ground cover, and land use and management practices.

WEPS

HYDROLOGY SUBMODEL

H-5

The combination of a hydrologic soil group (soil) and a land use and treatment class (cover) is referred to by the SCS as a hydrologic soil-cover complex. The standard SCS-CN procedure (Soil Conservation Service, 1972) uses a series of tables and graphs to assign runoff curve numbers (CN) for hydrologic soil-cover complexes. The CN of a soil-cover complex indicates the runoff potential of the complex when the soil is not frozen. The higher the CN, the higher is the runoff potential of the soil-cover complex. The procedure uses an antecedent rainfall index to estimate antecedent soil moisture as one of three types, I, II, and III for dry, normal, and wet conditions, respectively. The relationship between rainfall and runoff for these three conditions is expressed as a curve number (CN).

The SCS curve number equation is:

$$\begin{aligned} \text{RUNOFF} &= (\text{DH20} - 0.2\text{S})^2 / (\text{DH20} + 0.8\text{S}) & \text{DH20} > 0.2\text{S} \\ \text{RUNOFF} &= 0.0 & \text{DH20} \leq 0.2\text{S} \end{aligned} \quad (3)$$

where RUNOFF is the daily runoff (mm); DH20 is the total daily amount of water from precipitation, snow melt, and/or irrigation (mm); and S is the retention parameter (mm).

The retention parameter (S) varies according to the hydrologic properties of the soil-cover complex in the simulation region. It is estimated on the basis of a curve number, which reflects the effects of soil properties, antecedent soil moisture conditions, land use, and soil cover hydrologic conditions. The curve number (CN) is related to the retention parameter using the equation:

$$S = 254(100/\text{CN} - 1) \quad (4)$$

where CN is the calculated curve number.

A modification to the standard SCS-CN method similar to the one adopted by the SPAW model (Saxton and Bluhm, 1982; Saxton et al., 1974; 1984; Sudar et al., 1981) is used in the HYDROLOGY submodel to incorporate the predicted daily estimates of crop canopy by the CROP submodel of WEPS and improve the accuracy of runoff simulation. To adjust the curve number, the tabulated CN values (Table H1) under poor and good crop conditions are prorated according to the daily estimated value of crop canopy. The selection of the correct hydrologic soil group is based on the criteria listed in Table H-2.

H-6

HYDROLOGY SUBMODEL

WEPS

Table H-1. Runoff curve numbers for hydrologic soil-cover complexes (Class II antecedent moisture conditions).

Land use	Cover		Hydrologic soil group			
	Treatment or practice	Hydrologic condition	A	B	C	D
Fallow	straight row	---	77	86	91	94
Row crops	straight row	poor	72	81	88	91
	straight row	good	67	78	85	89
	contoured	poor	70	79	84	88
	contoured	good	65	75	82	86
	contoured and terraced	poor	66	74	80	82
	contoured and terraced	good	62	71	78	81
Small grain	straight row	poor	65	76	84	88
	straight row	good	63	75	83	87
	contoured	poor	63	74	82	85
	contoured	good	61	73	81	84
	contoured and terraced	poor	61	72	79	82
	contoured and terraced	good	59	70	78	81
Close-seeded legumes* or rotation meadow	straight row	poor	66	77	85	89
	straight row	good	58	72	81	85
	contoured	poor	64	75	83	85
	contoured	good	55	69	78	83
	contoured and terraced	poor	63	73	80	83
	contoured and terraced	good	51	67	76	80
pasture or range		poor	68	79	86	89
		fair	49	69	79	84
		good	39	61	74	80
	contoured	poor	47	67	81	88
	contoured	fair	25	59	75	83
	contoured	good	6	35	70	79
Meadow		good	30	58	71	78
Woods		poor	45	66	77	83
		fair	36	60	73	79
		good	25	55	70	77
Farmsteads		---	59	74	82	86
Roads	dirt**	---	72	82	87	89
	hard surface**	---	74	84	90	92

Source: Soil Conservation Service (1972)

* Close-drilled or broadcast-seeded

** Including right-of-way

Table H-2. Criteria for selecting the correct hydrologic soil group.

Hydrologic soil group	Final infiltration rate (m/s)	Soil characteristics
A	2.117E-06 - 3.175E-06	Deep sand, deep loess, aggregated silts
B	1.058E-06 - 2.117E-06	Shallow loess, sandy loam
C	3.528E-07 - 1.058E-06	Clay loams, shallow sandy loam, soils low in organic content, and soils usually high in clay
D	0 - 3.528E-07	Soils that swell significantly when wet, heavy plastic clays, certain saline soils, soils with permanent high water table, and shallow soils over nearly impervious material

Source: Hjelmfelt, Jr. and Cassidy (1975) and Soil Conservation Service (1972).

The difference (CNDIF) between the SCS curve numbers for poor (CNIP) and good (CNIIG) soil-cover hydrologic conditions for the average antecedent soil moisture conditions (class II) is calculated

$$CNDIF = CNIP - CNIIG \quad (5)$$

The calculated runoff curve number for class II antecedent soil moisture conditions is then adjusted according to the daily estimate of crop canopy using the equation

$$CNII = CNIP - (CNDIF * CANP) \quad (6)$$

where CANP is the daily estimate of crop canopy (ratio of ground cover), and CNII is the curve number for class II antecedent soil moisture conditions.

Furthermore, an adjustment similar to the one proposed by the EPIC model (Williams, 1989; Williams et al., 1984; 1990) is used to express the effects of slope on runoff. This adjustment is based on the assumption that the tabulated curve number values in the handbook (Soil Conservation Service, 1972) are appropriate only for a 5% slope. The equation for adjusting the handbook curve number values is

$$CNIIS = 1/3 (CNIII - CNII)(1 - 2 \exp(-13.86SLP)) + CNII \quad (7)$$

where CNIIS is the curve number for class II antecedent soil moisture conditions adjusted for slope, SLP is the average slope of the simulation region (m/m), and CNIII is the curve number for class III antecedent soil moisture conditions.

The class III antecedent soil moisture conditions (CNIII) is related to class II with the equation

$$CNIII = 6.9368 + 1.6425 CNII - 0.0071 CNII^2 \quad (8)$$

With the standard curve number method (Soil Conservation Service, 1972), the antecedent rainfall index is used to evaluate antecedent soil moisture conditions. However, this is no longer necessary, because direct evaluation of antecedent soil moisture conditions can be obtained from the simulation of soil water dynamics by the HYDROLOGY submodel. The surface runoff component of the submodel uses a procedure similar to the one used in the SPAW model (Saxton and Bluhm, 1982; Saxton et al., 1974; 1984; Sudar et al., 1981) to adjust the calculated curve number from Eq. H7 for the type II antecedent soil moisture condition according to the current status of surface soil moisture. If the soil water content of the uppermost simulation layer is less than 60% of the field capacity, the curve number is adjusted to the type I condition. On the other hand, if the soil water content of the top simulation layer is greater than field capacity, the curve number is adjusted to the type III condition. The slope-adjusted curve number values for antecedent soil moisture condition types I and III are related to type II with the following equations:

$$CNIS = 0.4678 (1.0113)^{CNIS} (CNIS)^{0.9191} \quad (9)$$

$$CNIIS = 6.9368 + 1.6425 CNIIS - 0.0071 CNIIS^2 \quad (10)$$

where CNIS is the slope-adjusted curve number for class I antecedent soil moisture conditions, CNIIS is the slope-adjusted curve number for class II antecedent soil moisture conditions, and CNIIS is the slope-adjusted curve number for class III antecedent soil moisture conditions. Therefore, the calculated curve number used in Eq. H4 to determine the retention parameter will be equal to one of the three curve numbers (CNIS, CNIIS, or CNIIS) according to the current status of surface soil moisture. Equations H9 and H10 were obtained by regression analysis of the tabulated data (Hjelmfelt, Jr. and Cassidy, 1975; Soil Conservation Service, 1972). The coefficients of determination (r^2 values) for Eq. H9 and Eq. H10 are 1.00 and 0.99, respectively.

Finally, a refinement of the retention parameter (S) will be added to account for the increase in runoff under frozen soil conditions. An equation similar to the one used in the EPIC model (Williams, 1989; Williams et al., 1984; 1990) is used to determine the frozen ground retention parameter when the temperature of the surface soil is less than 0°C.

$$SF = S [1 - \exp(-0.00292 S)] \quad (11)$$

where SF is the frozen ground retention parameter (mm).

Hence, the surface runoff component is linked with the rest of the HYDROLOGY submodel as well as other WEPS submodels, such as CROP, to maintain a continuous daily soil-water balance.

Soil Water Storage

The soil-water storage segment of the HYDROLOGY submodel of WEPS is similar to that of the SPAW model (Saxton and Bluhm, 1982; Saxton et al., 1974; 1984; Sudar et al., 1981). The submodel estimates the daily amount of water available for infiltration into the soil by subtracting the amount of daily surface runoff from the amount of daily precipitation, snow melt, and/or irrigation. However, the submodel does not give time distribution to the predicted daily infiltration.

The water is added to the uppermost simulation layer, until its water content reaches field capacity; then any excess water is cascaded downward to succeeding layers and stored without exceeding field capacity, until adequate storage is achieved. Any excess water that infiltrates below the lower boundary layer becomes a part of deep percolation. The soil-water redistribution segment of the submodel carries out all further water redistribution in the simulation.

Potential Evapotranspiration

Potential evapotranspiration is calculated using the revised combination method of Van Bavel (1966), which combines a surface energy balance equation and an approximate expression of water vapor and sensible heat transfer as influenced by surface roughness and ambient air properties. Van Bavel considered his method an improvement over the original version of the combination equation (Penman, 1948), because it contains no empirical constants or functions.

Van Bavel (1966) conducted an extensive validation of his method at Phoenix, Arizona, concluding that the method provides an excellent estimation of potential evapotranspiration on an hourly and daily basis under a wide variety of test conditions. Further evaluation of the combination method of Van Bavel in Kansas (Skidmore et al., 1969) and Texas (Wendt, 1970) showed that it can provide reasonably good estimates of potential evapotranspiration, particularly in areas with large amounts of advection. Furthermore, Jensen (1974) evaluated 16 different methods to estimate potential evapotranspiration at 10 different locations throughout the world. The elevations of these sites ranged from 30 m below sea level to 2774 m above sea level, and the latitudes ranged from 38°S at Victoria, Australia to 56°N at Copenhagen, Denmark. He then ranked Van Bavel's method as one of the best methods to estimate potential evapotranspiration especially in the inland semi-arid to arid regions.

For use on a daily basis, the Van Bavel equation is expressed as:

H-10

HYDROLOGY SUBMODEL

WEPS

$$ETP = \frac{(SVPG (H/VLH)) + ((TTC) (VPD))}{(SVPG + 1)} \quad (12)$$

where ETP is the potential evapotranspiration (mm/day), H is the sum of surface energy inputs (MJ/m²/day), and SVPG is the adjusted ratio of the slope of the saturation vapor pressure curve taken at mean air temperature to the psychrometric constant. The ratio is adjusted according to the ambient barometric pressure, TTC is the turbulent transfer coefficient for water vapor (kg/m²/kPa/day), and VPD is the saturation vapor pressure deficit of air (kPa).

Because the psychrometric constant is proportional to the ambient pressure, the adjusted ratio of the slope of the saturation vapor pressure curve to the psychrometric constant (SVPG) is estimated with the equation:

$$SVPG = SVPGO (101.325/ BP) \quad (13)$$

where SVPGO is the unadjusted ratio of the slope of the saturation vapor pressure curve taken at mean air temperature to the psychrometric constant, and BP is the ambient barometric pressure (kPa).

The (SVPGO) term in Eq. H13 is a dimensionless number dependent on air temperature. The tabulated values of the term are listed versus air temperature in Table 5 of Van Bavel's (1966) article. However, to simplify the computation of the term in our computer coding, the data of the table were regressed, and the following expression of (SVPGO) as a function of temperature was obtained:

$$SVPGO = 67.5242 \exp\left(\frac{(TAIR - 149.531)^2}{-4859.0665}\right) \quad (14)$$

where TAIR is the mean daily air temperature (°C). The coefficient of determination (r²) for Eq. H14 is 1.00.

The U.S. Standard Atmosphere, 1976 (NOAA, NASA, and USAF, 1976), which is an idealized, steady-state representation of the earth's atmosphere, provides an approximation of atmospheric pressure that is sufficiently accurate for estimating potential evapotranspiration. The tabulated data of that report were regressed, and the following expression of atmospheric pressure as a function of elevation was obtained:

$$BP = 824.4996 \exp\left(\frac{(ELEV + 35702.8022)^2}{-607940000}\right) \quad (15)$$

WEPS

HYDROLOGY SUBMODEL

H-11

where BP is the barometric pressure (kPa), and ELEV is the elevation of the site (m). The coefficient of determination (r^2) for Eq. H15 is 1.00. The range of elevations used in the regression analysis was between -500 m and 30,000 m.

The daily sum of surface energy inputs (H) can be computed using the equation

$$H = RN + G \quad (16)$$

where RN is the net radiation (MJ/m²/day), and G is the soil heat flux (MJ/m²/day).

However, soil heat flux data, are not always readily available, and the soil heat flux is often negligible on a daily basis. Therefore, the soil heat flux component of the daily surface energy balance is ignored, and the daily sum of surface energy inputs is assumed to equal the daily net radiation.

Whenever net radiation data are not available, the HYDROLOGY submodel of WEPS estimates daily net radiation from solar radiation, air temperature, and vapor pressure using Wright's modified version of Penman's general relationship outlined by Allen et al. (1989) as:

$$RN = [(1-ALBEDO)RS - BC \frac{(T_{max}^4 + T_{min}^4)}{2}] \quad (17)$$

$$(AI - 0.139\sqrt{E})(A \frac{RS}{RSO} + B)$$

where ALBEDO is the albedo (reflectance) of the surface; RS is the measured solar radiation (MJ/m²/day); BC is the Stephan-Boltzman constant (4.903×10^{-9} MJ/m²/day/K⁴); T_{max} is the maximum daily air temperature (K); T_{min} is the minimum daily air temperature (K); E is the saturation vapor pressure at the dew-point temperature (kPa); RSO is the clear sky short wave radiation (MJ/m²/day); and AI, A, B are empirical coefficients.

The empirical coefficients in Eq. H17 were estimated by Wright (1982) as:

$$AI = 0.26 + 0.1 \exp[-0.0154(IDOY - 180)]^2 \quad (18)$$

where IDOY is the day of year (1 to 366). A and B are affected by the ratio RS/RSO, which indicates cloudiness. For RS/RSO > 0.7, which indicates few clouds, A = 1.126 and B = -0.07. For RS/RSO < 0.7, which indicates prevalent clouds, A = 1.017 and B = -0.06.

RSO, which is the clear sky radiation, was estimated as:

H-12

HYDROLOGY SUBMODEL

WEPS

$$RSO = 0.75 RA \quad (19)$$

where RA is extraterrestrial radiation (MJ/m²/day). RA was estimated using the following equation by Duffie and Beckman (1980):

$$RA = (24(60)/\Pi)(GSC)(DR)[(WS)SIN(RLAT)SIN(SIGMA) + COS(RLAT)COS(SIGMA)SIN(WS)] \quad (20)$$

where GSC is the solar constant (MJ/m²/min), DR is the relative distance of the earth from the sun, RLAT is the latitude of the station in radians, WS is the sunset hour angle (radians), and SIGMA is the declination of the sun. GSC was determined to be 0.08202 MJ/m²/min (London and Frohlich, 1982). DR, WS, and SIGMA in Eq. H20 were determined from the following equations:

$$DR = 1 + 0.033 \cos(2\Pi IDOY/365) \quad (21)$$

$$WS = \text{ARCCOS}(-\text{TAN}(\text{RLAT})\text{TAN}(\text{SIGMA})) \quad (22)$$

$$SIGMA = 0.4093 \sin(2\Pi(284 + IDOY)/365) \quad (23)$$

The latent heat of vaporization (VLH) varies with temperature. A regression analysis was performed on the tabulated temperature-latent heat data in Table 2.1 of Hillel (1971), and the following expression of latent heat as a function of temperature was derived:

$$VLH = 2.500277 - 0.002364 \text{ TAIR} \quad (24)$$

where VLH is the latent heat of vaporization (MJ/kg), and TAIR is the mean daily air temperature (°C). The coefficient of determination (r^2) for Eq. H24 is 1.00. The range of temperatures used in the regression analysis was between -10 °C and 50 °C.

The saturation vapor pressure deficit of air is estimated using the equation

$$VPD = VPS - VPA \quad (25)$$

where VPD is the saturation vapor pressure deficit (kPa), VPS is the saturation vapor pressure (kPa), and VPA is the actual vapor pressure (kPa).

The daily saturation vapor pressure is calculated as the average of the saturation vapor pressure at minimum and maximum daily air temperatures.

WEPS

HYDROLOGY SUBMODEL

H-13

$$VPS = (VPSMN + VPSMX) / 2 \quad (26)$$

where VPSMN is the saturation vapor pressure at minimum air temperature (kPa), and VPSMX is the saturation vapor pressure at maximum air temperature (kPa).

The saturation vapor pressure at minimum and maximum air temperatures can be estimated using the equations

$$VPSMN = 129.07487 \exp\left(\frac{(TMIN - 149.195)^2}{-4160.7968}\right) \quad (27)$$

$$VPSMX = 129.07487 \exp\left(\frac{(TMAX - 149.195)^2}{-4160.7968}\right) \quad (28)$$

where TMIN is the daily minimum air temperature (°C), and TMAX is the daily maximum air temperature (°C).

The actual vapor pressure can be estimated as a function of dew-point temperature using the equation

$$VPA = 129.07487 \exp\left(\frac{(TDP - 149.195)^2}{-4160.7968}\right) \quad (29)$$

where TDP is the mean daily dew-point temperature (°C). Equations H27, H28, and H29 were obtained by regression analysis of the tabulated vapor pressure versus temperature data as listed in the Smithsonian meteorological tables (List, 1971). The coefficient of determination (r^2) for the equations is 1.00. The range of temperatures used in the regression analysis was between 0 °C and 40 °C.

The turbulent transfer coefficient for water vapor is estimated with the equation

$$TTC = \{(ARHO)(E)(VK)^2(U+86400)\} / \{(BP)[LOG(ZA/ZO)]^2\} \quad (30)$$

where TTC is the turbulent transfer coefficient (kg/m²/kPa/day), ARHO is the density of air (kg/m³), E is the water-air molecular weight ratio, VK is the Von Karman's constant, BP is the barometric pressure (kPa), U is the mean daily wind speed (m/s), ZA is the height of measurement of meteorological sensors (m), and ZO is the roughness parameter (m).

The Von Karman's constant (VK) is usually used as a universal, dimensionless constant in turbulent flow. Its value has been determined to be near 0.4, with a range of 0.36 to 0.43. However, for Eq. H30 calculations, the (VK) value is assumed to be equal to 0.41.

The (E) term in Eq. H30 is a dimensionless constant equal to 0.622, which represents the ratio of water-vapor/air molecular weights. The term (ZA) represents the height of temperature, humidity, radiation, and wind speed measurements.

The roughness parameter (ZO), which is sometimes referred to as the roughness thickness or length, is defined as the actual height above the bare soil surface at which the wind velocity extrapolates to zero. It is related directly to the maximum height of surface protuberances. When the wind blows across a bare soil surface, it is usually slowed down by any surface protuberance (i.e., surface ripples, clods, or individual soil grains) that cause its velocity to decrease to zero. The zero plane elevation is slightly above the average height of the bare soil surface but below the top of soil surface irregularities. Jensen (1974) evaluated 16 different methods to calculate potential evapotranspiration, including the Van Bavel's combination method with various values for (ZO) and found that the Van Bavel method with $ZO = 0.0025$ m gave the best estimates of potential evapotranspiration, particularly in the inland-semiarid to arid regions. Therefore, the (ZO) term in Eq. H30 was assumed as a constant equal to 0.0025 m. In the future validation of the submodel, we will evaluate changing the roughness parameter of vegetated surfaces using the equation proposed by Jacobs and Von Boxel (1988).

$$ZO = 0.063 CH \quad (31)$$

where CH is the crop height (m).

The air density (ARHO) is directly proportional to ambient pressure and inversely proportional to temperature. It is estimated by the equation:

$$ARHO = 1000 \{ [BP/101.325][0.001293/(1+0.00367(TAIR))] \} \quad (32)$$

where ARHO is the density of air (kg/m^3), BP is the ambient pressure (kPa), and TAIR is the mean daily air temperature ($^{\circ}\text{C}$). Eq. H32 is a revised version of the density of dry air equation listed in the CRC Handbook of Chemistry and Physics (Weast et al., 1983).

Furthermore, Skidmore et al. (1969) proposed that Van Bavel's (1966) combination equation can be separated into two terms to get estimates of the potential evapotranspiration by radiation and wind. Accordingly, Eq. H12 can be rewritten as follows:

$$ETPR = \frac{(SVPG (H/VLH))}{(SVPG + 1)} \quad (33)$$

$$ETPW = \frac{((TTC) (VPD))}{(SVPG + 1)} \quad (34)$$

where ETPR is the potential evapotranspiration by radiation (mm/day), and ETPW is the potential evapotranspiration by wind (mm/day).

Potential Soil Evaporation and Plant Transpiration

The total daily potential evapotranspiration (ETP) as computed with Eq. H12 is then partitioned on the basis of the plant leaf area index into potential soil evaporation (EP) and potential plant transpiration (TP). The plant leaf area index, which is defined as the area of plant leaves relative to the land area, is estimated on a daily basis by the CROP submodel of WEPS.

Firstly, the daily potential soil evaporation is estimated with an equation that was proposed originally by Richardson and Ritchie (1973).

$$EP = ETP \exp(-0.398 PLAI) \quad (35)$$

where ETP is the potential evapotranspiration (mm/day), EP is the potential soil evaporation (mm/day), and PLAI is the plant leaf area index.

Secondly, the potential plant transpiration then is estimated by subtraction

$$TP = ETP - EP \quad (36)$$

where TP is the potential plant transpiration (mm/day).

As described earlier in the snow melt section, snow is melted during days when the maximum daily air temperature exceeds 0°C. However, if there is any remaining snow cover, soil evaporation is considered to come first from the snow and then from the soil. Furthermore, the potential soil evaporation is reduced with increased plant residues using an equation similar to that of the WEPP model (Savabi et al., 1989), which is based on the research conducted by Steiner (1989)

$$EP = EP \exp(-0.000064 PRES) \quad (37)$$

where PRES is the amount of plant residues on the soil surface (kg/hectare). It is estimated on a daily basis by the DECOMPOSITION submodel of WEPS.

Furthermore, the daily potential rates of soil evaporation and plant transpiration are adjusted to actual rates on the basis of soil water availability.

Actual Plant Water Uptake and Water Stress Factor

The HYDROLOGY submodel estimates actual plant water uptake and plant growth water stress factor using an approach similar to that of the EPIC (Williams, 1989; Williams et al., 1984; 1990) and WEPP (Savabi et al., 1989) models. Firstly, the potential plant transpiration is distributed in the root zone with the equation

$$WUP(i) = \frac{TP}{(1-\exp(-WUD))} * (1 - \exp(-WUD * (\frac{DLAYR(i)}{PRTD}))) - TWU \quad (38)$$

where WUP(I) is the potential plant water-uptake from soil layer I (mm/day), TP is the potential plant transpiration (mm/day), WUD is the water use distribution parameter, DLAYR(I) is the depth to the bottom of soil layer I, from the soil surface (m), PRTD is the plant root zone depth (m), and TWU is the accumulated actual water use from the soil layers above layer I (mm).

The HYDROLOGY submodel of WEPS uses a depth parameter (WUD) of 3.065 based on the assumption that about 30% of the total water use comes from the top 10% of the soil root zone. Williams and Hann (1978) described in more detail how to evaluate the water use distribution parameter.

The potential water use in each soil layer is modified on the basis of soil water availability to obtain the actual water use.

$$\begin{aligned} WUA(i) &= WUP(i) & AWCR(i) &\geq 0.70 \\ WUA(i) &= WUP(i) * AWCR(i) & AWCR(i) &< 0.70 \end{aligned} \quad (39)$$

where WUA(I) is the actual plant water-uptake from soil layer I (mm/day), and AWCR(I) is the relative amount of available water content from soil layer I.

The relative amount of available water content (AWCR) for each simulation layer is a fraction (0-1.0), which can be computed using the equation

$$AWCR(i) = \frac{(THETA(i) - THETAW(i))}{AWCT(i)} \quad (40)$$

where AWCT(I) is the total amount of available water content (m^3/m^3), THETA(I) is the volumetric water content (m^3/m^3), and THETAW(I) is the soil water content at wilting point (m^3/m^3).

The total amount of available water content for each simulation layer is estimated using the equation

$$AWCT(i) = THETA(i) - THETAW(i) \quad (41)$$

where THETAF(I) is the soil water content at field capacity (m^3/m^3).

The actual water use equation (Eq. H39) stipulates that the rate of water uptake by plants from a given soil layer will proceed at the potential rate as long as 30% or less of the total available water from that soil layer is depleted. However, a linear decline will occur in the actual transpiration relative to the potential transpiration with increasing depletion of available soil water beyond the initial 30%. This approach represents a compromise among the various models that have been proposed in the literature to describe the relationship between actual and potential transpiration as influenced by soil water availability (Denmead and Shaw, 1962; Holmes and Robertson, 1963).

Finally, the water stress factor is computed by considering the demand and supply of soil water in the root zone

$$WSF = TA/TP \quad (42)$$

where WSF is the water stress factor, TP is the potential plant transpiration (mm/day), and TA is the actual plant transpiration (mm/day).

The water stress factor (WSF) is a fraction (0-1) that is used by the CROP submodel to adjust daily plant growth by accounting for water stress if it exists. The actual plant transpiration is the sum of actual water use from all of the soil layers.

$$TA = \sum_{i=1}^{LAYRSN} WUA(i) \quad (43)$$

where LAYRSN is the number of soil layers used in the simulation.

Soil Water Redistribution

Soil water is continually moving, mainly in response to gradients of soil water potential. Soil conductive properties also control soil water flow between the different layers of the soil profile.

Redistribution of soil water plays a significant role in the various components of the soil water balance, particularly soil evaporation, deep percolation, and water uptake by plants. Therefore, an accurate evaluation of soil water redistribution is an essential prerequisite for any realistic simulation of soil-water dynamics.

The governing principles that describe water flow in soils are Darcy's law and the equation of continuity. Darcy's law states that the flow of water is proportional to the driving force

of the soil hydraulic gradient. The continuity equation states that the time rate of change in water content is proportional to the divergence of water flux. Richards (1931) derived a water flow equation by combining Darcy's law with the continuity equation. A water flow equation based on Darcy's law similar to the one used by Hillel (1977) and the SPAW model (Saxton et al., 1984) is used by the HYDROLOGY submodel of WEPS to estimate redistribution of soil water. The WEPS water flow equation in finite-difference form is

$$WFLUX(i) = (SWH(i-1) - SWH(i)) * CONDA(i) * DTIME / DIST(i) \quad (44)$$

where WFLUX is the amount of soil water flow (m), SWH is the soil water hydraulic head (m), CONDA is the average hydraulic conductivity for flow between adjoining soil layers (I) and (I-1) (m/s), DTIME is the time step (s), and DIST is the distance of flow between adjacent soil layers (I) and (I-1) (m).

The flow distance (DIST) can be calculated using the equation

$$DIST(i) = 0.5 * (TLAYR(i-1) - TLAYR(i)) \quad (45)$$

where TLAYR(I) is the thickness of soil layer I (m).

The soil water hydraulic head (SWH) is obtained by summing the soil water matric head and the gravitational head (- DMLAYR(I))

$$SWH(i) = SWM(i) - DMLAYR(i) \quad (46)$$

where SWM is the soil water matric head (m), and DMLAYR(I) is the depth to the midpoint of soil layer I from the soil's surface (m).

The soil water matric head (SWM) can be computed by converting the soil water matric potential with the equation

$$SWM(i) = POTM(i) / 10 \quad (47)$$

where POTM is the soil water matric potential (Joules/kg).

The average hydraulic conductivity for flow between adjoining soil layers (I) and (I-1) is weighted according to the thicknesses of the two layers

$$CONDA(i) = (COND(i-1) * TLAYR(i-1) + COND(i) * TLAYR(i)) / (2 * DIST(i)) \quad (48)$$

where COND(I) is the unsaturated soil hydraulic conductivity (m/s).

The daily potential soil evaporation computed with Eq. H35 is partitioned to obtain hourly estimates of potential soil evaporation using a sine function of daytime

$$EPH = AMAX1(0, AMEP * SIN(2 * \pi * TIME/24)) \tag{49}$$

where EPH is the hourly potential soil evaporation (mm/hr), AMEP is the amplitude of the daily wave of potential soil evaporation (mm/hr), and TIME is the time from sunrise. The use of the specification (AMAX1) in Eq. H49 prevents the simulated hourly potential evaporation from becoming negative. Accordingly, the simulated hourly potential evaporation during nighttime is set at zero.

The (AMEP) term is computed using the equation

$$AMEP = \pi * AVEP \tag{50}$$

where AVEP is the time-average value of the daily potential soil evaporation (mm/hr).

The term (AVEP) is derived from the daily potential soil evaporation (EP)

$$AVEP = EP/24 \tag{51}$$

where EP is the daily potential bare soil evaporation (mm/day).

The time term (TIME) is computed by subtracting (IRISE + 1) from the hour of the day, where (IRISE) represents the hour of sunrise as an integer.

The time of sunrise for any simulation site is calculated based on the global position of the site and the day of the year as follows:

$$RISE = HANGL/15 + SN \tag{52}$$

where RISE is the time of sunrise, HANGL is the hour angle, and SN is the solar noon.

SN is determined by the following equation:

$$SN = 12 - E/60 - 4 * (DMER - DLONG)/60 \tag{53}$$

where E is the equation of time, DMER is the standard meridian of the site (degrees) and DLONG is the longitude of the site (degrees). The standard meridian for the site is calculated based on the fact that the earth rotates 15° per hour; therefore, the earth is divided into time zones that occupy 15° of longitude. Each time zone has a standard meridian which is its eastern boundary. For the central zone, the standard meridian is 90°. The central time

H-20

HYDROLOGY SUBMODEL

WEPS

zone extends from 90° to 105° west longitude. The prime meridian (0°) is at Greenwich, England.

E is defined by the following equation:

$$E = 9.87 * \sin(2 * \pi / 180) - 7.53 * \cos(B * \pi / 180) - 1.5 * \sin(B * \pi / 180) \quad (54)$$

where B is defined as:

$$B = (360/365) * (IDOY - 81.25) \quad (55)$$

and IDOY is the day of the year.

HANGL is defined by the following equation:

$$HANGL = \frac{[\pi/2 - \text{ATAN}(\text{COSHR}/\sqrt{1 - \text{COSHR}^2})] * 180}{\pi} \quad (56)$$

where COSHR is the cosine of the hour angle at sunrise and is defined as:

$$\text{COSHR} = \frac{-\sin(\text{DLAT} * \pi / 180) / \cos(\text{DLAT} * \pi / 180) * \sin(\text{DEC} * \pi / 180) / \cos(\text{DEC} * \pi / 180)}{\quad} \quad (57)$$

where DLAT is the latitude of the site and DEC is the angle of declination (RAD).

The angle of declination (DEC) is calculated as follows:

$$\text{DEC} = 23.5 * \sin(B * \pi / 180) \quad (58)$$

Soil water evaporation from the soil surface usually proceeds at a potential rate as long as there is an adequate supply of water from the interior of the soil profile. Accordingly, the water redistribution section of the HYDROLOGY submodel of WEPS assumes that the actual rate of soil evaporation is equal to the potential rate, if the water flux from the underlying layer exceeds the potential evaporation flux. However, if the incoming water flux to the uppermost soil layer is less than the potential evaporation, the actual evaporation rate is obtained by adjusting the potential rate of soil evaporation in accordance with soil water availability in the uppermost simulation layer. The approach is similar to the one used in the plant water-uptake segment of the submodel

$$\begin{aligned} EAH &= EPH & ASWCR &\geq 0.70 \\ EAH &= EPH * (ASWCR/0.7) & ASWCR &< 0.70 \end{aligned} \quad (59)$$

WEPS

HYDROLOGY SUBMODEL

H-21

where EAH is the hourly rate of actual soil evaporation (mm/hr), and ASWCR is the relative amount of available water content in the surface layer.

The relative amount of available water in the surface layer (ASWCR) is a fraction (0-1.0), which is computed using the equation

$$ASWCR = \frac{(THETEV - THETA(1))}{AWCT(1)} \quad (60)$$

where AWCT(1) is the total amount of available water in the uppermost simulation layer (m^3/m^3), THETEV is soil wetness of the evaporation zone of the surface layer (m^3/m^3), and THETA(1) is soil water content at wilting point for the uppermost simulation layer (m^3/m^3).

The total amount of available water in the uppermost simulation layer is estimated using the equation

$$AWCT(1) = THETA(1) - THETA(1) \quad (61)$$

where THETA(1) is soil water content at field capacity for the uppermost simulation layer (m^3/m^3).

The soil water content of the evaporation zone (THETEV) is dependent on the thickness of the first simulation layer. If the thickness of the first simulation layer is less than or equal to 10 mm, then THETEV is calculated as follows:

$$THETEV = (THETA(1) + THETA(1))/2 \quad (62)$$

where THETA(1) is the volumetric water content of the first simulation layer (m^3/m^3) and THETA(1) is the extrapolated water content at the soil surface (m^3/m^3). On the other hand, if the thickness of the first simulation layer is greater than 10 mm, then the soil water content of the evaporation zone (THETEV) is calculated as the weighted average water content based on the water contents of the first simulation layer and the extrapolated surface water content. This assumes that the extrapolated water content represents only the uppermost 5 mm of the soil. Accordingly, THETEV is calculated as follows:

$$THETEV = \frac{THETA(1) + 0.005 + [THETA(1) * (TLAYR(1) - 0.005)]}{TLAYR(1)} \quad (63)$$

where TLAYR(1) is the thickness of the first layer (mm). The extrapolated water content at the soil surface (THETA(1)) is obtained by extrapolating water content to the soil surface from the three uppermost simulation layers. A numerical solution known as Cramer's rule

H-22

HYDROLOGY SUBMODEL

WEPS

(Miller, 1982) is used to obtain an estimate of the extrapolated water content at the soil surface (THETAX) by solving the three simultaneous equations:

$$THETA(1) = THETAX + b * DLAYR(1) + c * (DLAYR(1))^2 \quad (64)$$

$$THETA(2) = THETAX + b * DLAYR(2) + c * (DLAYR(2))^2 \quad (65)$$

$$THETA(3) = THETAX + b * DLAYR(3) + c * (DLAYR(3))^2 \quad (66)$$

where THETA(1), THETA(2), and THETA(3) are the volumetric soil water contents for simulation layers 1, 2, and 3, respectively (m^3/m^3), and DLAYR(1), DLAYR(2), and DLAYR(3) are the depths to the bottom of simulation layers 1, 2, and 3, respectively (m).

The equation that calculates soil evaporation (Eq. H59) stipulates that the actual rate of evaporations from a given soil will proceed at the potential rate as long as 30% or less of the total amount of available water content in the surface layer is depleted. However, the soil evaporation rate will decline linearly relative to the potential rate with increasing depletion of available soil water beyond the initial 30%.

The water flux from the uppermost simulation layer is computed by converting the actual evaporation rate with the equation

$$WFLUX(1) = - EAHICMTOMM \quad (67)$$

where WFLUX(1) is the flux of water through the soil surface (m), and CMTOMM is a conversion factor from meters to millimeters (CMTOMM = 1000.0). The minus sign in Eq. H67 is used to indicate that latent heat flux in the upward direction from the soil surface represents an energy loss in accordance with the principles of the energy balance equation.

A unit hydraulic gradient approach is applied to the lower boundary condition for the one-dimensional water flow in the soil profile. The flux from the lowermost soil layer is set to equal the hydraulic conductivity

$$WFLUX(LAYRSN+1) = COND(LAYRSN) * DTIME \quad (68)$$

where LAYRSN is the number of soil layers used in the simulation, and WFLUX(LAYRSN+1) is the amount of soil water flow from the lowermost simulation layer (m).

Hourly estimates of deep percolation are obtained by converting the flux from the lowermost simulation layer

WEPS

HYDROLOGY SUBMODEL

H-23

$$DPH = WFLUX(LAYRSN+1) * CMTOMM \quad (69)$$

where DPH is the hourly deep percolation (mm).

According to the continuity equation, the change in water content of each simulation layer is related to the net flux of water into the layer. The net water flux for each layer is computed using the equation

$$WFLUXN(i) = WFLUX(i) - WFLUX(i-1) \quad (70)$$

where WFLUXN(I) is the net amount of soil water flow into layer I (m).

The net amount of water flux (WFLUXN) enters into the determination soil wetness using the equations

$$WC(i) = WCI(i) + (WFLUXN(i) * CMTOMM) \quad (71)$$

$$THETA(i) = WC(i) / (TLAYR(i) * CMTOMM) \quad (72)$$

where WC is the amount of soil layer wetness (mm), WCI is the initial amount of soil layer wetness (mm), and THETA is the volumetric soil water content (m^3/m^3).

The HYDROLOGY submodel of WEPS, thus, uses a simplified forward finite-difference technique to redistribute soil water with the one-dimensional Darcy equation for unsaturated water flow. Accordingly, the wetness of a soil layer at a future time increment is expressed in terms of the water contents of the same layer and the adjacent layers at the beginning of the time increment. The technique allows for an explicit expression of soil wetness in terms of the water contents at the previous time step. The main advantage of the explicit forward finite-difference procedure is the direct calculation of future soil water contents of the simulation layers.

The default time step (DTIME) of the soil water redistribution section is 1 hour, which allows for an hourly estimation of soil wetness as needed by the Wind Erosion Research Model. However, under certain situations, such as strong hydraulic gradients and/or high soil hydraulic conductivity, the default time step can result in significant changes in the simulated soil wetness, adversely affecting the stability and, consequently, the quality of the computation. To overcome this problem, a tolerance level is established as the maximum allowable change in soil water matric potential in each time step. The tolerance level is -20 Joules/kg soil matric potential (200 mb soil water tension). If the tolerance level is exceeded, the initial time step is halved, and all calculations are repeated until the tolerance level is not exceeded in that time step.

Estimating Soil Hydraulic Properties

Knowledge of the relationship between unsaturated hydraulic conductivity and soil water content is required for solving the governing transport equations of water movement through the soil. However, reliable estimates of unsaturated hydraulic conductivity (COND) as a function of soil water content are extremely difficult to obtain not only because of the extensive spatial variability of the parameter in the field but also because its determination in the field and/or laboratory is very difficult, laborious, and expensive. To overcome this problem, many methods have been proposed to predict the unsaturated hydraulic conductivity from more easily determined soil parameters. Most of these methods calculate the unsaturated hydraulic conductivity of the soil from the relatively more easily and routinely obtainable soil water characteristic curve and saturated hydraulic conductivity (Millington and Quirk, 1959; Brooks and Corey, 1964; 1966; Campbell, 1974; Mualem, 1976; and Van Genuchten, 1978; 1980).

The HYDROLOGY submodel of WEPS uses Campbell's (1974) relatively simple method to calculate the unsaturated hydraulic conductivity as a function of soil water content. This method assumes that the soil water characteristic curve can be represented by the equation

$$POTM = POTE * ESAT^{-CB} \quad (73)$$

where CB is the power of Campbell's model of the soil water characteristic curve, POTE is the air-entry potential of soil water (Joules/kg), POTM is the matric potential of soil water (Joules/kg), and ESAT is the effective saturation.

The effective saturation (ESAT) in Eq. H73 is a dimensionless term, which is referred to sometimes as the reduced water content. It is calculated using the equation:

$$ESAT = THETA / THETAS \quad (74)$$

where THETA is the volumetric soil water content (m^3/m^3), and THETAS is the soil water content at saturation (m^3/m^3).

Campbell's function of the soil unsaturated hydraulic conductivity is represented by the equation:

$$COND = SATK * ESAT^{CM} \quad (75)$$

where SATK is the saturated soil hydraulic conductivity (m/s), and CM is the exponent of Campbell's function of unsaturated hydraulic conductivity.

The exponent parameter (CM) in Eq. H75 is calculated using the equation:

$$CM = (2 * CB) + 3. \quad (76)$$

Both (POTE) and (CB) are considered as characteristic hydraulic parameters of the soil. The air-entry potential, which usually is referred to as the bubbling pressure, is related to the maximum pore size forming a continuous network of flow channels within the soil. The air entry potential is defined as the minimum capillary pressure on the drainage cycle at which a continuous nonwetting condition exists in the soil, i.e., the potential at which the largest water-filled pores start to drain and, hence, gas flow can be observed. The (CB) parameter is a function not only of the size of soil pores but also of the interfacial forces, contact angles, shape of soil pores, etc.

The (CB) parameter is the inverse of the pore size distribution (λ) term of the model developed by Brooks and Corey (1964) for the soil water characteristic curve. The parameter evaluates the distribution of sizes of the flow channels within the soil medium, which is a function of the microscopic geometry of the soil. Theoretically, the (CB) parameter can have any positive value greater than zero. However, the parameter is usually larger for soils with a wide range of pore sizes than for soils with a relatively uniform distribution of pore sizes.

Brooks and Corey (1964) proposed a graphical procedure for determining the air-entry potential and the pore size distribution index of the soil by plotting the water release data on a log-log graph paper and fitting a straight line to the data. The negative slope of the best-fit line is designated as the pore size distribution index of the soil and, hence, its inverse is the (CB) parameter of the soil. Furthermore, the extrapolation of the best-fit line to the ordinate representing the effective saturation value of 1.0 gives the air-entry potential of the soil.

Soil hydraulic parameters, including the air-entry potential (POTE) and the power of Campbell's model of the soil water characteristic curve (CB), are required as inputs to run the HYDROLOGY submodel of WEPS. However, these parameters are not always readily available. To circumvent the problem, the HYDROLOGY submodel provides an approximation of these properties from easily and routinely obtainable soil texture and bulk density data based on a set of equations proposed by Campbell (1985).

The air-entry potential at a standard bulk density of 1.3 Mg/m^3 is calculated using the equation

$$POTES = -0.2 * GMD^{-0.5} \quad (77)$$

where POTES is the air-entry potential at a standard bulk density of 1.3 Mg/m^3 (Joules/kg), and GMD is the geometric mean particle diameter (mm).

Originally, Campbell (1985) proposed a coefficient of -0.5 for use in Eq. H77, but more recently, Flerchinger (1987) reported that a better fit between predicted and measured soil hydraulic parameters can be obtained by using a coefficient of -0.2.

The (CB) term is calculated with the equation

$$CB = -2 * POTES + 0.2 * GSD \quad (78)$$

where GSD is the geometric standard deviation (mm).

The air-entry potential (POTE) adjusted to the soil bulk density can be computed using the equation

$$POTE = POTES * (BD/1.3)^{(0.67 * CB)} \quad (79)$$

where BD is the soil bulk density (Mg/m³).

The saturated hydraulic conductivity (SATK) is established by the following equation

$$SATK = 3.9167E-05 \left(\frac{BD}{1.3} \right)^{1.3b} \exp(-9.6CLAYM - 3.7SILTM) \quad (80)$$

The geometric mean particle diameter (GMD) and geometric standard deviation (GSD) are calculated from the particle size distribution using the following equations

$$GMD = \exp X \quad (81)$$

$$GSD = \exp((Y - X^2)^{0.5}) \quad (82)$$

where

$$X = SANDM * LOG(0.316) + SILTM * LOG(0.01) + CLAYM * LOG(0.0002) \quad (83)$$

$$Y = SANDM * (LOG(0.316))^2 + SILTM * (LOG(0.01))^2 + CLAYM * (LOG(0.0002))^2 \quad (84)$$

where SANDM is the mass fraction of sand, SILTM is the mass fraction of silt, and CLAYM is the mass fraction of clay.

The coefficients 0.316, 0.01, and 0.0002 listed in Eqs. H83 and H84 represent the geometric mean diameters of the sand, silt, and clay soil particle-size fractions, respectively.

The expected range for the geometric mean particle diameter (GMD) is 0.003 to 0.7 mm, whereas the expected range for the geometric standard deviation (GSD) is 1 to 30 (Campbell, 1985).

The detailed soil texture and bulk density data that are required to estimate soil hydraulic parameters are not always available. Therefore, the HYDROLOGY submodel of WEPS provides an additional approximation of the hydraulic parameters based exclusively on the textural class of the soil. McCuen et al. (1981) determined that soil hydraulic parameters, such as the pore size distribution index and the air entry potential, are unique for each soil texture class, i.e., these parameters differ collectively and not singularly across soil texture classes. Furthermore, Rawls et al. (1982) collected soil hydraulic properties from 1,323 soils with about 5,320 horizons from 32 states in an extensive search of literature and data sources. Table H3 is a revised summary of the means of soil hydraulic parameters for the 11 USDA soil texture classes as reported by Rawls et al. (1982). The silt textural class is missing; however, it is rare to find a soil sample having that textural class.

In summary, soil hydraulic parameters that are required to run the HYDROLOGY submodel of WEPS are relatively simple. The first and most desired option is to use measured values. However, the HYDROLOGY submodel provides other options to estimate soil hydraulic parameters in order to accommodate the varying degrees of data availability.

Table H-3. Soil hydraulic parameters classified by soil textural class (water contents on volumetric basis).

USDA Textural Class	(POTE) Air-entry potential (Joules/kg)	(CB) Campbell's b parameter	(THETAS) Saturation (m ³ /m ³)	(THETAF) Field capacity (m ³ /m ³)	(THETA W) Wilting point (m ³ /m ³)	(SATK) Saturated K (m/s)
Sand	-1.598	1.441	0.437	0.091	0.033	5.833E-05
Loamy sand	-2.058	1.808	0.437	0.125	0.055	1.697E-05
Sandy loam	-3.020	2.646	0.453	0.207	0.095	7.194E-06
Loam	-4.012	3.968	0.463	0.270	0.117	3.667E-06
Silt loam	-5.087	4.274	0.501	0.330	0.133	1.889E-06
Sandy clay loam	-5.941	3.135	0.398	0.255	0.148	1.194E-06
Clay loam	-5.643	4.132	0.464	0.318	0.197	6.389E-07
Silty clay loam	-7.033	5.650	0.471	0.366	0.208	4.167E-07
Sandy clay	-7.948	4.484	0.430	0.339	0.239	3.333E-07
Silty clay	-7.654	6.667	0.479	0.387	0.250	2.500E-07
Clay	-8.560	6.061	0.475	0.396	0.272	1.667E-07

Source: Rawls, et al. (1982).

Table H-4. Soil hydraulic parameters classified by soil textural class (water contents on gravimetric basis).

USDA Textural Class	(aheaep) Air-entry potential (Joules/kg)	(ah0cb) Campbell's b Parameter	(ahrwcs) Saturation (kg/kg)	(ahrwcf) Field capacity (kg/kg)	(ahrwcw) Wilting point (kg/kg)	(ahrsk) Saturated K (m/s)
Sand	-1.598	1.441	0.293	0.061	0.022	5.833E-05
Loamy sand	-2.058	1.808	0.293	0.084	0.037	1.697E-05
Sandy loam	-3.020	2.646	0.312	0.143	0.066	7.194E-06
Loam	-4.012	3.968	0.325	0.190	0.082	3.667E-06
Silt loam	-5.087	4.274	0.379	0.250	0.101	1.889E-06
Sandy clay loam	-5.941	3.135	0.250	0.160	0.093	1.194E-06
Clay loam	-5.643	4.132	0.327	0.224	0.139	6.389E-07
Silty clay loam	-7.033	5.650	0.336	0.261	0.148	4.167E-07
Sandy clay	-7.948	4.484	0.285	0.224	0.158	3.333E-07
Silty clay	-7.654	6.667	0.347	0.280	0.181	2.500E-07
Clay	-8.560	6.061	0.341	0.285	0.196	1.667E-07

Source: Rawls et al., (1982).

Soil Wetness at the Soil-Atmosphere Interface

The water redistribution section of the HYDROLOGY submodel of WEPS accounts for water flux only in the liquid phase. However, when the soil is relatively dry, significant water flux can occur in the vapor phase. Campbell (1985) compared simulated water content profiles with and without vapor flux. He showed that the profile with the vapor flux was significantly drier particularly at the surface and, therefore, resulted in a better fit with the observed water content profile of the drying soil. Therefore, it is essential to account somehow for vapor flux in any attempt to correctly predict surface-soil wetness, particularly at or below the critical level of threshold of erodibility. This is not a simple task, because many factors have to be considered. For example, heat flux, because thermally induced vapor flow can be an important factor in soil drying. However, a complete simulation that accounts for linked fluxes of liquid, vapor, and heat is probably too complex, long, and slow to meet the unique requirements of WEPS for fast simulation of the diurnal changes in soil water content, particularly at the soil-atmosphere interface. Therefore, the HYDROLOGY submodel of WEPS neglects vapor flux except at the soil surface, where the relationship

between actual and potential evaporation is used as an estimator of surface soil wetness. Water usually evaporates from the soil surface at the potential rate only when the soil is adequately wet. However, when the soil begins to dry and water is not conducted to the soil-atmosphere interface fast enough to meet the atmospheric evaporation demand, actual evaporation falls behind the potential rate. Holmes and Robertson (1963) verified the unique relationship between soil wetness and the ratio of actual to potential evaporation in a growth chamber experiment conducted with samples from three soil materials (North Gower clay, Matilda silt loam, and 26-mesh quartz sand). In order to make the relationship between evaporation ratio and soil wetness useful in predicting surface soil wetness as needed by WEPS, the functional relationship between equivalent water content and the ratio of actual to potential evaporation has to be determined first. We used Jackson's (1973) original soil water and meteorological data from a 1971 bare soil evaporation experiment conducted on an Avondale loam (fine-loamy, mixed (calcareous), hyperthermic Typic Torrifuvent) at the U.S. Water Conservation Laboratory, Phoenix, Arizona to derive the relationship between equivalent water content and the evaporation ratio. On the afternoon of March 2, 1971, the bare field was irrigated thoroughly with about 10 cm of water. After irrigation, actual soil evaporation was monitored at 0.5-hour intervals by measuring weight loss from two lysimeters located within the experimental field. Intensive soil sampling at 0.5-hour intervals was carried out from 2300 on March 4, 1971 to 0130 on March 19, 1971. Six sites were sampled each time and composited for the surface soil layer of 0-5 mm. Soil water content was measured gravimetrically. Water contents were converted to the volumetric basis by multiplying the gravimetric data by the soil bulk density. Net radiation, wind speed, vapor pressure, and air temperature were recorded at 0.5-hour intervals by a data acquisition system. We converted the raw data from Jackson's experiment to obtain hourly estimates of lysimeter evaporation and meteorological variables from 0000 on March 5 to 2400 on March 18. Furthermore, we smoothed the raw hourly water-content data for the surface soil using a 1-2-3-2-1 weighted running average procedure similar to the one described by Jackson et al. (1973). We also used the hourly meteorological data to calculate the hourly potential evaporation using Van Bavel's (1966) combination equation.

Figure H-1 depicts the relationship between the hourly evaporation ratios of actual lysimeter evaporation to potential evaporation and surface soil wetness expressed as equivalent water content. The hourly values of equivalent water content were obtained by dividing the smoothed water content data by $0.146 \text{ m}^3/\text{m}^3$, which represents the amount of water retained by the Avondale loam at -1500 J/kg soil water potential. Figure H-1 shows two clusters of data points on the graph; the first at an evaporation ratio of 0.2, and the second at an evaporation ratio of 0.7. The relationship between measured hourly soil water contents at the soil-atmosphere interface and measured evaporation ratios can be well-represented with a sigmoid function. We would have preferred more data points to confirm the sigmoidal functional relationship; however, because of equipment malfunctions, no hourly lysimeter data were available during March 6 and 7, 1971. However, for the available data, agreement was good between hourly measured lysimeter evaporation rates and the simulated hourly

evaporation rates by the HYDROLOGY submodel of WEPS (Figure H-2). Therefore, to overcome the problem of the missing data, simulated evaporation data for the 2 days were substituted. Figure H3 depicts the functional relationship between the hourly measured surface soil-water contents at the soil-atmosphere interface and the simulated evaporation ratios for March 6 and 7 and the measured evaporation ratios for the remainder of the experiment.

The functional relationship between equivalent water content of the soil surface and hourly evaporation ratios is described with the equation.

$$THETA_E = 0.24308 + \frac{1.37918}{1 + \exp\left[-\left(\frac{ERATIO - 0.44882}{0.08100}\right)\right]} \quad (85)$$

where THETA_E is the equivalent water content defined as the ratio of volumetric soil-water content (m³/m³) to volumetric soil-water content for the same soil at -1.5 kJ/kg soil matric potential, and ERATIO is the ratio of hourly actual evaporation (E_{ah}) to hourly potential evaporation (E_{ph}).

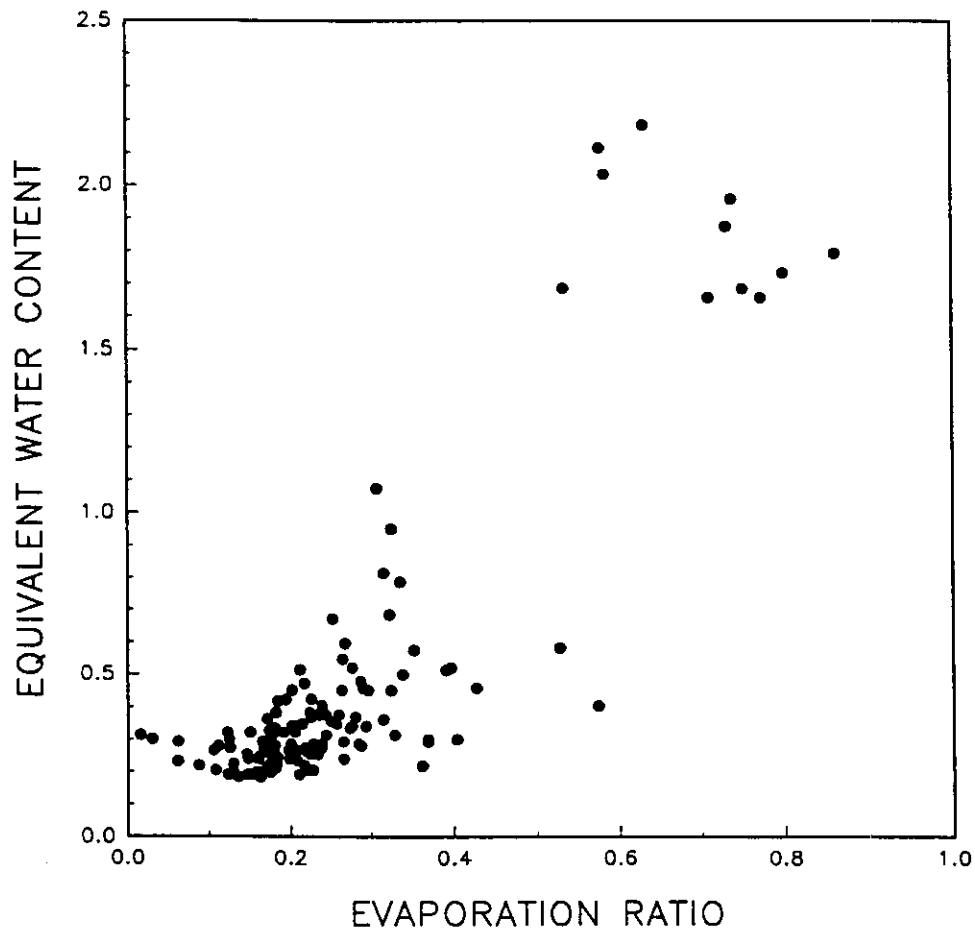


Figure H-1. Measured hourly soil water contents at the soil-atmosphere interface versus measured evaporation ratios from the 1971 Arizona experiment (data for March 6 & 7 were missing).

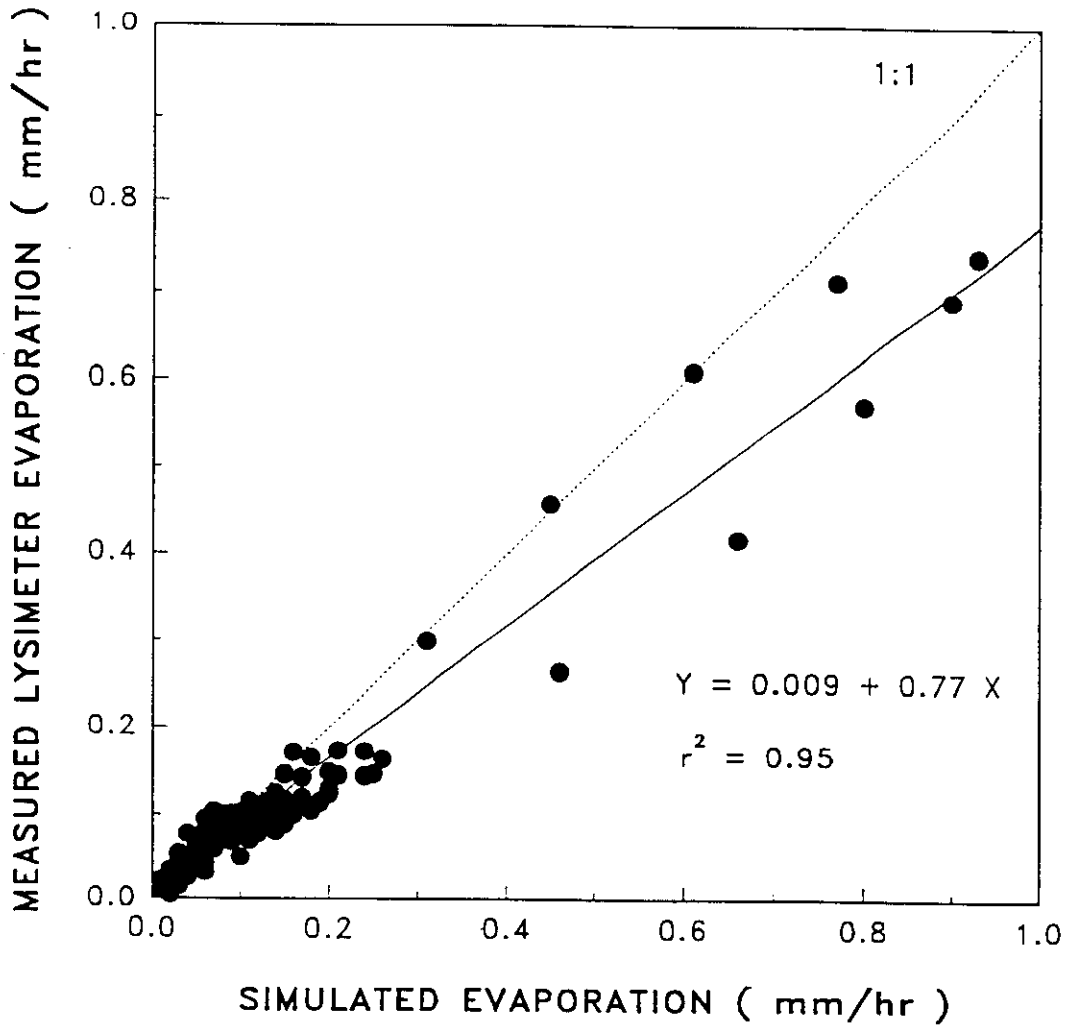


Figure H-2. Regression analysis between measured and simulated hourly evaporation ratios from the 1971 Arizona experiment excluding March 6 & 7.

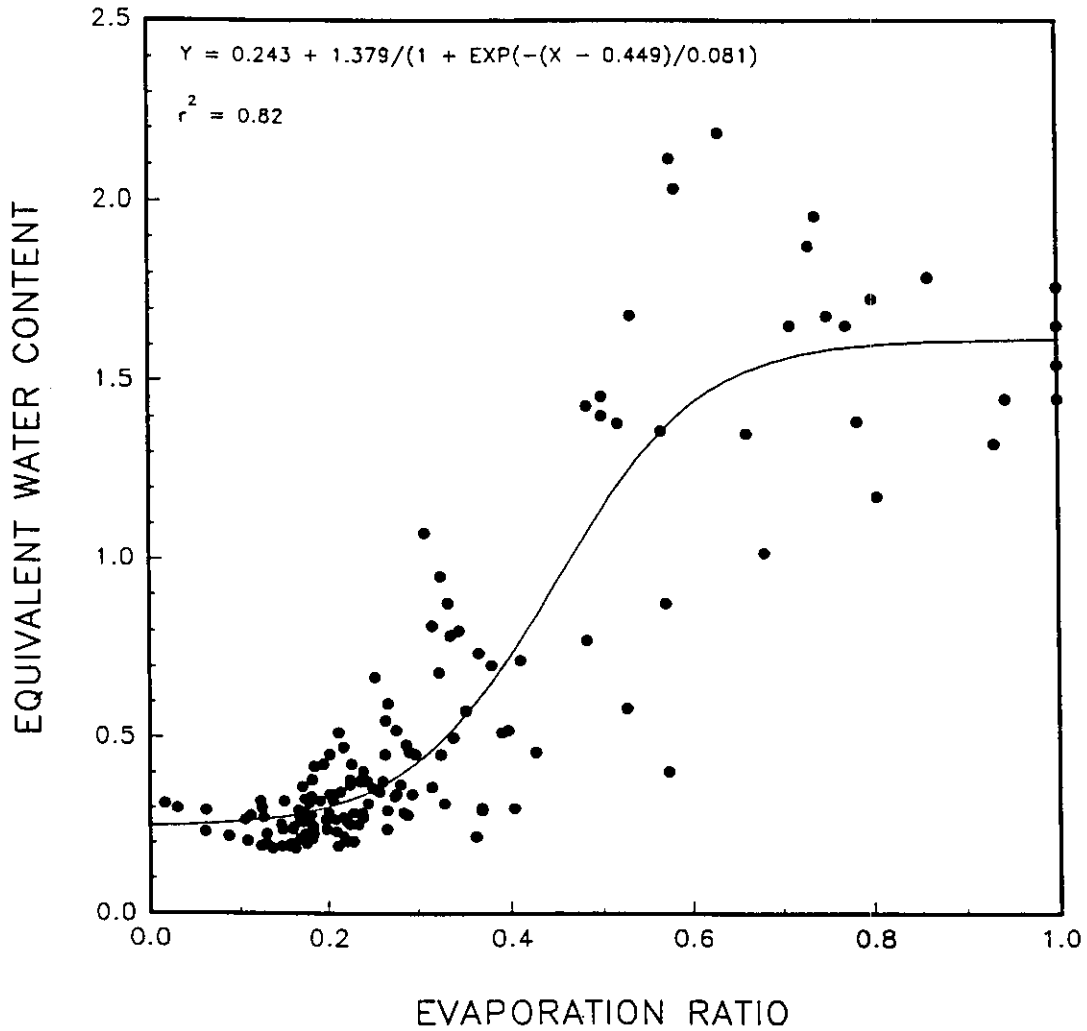


Figure H-3. Measured hourly soil water contents at the soil-atmosphere interface versus measured and simulated evaporation ratios from the 1971 Arizona experiment (March 6 & 7 evaporation ratios were simulated).

The surface soil water content (*THETER*) as interpolated from the relationship between evaporation ratio and equivalent surface soil water content is calculated with the equation

$$THETER = THETA E * THETA W(1) \quad (86)$$

where *THETER* is the surface soil water content based on the relationship between evaporation ratio and equivalent surface water content (m^3/m^3).

At the start of simulation, the initial soil wetness at the soil-atmosphere interface (*THETOI*) is estimated using the equations

$$THETOI = AMAX1(THETAX, THETI3) \quad THETI3 \geq THETF3 \quad (87)$$

$$THETOI = THETAX \quad THETI3 < THETF3 \quad (88)$$

where *THETI3* is the weighted average of the initial soil water contents from the three uppermost simulation layers (m^3/m^3), and *THETF3* is the weighted average of soil water contents at field capacity of the three uppermost simulation layers (m^3/m^3).

Furthermore, soil wetness at the soil-atmosphere interface (*THETA0*) is estimated throughout the rest of the simulation period by using the equations

$$THETA0 = AMINI(THETER, THETAX, THETOI) \quad EPH > 0.0 \quad (89)$$

$$THETA0 = AMAX1(THETAX/2, THETOI) \quad EPH = 0.0 \quad (90)$$

where *THETA0* is the soil water content at the soil-atmosphere interface (m^3/m^3), *THETOI* is the soil water content at the soil-atmosphere interface from the previous time increment (m^3/m^3), *THETAX* is the extrapolated water content at the soil surface (m^3/m^3), and *EPH* is the hourly potential of soil evaporation (mm/hr).

If an irrigation, precipitation, and/or snow melt event occurs on a given simulation day, the amount of water available for infiltration is distributed in the soil profile as described in the soil water storage section of the submodel. Furthermore, the extrapolated soil wetness (*THETAX*) is used exclusively to represent soil wetness at the soil-atmosphere interface at the first hour of the day.

The extrapolated soil wetness (*THETAX*) also is used as the sole indicator of soil wetness at the soil-atmosphere interface, when an abundance of water is present in the surface soil, i.e., only 30% or less of the surface available water is depleted.

Simulation of Soil Temperature

Subroutine HEAT simulates soil temperature based on the algorithm described by Campbell (1985). The subroutine estimates daily minimum, maximum, and average soil temperatures at the center of each simulation layer. The inputs needed to run the program are maximum and minimum daily air temperatures. In addition, soil bulk density, volumetric water content, and clay fraction are used to calculate soil thermal properties.

The basic assumption is that the hourly soil temperature is estimated about an average soil temperature distributed over a sine function. The following equation gives the estimated hourly soil temperature:

$$TSOIL(K,J) = TSAVG(K) + TAMP * EXP(-DMLAYR(K)/ZDAMP) * SIN((FREQ * TIME(J)) - (DMLAYR(K)/ZDAMP) + PHI) \quad (91)$$

where TSOIL is the hourly soil temperature ($^{\circ}\text{C}$), TSAVG is the average soil temperature ($^{\circ}\text{C}$), TAMP is amplitude of the temperature wave at the soil surface ($^{\circ}\text{C}$), DMLAYR is the depth from the soil surface to the center of the simulation layer (m), ZDAMP is the diurnal damping depth, FREQ is the angular frequency of the temperature oscillation, TIME is the time of simulation (s), PHI is the phase constant, J is the simulation hour (h), and K is the simulation layer.

TAMP and PHI are determined by the following as:

$$TAMP = TMAX - TAIR \quad (92)$$

$$PHI = -(7.0 * \pi) / 12 \quad (93)$$

where TMAX is the daily maximum air temperature ($^{\circ}\text{C}$), and TAIR is the mean air temperature ($^{\circ}\text{C}$).

The basic assumption in simulating soil temperature is that the temperature at the upper boundary condition, i.e., the soil-atmosphere interface over a 24-hour period is equal to the average air temperature for the same period. Furthermore, the temperature at the lower boundary condition is equal to the average annual air temperature at the site. The average soil temperature for each simulation layer is interpolated between the temperatures at the upper and lower boundary conditions and is given as:

$$TSAVG(K) = TUBC + (TDIF * (DMLAYR(K)/DLBC)) \quad (94)$$

where TUBC is the temperature at the upper boundary condition ($^{\circ}\text{C}$), TDIF is the temperature difference between the upper and lower boundary conditions ($^{\circ}\text{C}$), and DLBC is the depth of the lower boundary condition (m).

The depth of the lower boundary condition (DLBC) is determined by taking the larger of either the annual damping depth or the depth of the lowermost simulation layer. The annual damping depth is defined as:

$$ZDAMPY = ZDAMP * \sqrt{365} \quad (95)$$

where ZDAMPY is the annual damping depth (m).

The diurnal damping depth, ZDAMP, is calculated using the following equation:

$$ZDAMP = \sqrt{(2 * (THERMK / VSHEAT)) / \text{FREQ}} \quad (96)$$

where THERMK is the soil thermal conductivity ($\text{W}/\text{m}\cdot\text{C}$), and VSHEAT is the volumetric specific heat ($\text{J}/\text{m}^3\cdot\text{C}$).

The angular frequency of the temperature oscillation, FREQ, is calculated as:

$$\text{FREQ} = (2 * \pi) / (86400 * \text{PERIOD}) \quad (97)$$

where PERIOD is the length of the simulation in days.

The volumetric specific heat is determined by the following equation:

$$\text{VSHEAT} = \text{CMJTOJ} * (((\text{CM} * \text{PBD}) / 2.65) + (\text{CW} * \text{PTHETA})) \quad (98)$$

where CMJTOJ is the conversion factor to convert from MJ to J (1×10^6), CM is the volumetric specific heat for the soil mineral fraction ($\text{MJ}/\text{m}^3\cdot\text{C}$, $\text{CM} = 2.26$), CW is the volumetric specific heat for the soil water fraction ($\text{MJ}/\text{m}^3\cdot\text{C}$, $\text{CW} = 4.18$), PBD is the weighted average bulk density of the soil profile (Mg/m^3), and PTHETA is the weighted average water content of the soil profile (m^3/m^3).

The soil thermal conductivity, THERMK, is defined as:

$$\text{THERMK} = A + (B * \text{PTHETA}) - (A - D) * \text{EXP}(-(C * \text{PTHETA})^4) \quad (99)$$

where,

H-38

HYDROLOGY SUBMODEL

WEPS

$$A = 0.65 - 0.78 * PBD + 0.6 * PBD^2 \quad (100)$$

$$B = 1.06 * PBD \quad (101)$$

$$C = 1.0 + (2.6 / \sqrt{PCLAYM}) \quad (102)$$

$$D = 0.03 + (0.1 * PBD^2) \quad (103)$$

Subroutine STAT is called to calculate the maximum and minimum temperatures at the center of each simulation layer.

The Structure and Procedures of the HYDROLOGY Submodel

The processes that were described in the previous sections of this chapter play a significant role in the water balance of the soil. The physical basis of these processes were defined, and a set of algorithms were developed to complete the simulation of each process. These algorithms were coded using FORTRAN 77 programming language and then arranged in an orderly computational sequence to form the HYDROLOGY submodel of WEPS.

The structure of the submodel is modular; therefore, the submodel can be updated easily by substituting alternative algorithms for specific processes when needed. The HYDROLOGY submodel of WEPS contains 10 subroutines and 3 function calls.

Subroutine HYDRO is the main (supervisory) program for the HYDROLOGY submodel. The subroutine controls the calling of the major subprograms of the HYDROLOGY submodel and also initializes the depth variables of the simulation layers and converts the water content variables from mass basis to volume basis.

Subroutine HINIT controls the initialization of the HYDROLOGY submodel of WEPS.

Subroutine EXTRA extrapolates soil water content to the surface from the three upper simulation layers. A numerical solution known as Cramer's rule is used to obtain an estimate of the extrapolated water content at the soil surface by solving the three simultaneous equations that describe the relationship between soil water content and soil depth for the three uppermost simulation layers.

Subroutine SNOMLT predicts daily snow melt when the maximum daily air temperature exceeds 0°C. The melted snow is added to the daily precipitation.

Function SCSQ estimates daily surface runoff using a modification of the Soil Conservation Service soil-cover complex method, which is known commonly as the curve number method (Soil Conservation Service, 1972).

Subroutine STORE stores the daily amount of water available for infiltration into the soil profile. First, water is stored in the uppermost simulation layer, until its water content reaches field capacity. The excess water is then added to the succeeding lower soil layer, where it is stored with the same maximum storage restriction. This is repeated, until complete water storage is obtained. Any excess water that flows out from the lowermost simulation layer becomes a part of deep percolation.

Subroutine ET calculates daily potential evapotranspiration using Van Bavel's (1966) revised combination method.

Subroutine DARCY uses a simplified forward finite-difference technique to redistribute soil water in the soil profile using Richards (1931) water flow equation. This subroutine predicts on an hourly basis soil water profile, soil water content at the soil-atmosphere interface, potential and actual soil evaporations, and deep percolation.

Subroutine TRANSP predicts the daily actual plant transpiration rate by distributing the potential amount of plant transpiration throughout the root zone and then adjusting the potential rate on the basis of soil water availability.

Subroutine PSD calculates the geometric mean diameter and geometric standard deviation of primary soil particles on the basis of particle size distribution (percent sand, silt, and clay) of the soil. The geometric mean diameter and geometric standard deviation are used to estimate soil hydraulic parameters that are needed as inputs to the submodel when they are not readily available.

Subroutine HEAT simulates soil temperature based on the algorithm described by Campbell (1985). The subroutine estimates daily minimum, maximum, and average soil temperatures at the center of each simulation layer. The inputs needed to run the program are maximum daily air temperature and minimum daily air temperature. The basic assumption is that the temperature at the upper boundary condition, i.e., the soil-atmosphere interface, over a 24-hour period is equal to the average air temperature for the same period. Furthermore, the temperature at the lower boundary condition, i.e., the center of the lowermost simulation layer, is equal to the average annual air temperature at the site. Furthermore, soil bulk density, volumetric water content, and clay fraction are used to calculate soil thermal properties.

Function RADNET converts the radiation data from global radiation (ly/day) as read from the climate generator (CLIGEN) files into net radiation (MJ/m²/day) as needed by

subroutine ET of the HYDROLOGY submodel of WEPS. Using Wright's modified version of Penman's general relationship outlined by Allen et al. (1989), the subroutine initially estimates the surface albedo by considering the soil, crop, and snow cover. If a snow cover exists with 5 mm or greater water content, the value of albedo is set to 0.6. If the snow cover is less than 5 mm and no crop is growing, the soil albedo is the appropriate value. When crops are growing, albedo is estimated on the basis of soil albedo, crop albedo, and soil cover index.

Function DAWN calculates the time of sunrise for any simulation day based on the position of the simulation site and day of the year. Time of sunrise is used by subroutine DARCY of the HYDROLOGY submodel of WEPS to partition the daily soil evaporation and obtain hourly estimates of potential soil evaporation.

Function WATERK estimates the soil saturated hydraulic conductivity, if it is not readily available as a function of percent silt, percent clay, and soil bulk density.

Figures H4-H8 show the computational sequence of the major subroutines of the HYDROLOGY submodel of WEPS in a flowchart form.

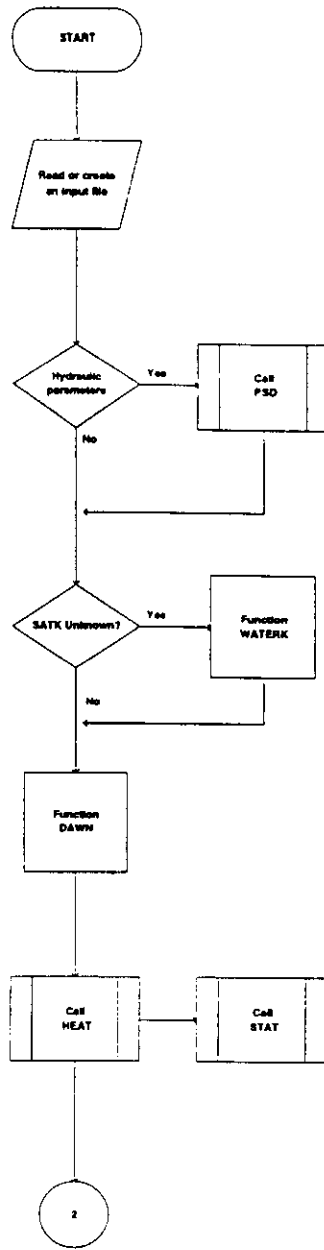


Figure H-4. Simplified flowchart of the HYDROLOGY submodel of WEPS.

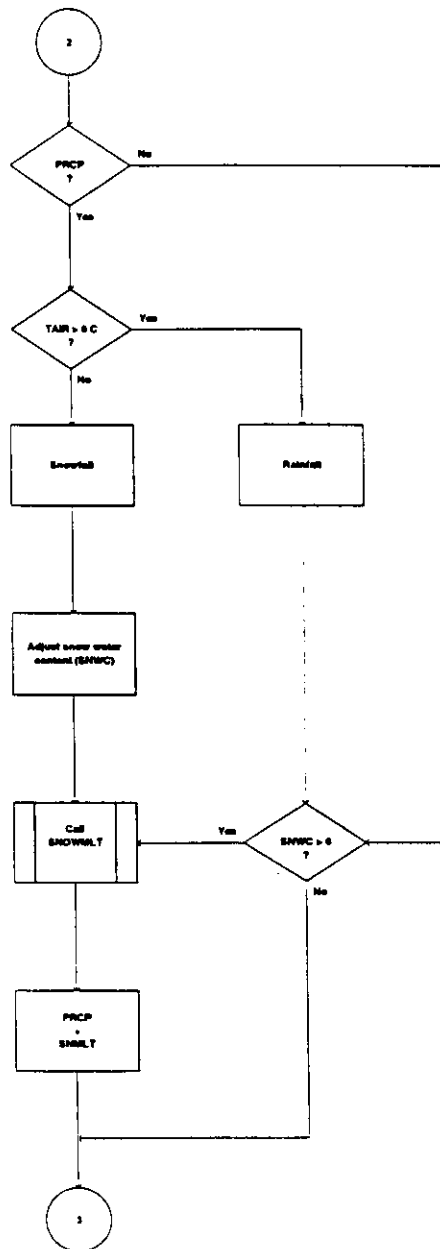


Figure H-5. Simplified flowchart of the HYDROLOGY submodel of WEPS (continued).

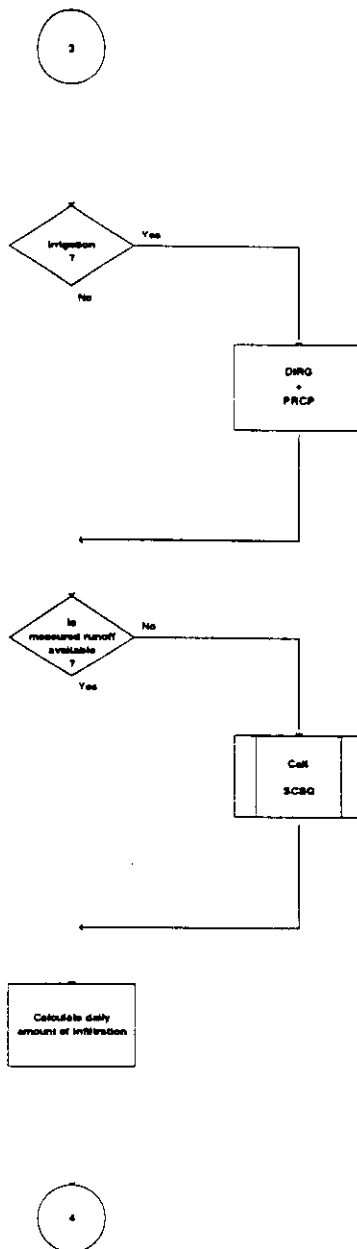


Figure H-6. Simplified flowchart of the HYDROLOGY submodel of WEPS (continued).

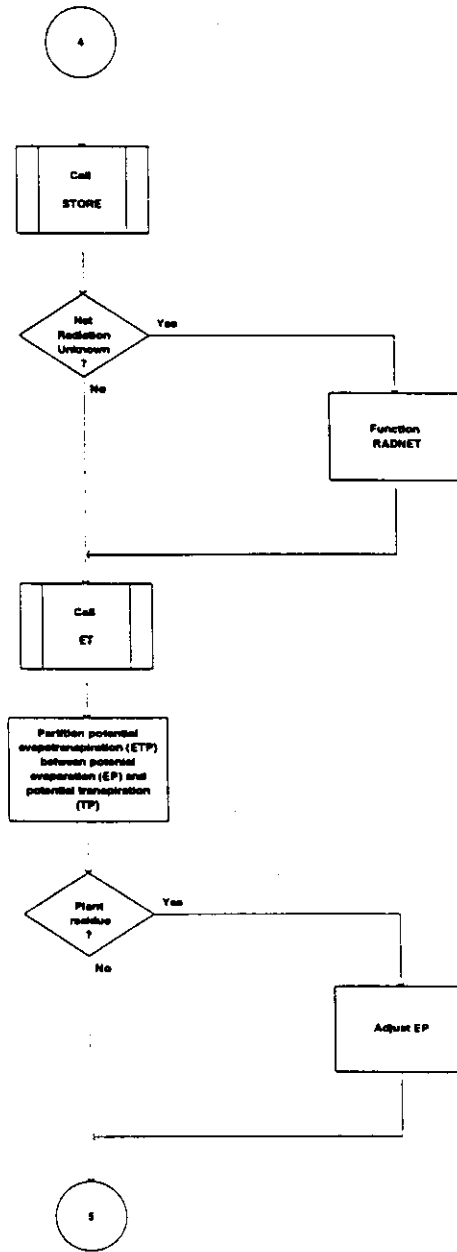


Figure H-7. Simplified flowchart of the HYDROLOGY submodel of WEPS (continued).

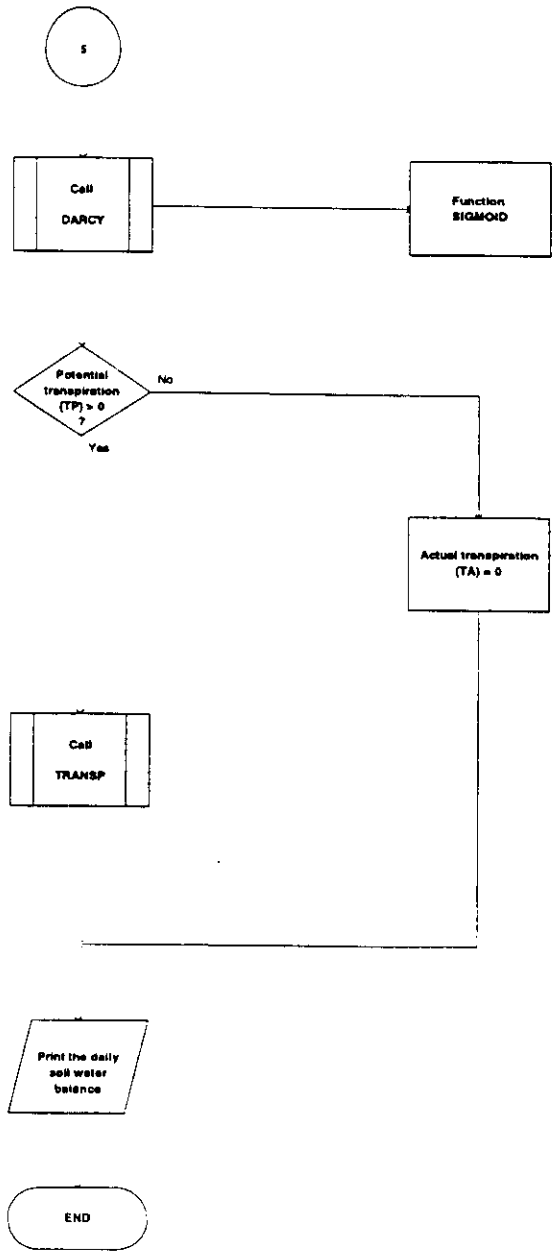


Figure H-8. Simplified flowchart of the HYDROLOGY submodel of WEPS (continued).

Winter Routines

The winter routines from the most-recent version of the SPAW model (Saxton, 1995; K.E. Saxton, 1995, personal communication) are in the process of being adapted with some modifications to the HYDROLOGY submodel of WEPS. The routines consist of three interactive components which deal with snow melt, soil frost formation, and snow drifting. The interactions of the three components allow for simulating the extent and timing of snow cover, the number of freeze-thaw cycles, and the changes in soil moisture during winter. These parameters significantly influence the soil susceptibility to wind erosion, particularly in the spring.

The snow melt component of the winter routines is based on Eq. H-2. If snow is present on any given day, it begins to melt when the maximum daily air temperature exceeds 0°C. The daily amount of snow melt depends on the maximum air temperature of that day and the initial water content of the snow. As described by Male and Gray (1981) the temperature index methods for predicting snow melt often give melt estimates that are comparable to those determined from more complex methods that take into account other factors such as radiation, wind velocity, atmospheric humidity, and albedo of the snow.

The soil freeze-thaw component of the winter routines is based on the method outlined by Jumikis (1966) with some minor modifications. The approach is to estimate the cumulative freezing degree-days required from the surface downward through a multilayered soil system. Each additional layer has a freezing requirement and the thermal resistance of the overlying soil layers and snow. The soil freezing depth is estimated by comparing the soil freezing index with the cumulative degree day climatic freezing index. Soil freezing sets the soil freezing coefficient of each soil layer. The freezing coefficients reduce the soil hydraulic conductivity of frozen soil layers by 90%.

The snow drift component of the winter routines assumes that snow depth accumulate until surface storage capacity is filled. The surface storage capacity for snow is influenced by soil random roughness, ridges, and vegetative cover. When the surface storage capacity is filled, a fraction of the new snow is assumed to drift, if it falls during low temperatures and high wind speeds.

SUBMODEL TESTING AND EVALUATION

The HYDROLOGY submodel of WEPS uses tested technology from well-established watershed models such as SPAW (Saxton and Bluhm, 1982; Saxton et al., 1974; Sudar et al., 1981), CREAMS (Smith and Williams, 1980), and EPIC (Williams et al., 1984, 1990) to simulate the different components of the soil water balance such as snow melt, runoff, infiltration, deep percolation, soil evaporation, and plant transpiration. The unique ability of the submodel to predict soil wetness at the soil-atmosphere interface has been tested using data set from two soils.

As a first step in the validation of the submodel, its performance was evaluated by comparing its predictions with the measured soil water content and evaporation data from a 14-d field experiment conducted during March 1971 (Jackson, 1973; Jackson et al., 1973) on an Avondale loam (fine-loamy, mixed (calcareous), hyperthermic Typic Torrifluent). In general, the submodel predictions compared favorably to actual measurements of daily evaporation ($r^2= 0.99$) and soil water content measurements ($r^2= 0.91$) throughout the experiment. Furthermore, the submodel provided good hourly estimates of soil wetness at the soil-atmosphere interface as compared with the measured water contents from the uppermost 5 mm of soil (Durar, 1991). However, the data from Jackson (1973) were used to develop a key algorithm in the submodel that defines the functional relationship between surface soil wetness and the ratio of actual to potential evaporation.

Another study was conducted to independently evaluate the performance of a stand-alone version of the HYDROLOGY submodel of WEPS in predicting surface soil drying with different soil and climatic conditions (Durar, 1995). The field experiment was conducted during July-August 1991 on a Pullman clay loam (fine, mixed, thermic Torrertic Paleustoll). The experimental site was a 210- by 250-m field situated at the USDA-ARS Conservation and Production Research Laboratory at Bushland, TX (35° 11' N, 102° 6' W, and 1169 m above MSL). A lysimeter was located at the center of the 5-ha rectangular field. The lysimeter (NE) was one of four weighing lysimeters located at the research center. Water content was measured gravimetrically in a bare 5 x 30-m plot for 14 d after irrigation. The plot was located 5 m directly north of the bare NE lysimeter. Hourly samples were taken from 0 to 2, 2 to 6, 6 to 10, 10 to 30, and 30 to 50-mm depth increments. Furthermore, soil cores were taken to 900 mm at 6-h intervals. Water content also was measured daily at the lysimeter and between the lysimeter and gravimetric sampling plot using a neutron probe to 2.1 m. Simulation with the HYDROLOGY submodel of WEPS started on 1 Aug. 1991 (DOY 213) and continued for 14 d. Daily weather variables, soil hydrological and physical properties, and the initial water content profile were required as inputs in the simulation. The soil profile was divided into eight simulation layers: 0 to 0.05, 0.05 to 0.15, 0.15 to 0.3, 0.3 to 0.5, 0.5 to 0.9, 0.9 to 1.3, 1.3 to 1.7, and 1.7 to 2.1 m.

The submodel accurately predicted that no deep percolation occurred throughout the simulation period. Figure H-9 shows that simulation results agreed well with the measured daily evaporation rates from the lysimeter ($r^2=0.96$). The fit between simulated and measured hourly soil water content was good for the eight simulation layers throughout the experiment (Fig. H-10). The mean absolute error, which describes the average absolute deviation between measured and simulated soil water contents, was $0.015 \text{ m}^3/\text{m}^3$. Figure H-11 shows that the hourly simulated soil water content at the soil-atmosphere interface exhibited the same diurnal pattern of soil drying during daytime and partial rewetting during nighttime as was observed in the 0- to 2-mm sampling layer throughout the experiment. Hence, the submodel reasonably estimated the soil water content profiles, particularly the status of soil water at the soil-atmosphere interface. The submodel successfully predicts the changes in water content at the soil surface, which relate to the susceptibility of the soil to wind erosion. The stand-alone version of the submodel used in the Bushland, TX, validation experiment has one additional climatic input parameter i.e., hour of precipitation during days on which precipitation occurs. The HYDROLOGY submodel of WEPS does not require hour of precipitation as an input parameter because the climate component (CLIGEN) of the WEATHER submodel of WEPS does not generate values for the parameter.

Based on our limited testing, the HYDROLOGY submodel of WEPS shows a potential to accurately simulate soil water dynamics, as needed for wind erosion modeling. The development of the HYDROLOGY submodel of WEPS has highlighted the need for further research. Areas for future research include:

1. Broaden the validation efforts to include a wider range of soils, hydrologic, surface and cover conditions;
2. Combine the HYDROLOGY submodel with the WEATHER, SOIL, and perhaps other WEPS submodels to simulate the impact of soil wetness on the threshold wind velocity over time;
3. Analyze the sensitivity of the submodel by evaluating the changes in the prediction of soil wetness by the submodel as influenced by the changes in the values of the input variables that are needed to run the submodel.

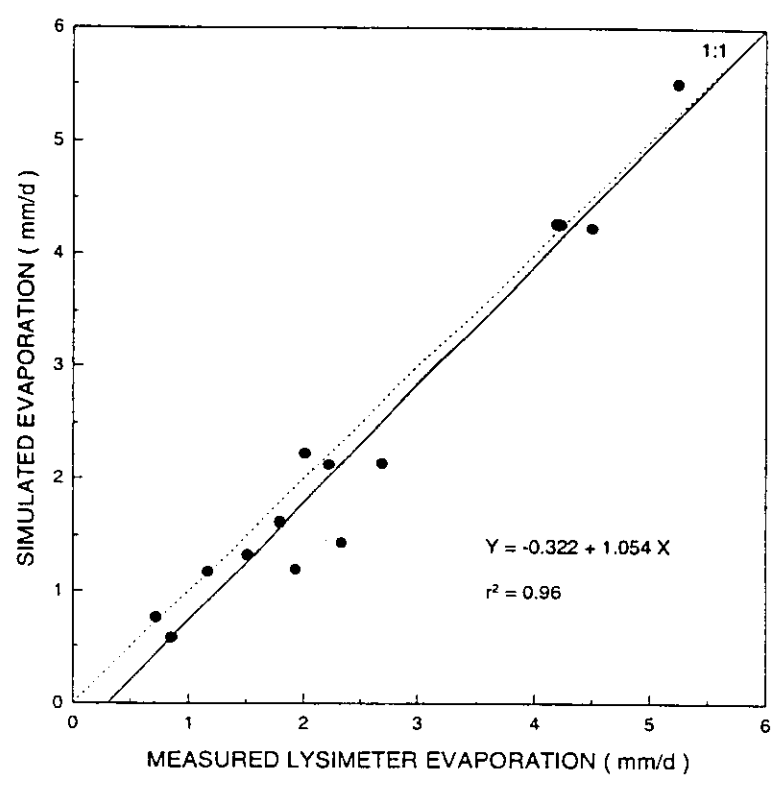


Figure H-9. Regression analysis between measured and simulated daily evaporation rates from Bushland, TX, 1991 validation experiment.

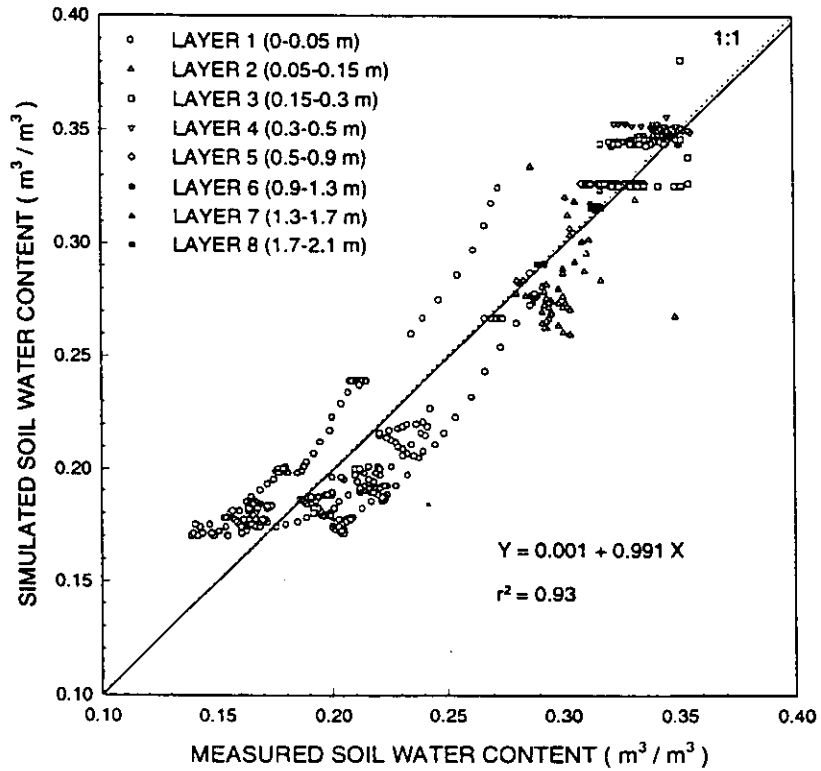


Figure H-10. Measured vs. simulated hourly soil water contents from the eight simulation layers, Bushland, TX 1991, validation experiment.

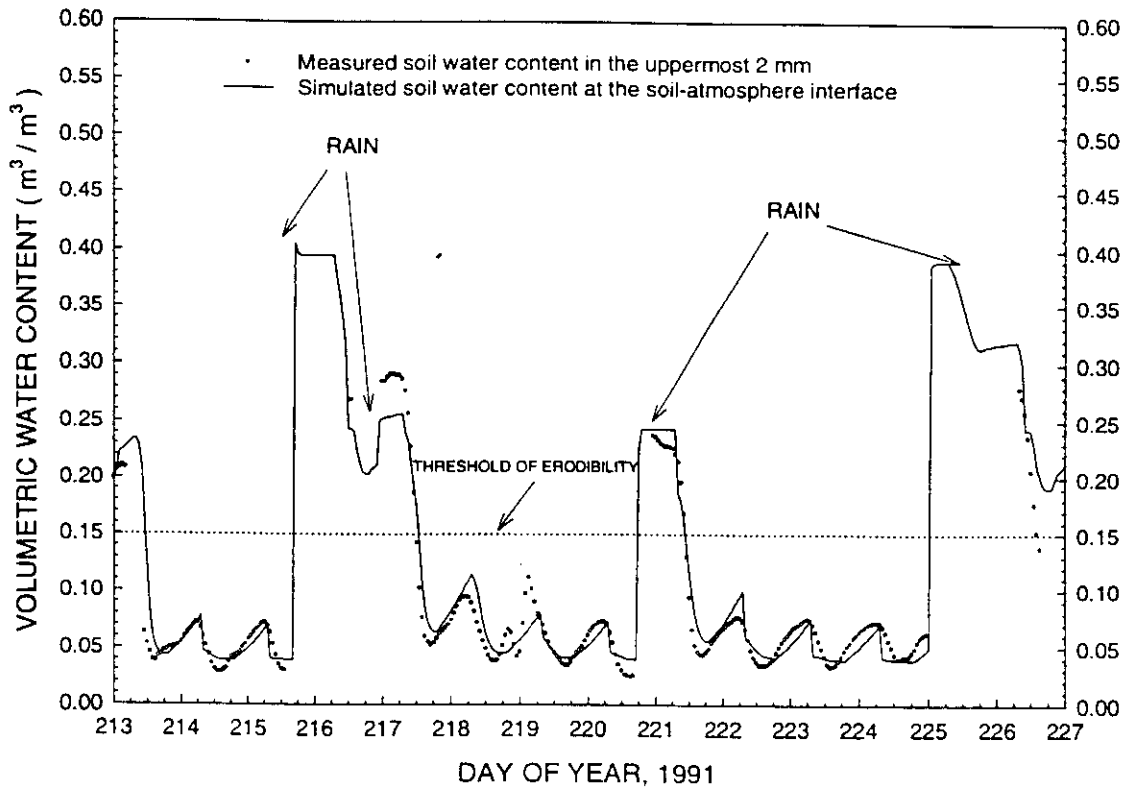


Figure H-11. Measured soil water contents in the uppermost 2 mm versus simulated hourly soil water contents at the soil-atmosphere interface, Bushland, TX. validation experiment.

LIST OF SYMBOLS

This list contains symbols that are used in the source code and the technical description document of the HYDROLOGY submodel of WEPS. Where two symbols are given, they both may be used in the source code, changing from one to another when passed as arguments between the HYDROLOGY submodel and the MAIN supervisory program of WEPS.

<u>Symbol</u>	<u>Description</u>	<u>Units</u>
am0hfl	Switch for production of hydrology outputs	--
am0ifl	Initialization flag for printing output headers	--
AMEP	Amplitude of the daily wave of potential soil evaporation	mm/hr
ARHO	Air density	kg/m ³
ASWC	Actual amount of available water in the surface layer	m ³ /m ³
ASWCR	Ratio of actual to total amounts of available water in the surface layer	--
AVEP	Time-average value of the daily potential soil evaporation	mm/hr
AWCR	Ratio of actual to total amounts of available water in the soil	--
AWCT	Total amount of available soil water content	m ³ /m ³
BD (asdblk)	Soil bulk density	Mg/m ³
bhrwc0	Hourly surface soil water content on a mass basis	kg/kg
BP	Barometric pressure	kPa
CANP	Daily crop canopy (ratio of ground cover)	--
CB	Power of Campbell's model of the soil water characteristic curve	--

WEPS	HYDROLOGY SUBMODEL	H-53
(ah0cb)		
CLAY	Percent clay	%
CLAYG	Geometric mean diameter of the clay-size fraction (CLAYG = 0.0002)	mm
CLAYM (asfcla)	Clay mass fraction	--
CM	Exponent of Campbell's model of the soil unsaturated hydraulic conductivity	--
CMTOMM (mTOmm)	Conversion factor from meters to millimeters (CMTOMM = 1000)	--
CN	Curve number	--
CNDIF	Difference between condition II SCS curve numbers for poor and good hydrologic conditions	--
CNI	SCS curve number for class I antecedent soil moisture conditions (dry soil moisture conditions)	--
CNII	SCS curve number for class II antecedent soil moisture conditions (average soil moisture conditions)	--
CNIIG (ah0cng)	SCS curve number for class II antecedent soil moisture conditions, under good cover conditions	--
CNIII	SCS curve number for class III antecedent soil moisture conditions (wet soil moisture conditions)	--
CNIIS	Slope-adjusted SCS curve number for class III antecedent soil moisture conditions	--
CNIP (ah0cnp)	SCS curve number for class II antecedent soil moisture conditons, under poor cover conditions	--
CNIIS	Slope-adjusted SCS curve number for class II antecedent soil moisture conditions	--

H-54	HYDROLOGY SUBMODEL	WEPS
CNIS	Slope-adjusted SCS curve number for class I antecedent soil moisture conditions	--
COND	Unsaturated soil hydraulic conductivity	m/s
CONDA	Average hydraulic conductivity for flow between adjoining soil layers	m/s
DFLOUT	Daily amount of infiltration water that flows out from the bottom of the lowermost layer and treated as deep percolation during soil water storage	mm/day
DH2O	Daily amount of water available from precipitation, snow melt, and/or irrigation	mm
DINF	Daily amount of water infiltration into the soil profile	mm/day
DIRG	Daily amount of irrigation water	mm
DIST	Distance of flow between adjacent soil layers	m
DLAYR (aszlyd)	Depth to the bottom of soil layer from the soil surface	m
DMLAYR (aszlym)	Depth to the midpoint of soil layer from the soil surface	m
DPH	Hourly amount of deep percolation	mm
DPRC	Daily amount of deep percolation	mm/day
DTIME	Time step in subroutine DARCY	s
E	Ratio of the molecular weights of water to air (E = 0.622)	--
EA (ahzea)	Daily rate of actual soil evaporation	mm/day
EAH	Hourly rate of actual soil evaporation	mm/hr
ELEV	Elevation of the simulation region above sea level	m

WEPS (amzele)	HYDROLOGY SUBMODEL	H-55
EP (ahzep)	Daily rate of potential soil evaporation	mm/day
EPH	Hourly rate of potential soil evaporation	mm/hr
ERATIO	Ratio of actual to potential soil evaporation	--
ESAT	Effective saturation	Dec. %
ETA (ahzeta)	Daily amount of actual evapotranspiration	mm/day
ETP (ahzeta)	Daily amount of potential evapotranspiration	mm/day
ETPR	Potential evapotranspiration by radiation	mm/day
ETPW	Potential evapotranspiration by wind	mm/day
G	Soil heat flux	MJ/m ²
GMD	Geometric mean diameter of primary soil particles	mm
GSD	Geometric standard deviation of primary soil particles	mm
H	Sum of energy inputs at the soil surface	MJ/m ²
IRISE	Time of sunrise	--
LAYRSN (nslay)	Number of soil layers used in the simulation	--
mc	Soil water content on a mass basis	kg/kg
mcfs	Soil water content at field capacity mass basis	kg/kg
mcs	Soil water content at saturation on a mass basis	kg/kg
mcw	Soil water content at wilting point on a mass basis	kg/kg

H-56	HYDROLOGY SUBMODEL	WEPS
PLAI (acrlai)	Plant leaf area index	--
POTE (aheaep)	Air entry potential of soil water	J/kg
POTES	Air entry potential at a standard bulk density of 1.3 Mg/m ³	J/kg
POTM	Matric potential of soil water	J/kg
POTMI	Initial matric potential of soil water	J/kg
PRCP (awzdpt)	Daily amount of precipitation	mm
PRES	Amount of plant residues on the soil surface	kg/ha
PRTD (aczrtd)	Depth of the root zone of the plant	m
RN	Net radiation	MJ/m ²
RNOFFM	Daily amount of measured surface runoff	mm
RUNOFF	Daily amount of estimated surface runoff	mm
S	Retention parameter	mm
SAND	Percent sand	%
SANDG	Geometric mean diameter of the sand-size fraction (SANDG = 0.316)	mm
SANDM (asfsan)	Sand mass fraction	--
SATK (ahrsk)	Saturated hydraulic conductivity of the soil	m/s
SILT	Percent silt	%
SILTG	Geometric mean diameter of the silt-size fraction	mm

WEPS	HYDROLOGY SUBMODEL	H-57
	(SILTG = 0.01)	
SILTM (asfsil)	Silt mass fraction	--
SLP (amrslp)	Average slope of the simulation region	m/m
SNMLT (ahzsmt)	Rate of snow melt	mm/day
SNOW	Daily snow melt minus daily snow accumulation	mm
SNWC (ahzsno)	Water content of snow	mm
SNWCI	Initial water content of snow	mm
SVPG	Ratio of the slope of the saturation vapor pressure curve to the psychrometric constant, adjusted to ambient barometric pressure	--
SVPG0	Unadjusted ratio of the slope of the saturation vapor pressure curve to the psychrometric constant	--
SWC	Amount of water in the soil profile in any given day	mm
SWCI	Initial amount of water in the soil profile	mm
SWH	Hydraulic head of soil water	m
SWM	Matric head of soil water	m
SWMI	Initial matric head of soil water	m
TA (ahzpta)	Actual plant transpiration	mm/day
TAIR (awtdav)	Daily mean air temperature	°C
TDP (awtdpt)	Daily mean dew-point temperature	°C

H-58	HYDROLOGY SUBMODEL	WEPS
THETOI	Initial soil water content at the soil-atmosphere interface	m^3/m^3
THETA	Volumetric water content of the soil	m^3/m^3
THETA0	Soil water content soil at the soil-atmosphere interface	m^3/m^3
THETAE	Equivalent water content of the surface layer	m^3/m^3
THETA F	Soil water content at field capacity	m^3/m^3
THETA I	Initial soil water content	m^3/m^3
THETA S	Soil water content at saturation	m^3/m^3
THETA W	Soil water content at wilting point	m^3/m^3
THETA X	Extrapolated water content at the soil surface	m^3/m^3
THETER	Soil water content of the surface layer based on the relationship between evaporation ratio and equivalent water content	m^3/m^3
THETE V	Soil water content of the evaporation zone of the surface layer	m^3/m^3
THETF3	Weighted average field capacity of the three uppermost simulation layers	m^3/m^3
THETI3	Weighted average initial water content of the three uppermost simulation layers	m^3/m^3
THETOI	Initial soil water content at the soil-atmosphere interface	m^3/m^3
TLAYR (aszlyt)	Thickness of soil layer	m
TOL	Tolerance value in subroutine DARCY. Maximum change in soil matric potential values between iterations in any soil layer (TOL = 2 m = 20 J/kg = 200 mb)	m
TMAX (awtdmx)	Daily maximum air temperature	$^{\circ}C$
TMIN	Daily minimum air temperature	$^{\circ}C$

WEPS	HYDROLOGY SUBMODEL	H-59
(awtdmx)		
TP (ahzptp)	Potential plant transpiration	mm/day
TTC	Turbulent transfer coefficient of water vapor	kg/m ² /kPa
TWU	Accumulated actual water use from the overlying soil layers	mm
U (awudav)	Mean daily wind speed	m/s
VK	Von Karman's constant (VK = 0.41)	--
VLH	Latent heat of vaporization	MJ/kg
VPA	Actual vapor pressure	kPa
VPD	Saturation vapor pressure deficit	kPa
VPS	Saturation vapor pressure	kPa
VPSMN	Saturation vapor pressure at minimum air temperature	kPa
VPSMX	Saturation vapor pressure at maximum air temperature	kPa
WC	Amount of water in the soil layer	mm
WCI	Initial amount of water in the soil layer	mm
WCS	Amount of water in the soil layer at saturation	mm
WFLUX	Amount of soil water flow in subroutine DARCY	m
WFLUXN	Net amount of soil water flow into a given soil layer	m
WSF	Water stress factor of plant growth	--
WUA	Actual rate of water use from a given layer	mm/day
WUD	Water use distribution parameter	--

H-60	HYDROLOGY SUBMODEL	WEPS
	(WUD = 3.065)	
WUP	Potential rate of water use from a given layer	mm/day
Z0	Roughness thickness	m
ZA	Height of measurements of meteorological sensors	m

REFERENCES

- Allen, R. G., M. E. Jensen, J. L. Wright, and R. D. Burman. 1989. Operational estimates of reference evapotranspiration. *Agron. J.* 81(4):650-662.
- Brooks, R. H., and A. T. Corey. 1964. Hydraulic properties of porous media. *Hydrology Papers No. 3*, Civil Engineering Dep., Colorado State Univ., Fort Collins, CO.
- Brooks, R. H., and A. T. Corey. 1966. Properties of porous media affecting fluid flow. *J. Irrig. Drain. Div., Am. Soc. Civil Eng.* 92(IR 2):61-88.
- Campbell, G. S. 1974. A simple method for determining unsaturated conductivity from moisture retention data. *Soil Sci.* 117(6):311-314.
- Campbell, G. S. 1985. *Soil physics with BASIC: transport models for soil-plant systems.* Elsevier Science Publishers B.V. Amsterdam, The Netherlands.
- Denmead, O. T., and R. H. Shaw. 1962. Availability of soil water to plants as affected by soil moisture content and meteorological conditions. *Agron. J.* 45:385-390.
- Duffie, J. R., and W. A. Beckman. 1980. *Solar engineering of thermal processes.* John Wiley and Sons, New York.
- Durar, A. A. 1991. Simulation of soil-water dynamics for wind erosion modeling. Ph.D. diss. Kansas State Univ., Manhattan (Diss. Abstr. 91-28491).
- Durar, A. A., J. L. Steiner, S. R. Evett, and E. L. Skidmore. 1995. Measured and simulated surface soil drying. *Agronomy J.* 87(2):235-244.
- Flerchinger, G. N. 1987. Simultaneous heat and water model of a snow-residue-soil system. Ph.D. diss. Washington State Univ., Pullman (Diss. Abstr. 88-13071).
- Hillel, D. 1971. *Soil and water: physical principles and processes.* Academic Press, New York, NY.
- Hillel, D. 1977. *Computer simulation of soil-water dynamics: a compendium of recent work.* International Development Res. Centre, Ottawa, Canada.
- Hjelmfelt, Jr., A. T., and J. J. Cassidy. 1975. *Hydrology for engineers and planners.* Iowa State University Press, Ames, IA.
- Holmes R. M., and G. W. Robertson. 1963. Application of the relationship between actual and potential evapotranspiration in dry land agriculture. *Trans. ASAE* 6(1):65-67.
- Jackson, R. D. 1973. Diurnal changes in soil-water content during drying. p. 37-55. *In* R. R. Bruce et al. (ed.) *Field soil water regime.* Special Pub. 5. Soil Sci. Soc. Am., Madison, WI.
- Jackson, R. D., S. B. Idso, and R. J. Reginato. 1976. Calculation of evaporation rates during the transition from energy-limiting to soil-limiting phases using albedo data. *Water Resour. Res.* 12(1):24-26.
- Jackson, R. D., B. A. Kimball, R. J. Reginato, and F. S. Nakayama. 1973. Diurnal soil water evaporation: time-depth-flux patterns. *Soil Sci. Soc. Am. Proc.* 37(4):505-509.
- Jacobs, A. F. G. and J. H. Van Boxel. 1988. Changes of the displacement height and roughness length of maize during a growing season. *Agric. Forest Meteor.* 42:53-62.

- Jensen, M. E. (ed.). 1974. Consumptive use of water and irrigation water requirements. A report prepared by the Tech. Committee on Irrig. Water Requirements, Irrig. and Drain. Div., Am. Soc. Civ. Eng., New York, NY.
- Jumikis, A. R. 1966. Thermal soil mechanics. Rutgers University Press. New Brunswick, NJ.
- List, R. J. 1971. Smithsonian Meteorological Tables. 6th ed. Smithsonian Institute Press, Washington, D.C.
- London, J., and C. Frohlich. 1982. Extended abstracts presented at the symposium on the solar constant and the spectral distribution of solar irradiance, Int. Assoc. of Meteorology and Atmospheric Physics Third Scientific Assembly, Hamburg, Federal Rep. Germany. 17-28 Aug. 1981. IAMAP, Innsbruck, Austria.
- Male, D.H., and D.M. Gray. 1980. Snowcover ablation and runoff. p. 360-436 in D.M. Gray and D.H. Male (ed.) Handbook of snow: principles, processes, management & use. Pergamon Press Canada Ltd. Ontario, Canada.
- McCuen, R. H., W. J. Rawls, and D. L. Brakensiek. 1981. Statistical analysis of the Brooks-Corey and the Green-Ampt parameters across soil textures. Water Resour. Res. 17(4):1005-1013.
- Miller, A. R. 1982. FORTRAN programs for scientists and engineers. SYBEX Inc., Berkeley, CA.
- Millington, R. J., and J. P. Quirk. 1959. Permeability of porous media. Nature. 183:387-388.
- Mualem, Y. 1976. A new model for predicting the hydraulic conductivity of unsaturated porous media. Water Resour. Res. 12(3):513-522.
- National Oceanic and Atmospheric Administration, National Aeronautic and Space Administration, and United States Air Force. 1976. U.S. Standard Atmosphere, 1976. U.S. Government Printing Office, Washington, DC.
- Penman, H. L. 1948. Natural evaporation from open water, bare soil, and grass. Proc. Roy. Soc. (London), Series A 193:120-146.
- Rawls, W. J., D. L. Brakensiek, and K. E. Saxton. 1982. Estimation of soil water properties. Trans. ASAE 25(5):1316-1328.
- Richards, L. A. 1931. Capillary conduction of liquids through porous mediums. Physics 1:318-324.
- Richardson, C. W., and J. T. Ritchie. 1973. Soil water balance for small watersheds. Trans. ASAE 16(1):72-77.
- Savabi, M. R., A. D. Nicks, J. R. Williams, and W. J. Rawls. 1989. Chapter 7, Water Balance and Percolation. In L. J. Lane and M. A. Nearing (ed.) USDA-Water Erosion Prediction Project: Hillslope Profile Model Documentation. NSERL Report No. 2. USDA-ARS National Soil Erosion Research Laboratory, West Lafayette, IN.
- Saxton, K. E. 1995. SPAW: a Soil Plant Atmosphere Water model. Users Manual. Draft of March 1995. USDA-ARS in cooperation with Washington State University.
- Saxton, K. E., and G. C. Bluhm. 1982. Regional prediction of crop water stress by soil water budgets and climatic demand. Trans. ASAE 25(1):105-110 & 115.

- Saxton, K. E., H. P. Johnson, and R. H. Shaw. 1974. Modeling evapotranspiration and soil moisture. *Trans. ASAE* 17(4):673-677.
- Saxton, K. E., P. F. Brooks, R. Richmond, and J. S. Romberger. 1984. Users manual for SPAW--a Soil-Plant-Air-Water model. Revision No.3 (8/6/84). USDA-ARS in cooperation with Washington State Univ., Pullman, WA.
- Skidmore, E. L., H. S. Jacobs, and W. L. Powers. 1969. Potential evapotranspiration as influenced by wind. *Agron. J.* 61(4):543-546.
- Smith, R. E., and J. R. Williams. 1980. Simulation of the surface water hydrology. p. 13-35. *In* W. G. Knisel (ed.) *CREAMS: A Field Scale Model for Chemicals, Runoff, and Erosion from Agricultural Management Systems*. USDA Conservation Research Report No. 26, U.S. Dept. of Agric., Washington DC.
- Soil Conservation Service. 1972. *SCS National Engineering Handbook, Section 4, Hydrology*. NEH-Notice 4-102. SCS, U.S. Dept. of Agric., Washington DC.
- Steiner, J. L. 1989. Tillage and surface residue effects on evaporation from soils. *Soil Sci. Soc. Am. Proc.* 53(3):911-916.
- Sudar, R. A., K. E. Saxton, and R. G. Spomer. 1981. A predictive model of water stress in corn and soybeans. *Trans. ASAE* 24(1):97-102.
- Van Bavel, C. H. M. 1966. Potential evaporation: the combination concept and its experimental verification. *Water Resour. Res.* 2(3):455-467.
- Van Genuchten R. 1978. Calculating the unsaturated hydraulic conductivity with a new closed-form analytical model. Research Report 78-WR-08, Water Resources Program, Dept. of Civil Engineering, Princeton Univ., Princeton, NJ., 63 p.
- Van Genuchten M. Th. 1980. A closed-form equation for predicting the hydraulic conductivity of unsaturated soils. *Soil Sci. Soc. Am. J.*, 44(5):892-898.
- Weast, R. C., M. J. Astle, and W. H. Beyer. 1983. *CRC Handbook of Chemistry and Physics*. 64th ed. (1983-1984), Chemical Rubber Company Press, Inc., Boca Raton, FL.
- Wendt, C. W. 1970. Water transfer from soil to the atmosphere as related to climate and soil properties. Tech. Rep. 24. *Water Resour. Inst. Texas A&M Univ., College Station, TX.*
- Williams, J. R. 1989. EPIC: the erosion-productivity impact calculator. p. 676-681. *In* Proc. 1989 Summer Computer Simulation Conference, Austin, TX. July 24-27, 1989. The Society for Computer Simulation, San Diego, CA.
- Williams, J. R., and R. W. Hann, Jr. 1978. Optimal operation of large agricultural watersheds with water quality constraints. Tech. Rep. 96. *Texas Water Resour. Inst. Texas A&M Univ., College Station, TX.*
- Williams, J. R., C. A. Jones, and P. T. Dyke. 1984. A modeling approach to determining the relationship between erosion and soil productivity. *Trans. ASAE* 27(1):129-144.
- Williams, J. R., C. A. Jones, and P. T. Dyke. 1990. The EPIC Model. p. 3-92. *In* A. N. Sharpley and J. R. Williams. (ed.) *EPIC--Erosion/Productivity Impact Calculator: 1. Model Documentation*. USDA Technical Bulletin No. 1768, U.S. Dept. of Agric., Washington DC.

H-64

HYDROLOGY SUBMODEL

WEPS

Wright, J. L. 1982. New evapotranspiration crop coefficients. J. Irrig. Drain. Div. , Am. Soc. Civ. Eng. 108(2):57-74.